CANMET

POTASH MINING PROJECT

PROJET D'EXPLOITATION DE LA POTASSE

MRL 90-145

HANGING WALL RESPONSE TO MINING OF DENISON-POTACAN

PHASE III

Final Report By:

DENISON-POTACAN POTASH COMPANY
Sussex, New Brunswick

Prepared By:

DENISON-POTACAN POTASH COMPANY
Sussex, New Brunswick

Work on the project was conducted under the auspices of the Canada Centre for Mineral and Energy Technology, Energy, Mines and Resources Canada as part of the Canada/New Brunswick Mineral Development Agreement.

DSS FILE NO: 14SQ.23440-8-9041

DSS CONTRACT SERIAL NO: 23440-8-904101-SQ
CANMET PROJECT NO: 144.603.02.3
CANMET SCIENTIFIC AUTHORITY: Dr. G Herget

180 pp + figs.

MICROMEDIA

July, 1990

ACKNOWLEDGMENTS

This report was prepared by Denison-Potacan Potash Company, Sussex, New Brunswick. The work on the project was largely sub-contracted to outside specialists. Assistance was greatly appreciated from the following:

* On site management, supervision and control of the microseismic project was handled by D.C.E. Waugh, Superintendent of Engineering, and C. Monahan, S. Munroe and R. Fry, Rock Mechanics Group.

* The bulk of the project involved conducting an on-site microseismic monitoring trial. This work was sub-contracted to A. Prugger, geophysicist, of Prugger Geophysical Services, Saskatoon, Saskatchewan. The report of that work is found in Appendix A.

* Comparison of the numerical codes GEOROC and VISCOT was sub-contracted to Mraz Project Consultants Ltd., Saskatoon, Saskatchewan. The results of that work is in Appendix B to this report.

LIST OF FIGURES

FIGURE	2.1	Location of Mine Site
	2.2	Geology of the Moncton Subbasin in New Brunswick (after Waugh and Urquhart, 1983)
	2.3	Stratigraphic Column Marchbank Syncline (after Waugh and Urquhart, 1983)
	2.4	Schematic of Cassidy Lake Formation Potash Members (after Waugh and Urquhart, 1983)
	2.5	Mohr-Coulomb Diagram for Poodiac Sandstone.
	2.6	Mohr-Coulomb Diagram for Poodiac Siltstone.
	2.7	Mohr-Coulomb Diagram for Fractured Poodiac Sandstone.
	2.8	Mohr-Coulomb Diagram for Siltstone Caprock Breccia.
	2.9	Plan, Clover Hill Mine, Mine Development April 1989, Showing Subsidence, Geophone Locations and Seismic Events. Scale 1:8000.
	2.10	Typical Geological Cross-Section.
	2.11	Plan, Clover Hill Mine, Mine Development April 1989, Showing Geophone Locations and Seismic Events. Scale 1:4000.
	2.12	North South Section 11 Panel.

TABLE OF CONTENTS

LIST OF FIGURES

LIST OF TABLES

1.0 EXECUTIVE SUMMARY (English/Francais)

2.0 INTRODUCTION

2.1 Background to Mine Development

2.2 Stratigraphy and General Description

2.3 Description of Mine and Mining Methods

2.4 Summary - Rock Mechanics Work
2.4.1 Material and Mechanical Properties - Summary
2.4.2 In-Situ Monitoring and Testing
2.4.3 Numerical Analysis

2.5 Phase III Work - Background

3.0 Microseismic Monitoring Trial

3.1 Introduction

3.2 Purposes of the Monitoring Trial

3.3 Summary - Details of Monitoring Trial

3.4 Summary - Main Results of the Trial

APPENDIX A

A.1 Report of Microseismic Monitoring at the Denison-Potacan Potash Mine at Clover Hill, New Brunswick in the period January 24, 1989 through April 7, 1989 - Final Report (draft). Report by A. Prugger, Consultant.

A.2 Recursive or feedback digital filters. Report by A. Prugger.

A.3 Discussions of electrical interference problems encountered during seismic monitoring, January - April 1989, at the Clover Hill Mine, New Brunswick. Report by A. Prugger.

A.4 Summary of Seismic event locations, Clover Hill Potash Mine, New Brunswick, January - April, 1989. Summary by A. Prugger.

A.5 System Overview - Microseismic Systems Inc - Microseismic Monitoring System.

APPENDIX B

B.1 Numerical Modelling using GEOROC. Report be Mraz Project Consultants Ltd. (MPC)

LIST OF TABLES

TABLE 2.1 SUMMARY MECHANICAL PROPERTIES - ORE ZONE AND UPPER HALITE

TABLE 2.2 SUMMARY MATERIAL AND MECHANICAL PROPERTIES - OVERBURDEN ROCKS

SECTION 1.0

1.0 EXECUTIVE SUMMARY

1.1 Background - Mine Development and Design

The Denison-Potacan Potash Company mine site is located southwest of Sussex, New Brunswick, as shown in Figure 2.1. The Clover Hill deposit was first identified by surface exploratory drilling conducted in 1973 under the direction of the New Brunswick Department of Natural Resources.

In 1975, the Government of New Brunswick granted International Minerals and Chemical Corporation (Canada) Limited (IMC) exclusive rights to explore and develop the Clover Hill property.

IMC subsequently conducted a surface exploration drilling program which defined approximately 200 million tonnes of potash ore grading 28% K_2O, which makes this deposit one of the highest grades in the world.

Potash production commenced in July 1985. Annual production projected for year 1990 is about 1.1 million tonnes of product.

The potash deposit is confined to the Marchbank Syncline, which is the most southern major structural feature of the Moncton Subbasin. It is shown in Figure 2.2 of the report. The potash deposit is part of the Cassidy Lake Evaporite Formation of the Windsor group as shown in the Marchbank Syncline stratigraphic column, Figure 2.3.

The evaporite interval has been subdivided into four members:

1. Basal Halite;
2. Middle Halite;
3. Potash;
4. Upper Halite.

DENISON POTACAN POTASH COMPANY

TITLE:
LOCATION OF MINE SITE

SCALE:
N.T.S.

FIGURE:
2.1

DENISON POTACAN POTASH COMPANY

TITLE:

GEOLOGY OF THE MONCTON SUBBASIN IN NEW BRUNSWICK
(After Waugh and Urquhart, 1983)

SCALE:
N.T.S.

FIGURE:
2.2

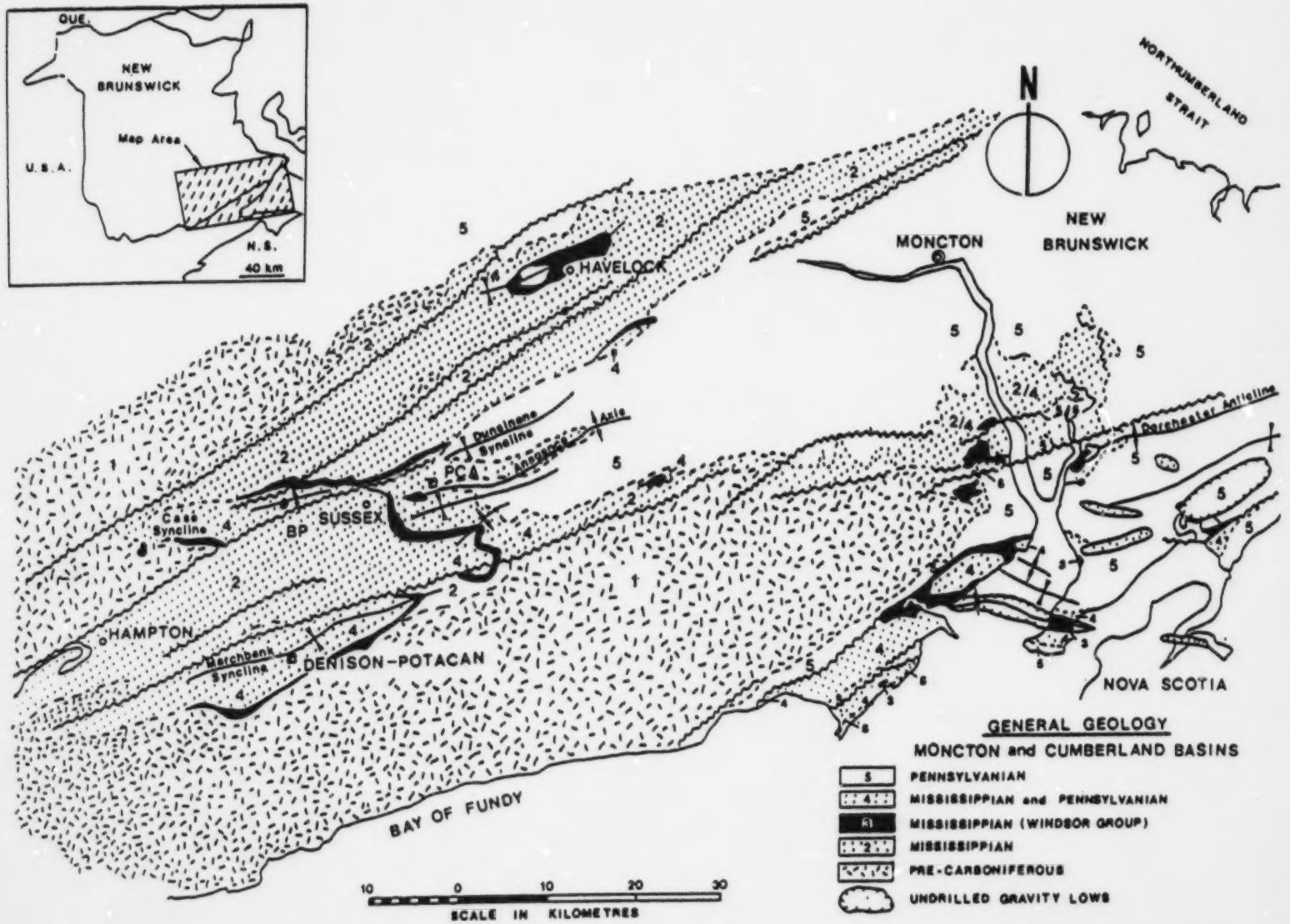

MARCHBANK SYNCLINE – STRATIGRAPHIC COLUMN

GROUP	FORMATION	MEMBER	BED		GENERAL LITHOLOGIES
HOPEWELL	Wanamaker	Fowler Brook			Grey red sandstone and siltstone numerous grey limestone nodules
		DeForest Lake			Grey red to grey brown conglomerate and sandstone
		Scoodic Brook			Grey red sandstone and siltstone
					unconformity
	Campbell Settlement				Pale red vuggy siltstone/sandstone
	Poodiac				Grey brown siltstone
					Grey to grey brown sandstone/siltstone
					Grey brown siltstone and sandstone
					Variable collapse breccia
WINDSOR	Plumweseep	Grey Clay			Green grey claystone
		Upper Salt			Not present in Marchbank Syncline
		Upper Anhydrite			Grey to bluish grey anhydrite
	Cassidy Lake	Upper Halite			Fine to medium grain orange to brown halite interbedded with numerous argillaceous and red sylvite beds and borate minerals
		Potash	Sylvinite Bed		Brick red very fine to fine grain sylvinite
			L.G.B.		Light orange halite with sylvite clusters
		Middle Halite			Light brown medium grain halite with irregular bands of dark brown to dark gray argillaceous halite
		Basal Halite			Very light grey to clear medium to coarse grain halite with irregular dark brown black argillaceous halite bands
	Upham	Upperton			Grey anhydrite
		Devine Corner			Light grey to buff limestone

DENISON POTACAN POTASH COMPANY

TITLE:
STRATIGRAPHIC COLUMN
MARCHBANK SYNCLINE
(After Waugh and Urquhart, 1983)

SCALE:
N.T.S.

FIGURE:
2.3

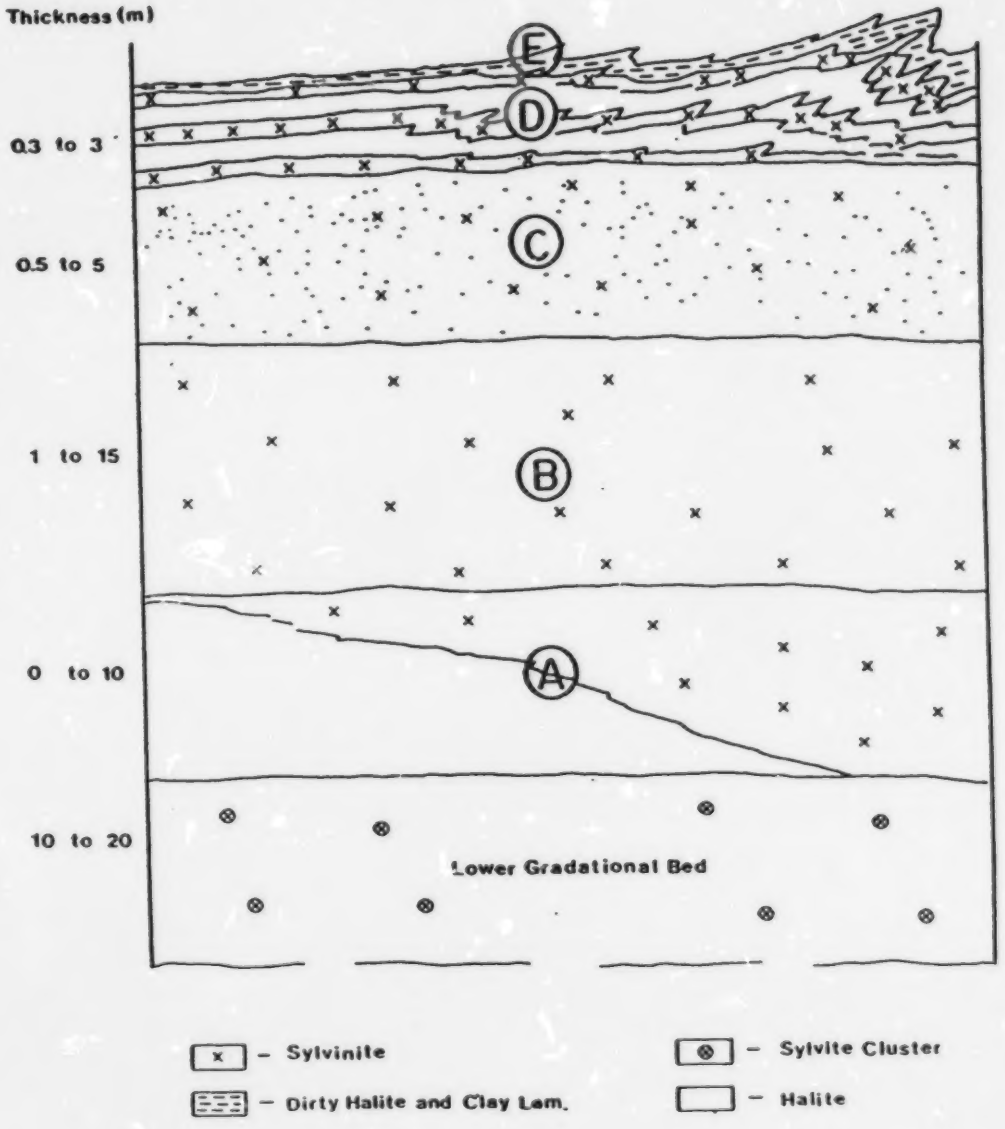

DENISON POTACAN POTASH COMPANY

TITLE:
SCHEMATIC OF CASSIDY LAKE FORMATION POTASH MEMBER
(After Waugh and Urquhart, 1983)

SCALE:
N.T.S.

FIGURE:
2.4

The potash member consists of the Sylvinite Bed and Lower Gradational Bed.

The Sylvinite Bed is composed of fine-grained sylvite and halite. It is subdivided into five distinct zones based on mineralization, percent insolubles and colour. These have been designated from oldest to youngest as the A, B, C, D and E zones. The B and C zones comprise the main ore bed illustrated in Figure 2.4.

The formations comprising the overburden overlying the potash and halite members of Cassidy Lake Formation consists of a sedimentary sequence including collapse breccia, siltstones, sandstones, conglomerate and limestone.

The Denison-Potacan Potash deposit is at a depth of approximately 880 metres below surface. It is approximately 10 kilometres in length along the strike and has a maximum plan width of about 3.5 kilometres.

A modified room and pillar method of mining with delayed backfill is used. The mining method uses either/or a combination of cutting machines and drill and blast methods for development of mining panels access and for top slicing and benching in the stopes. The mining panel entries are driven typically with three parallel drifts so that the center heading which is normally used as the travelway is in stress relieved ground. Stoping widths vary from 20 m to 30 m and stope heights range from about 5 m to 30 m with average height of 10 to 15 m. Pillars breadths vary from 20 m to 40 m. The final stope backs are supported with full length resin-grouted rebars. Slurried tailing fill using the halite waste fraction of the ore and a saturated brine for hydraulic transport

is placed in stopes after mining.

Conveyor belt systems are used to transport ore from the mining areas to underground storage bins and then to a loading pocket and production shaft. It is hoisted in 25 tonne skips to surface.

A comprehensive in-situ testing and monitoring program was conducted in the early stage of mining in order to determine time dependent stress - strain behaviour of the sylvinite and host salt rock. The results were used for development of a site specific creep model and as input data for numerical simulations.

Laboratory testing for the determination of the mechanical properties of the evaporites and overlying clastic sediments was also conducted. Creep tests and brittle yield tests were carried out on the evaporites. They exhibit elasto-plastic behaviour in response to applied stress. The sediments, which exhibit elastic behaviour, were subjected to brittle failure tests. Results were fitted to a creep failure criterion and classical Mohr-Coloumb shear failure criterion respectively. The details of the in-situ monitoring program as well as laboratory testing methods and the results are reported in previously published Phases I and II reports. The titles of these reports were: "Use of Backfill in New Brunswick Potash Mines". They were published in 1985 and 1989, respectively.

In summary, the results showed that the evaporites are mechanically weak and the behaviour is dominated by plastic flow. A brittle type failure mechanism is limited to a region of low confinement and a uniaxial condition. Beyond a low range of confining stresses the salt and potash rock yields rapidly and

exhibits plastic flow behaviour.

The sediments are mechanically stronger and stiffer than the evaporites. Failure mechanism is by brittle type fracture. The rock types comprising these geological formations are locally fractured. The fracturing would have the effect of reducing rock mass strength and rock mass stiffness. This becomes significant for assessing the response of this sequence to closure of the underlying mine openings and as well indirectly for evaluating groundwater flow conditions.

1.2 Background - Phase III Research

As a follow-up to the work done in Phases I and II, a decision was made that a study should be conducted to assess the hanging wall response to mining. This was based on some concern that the overburden rocks may be capable of storing a large magnitude of strain energy such that sudden brittle failure of that sequence would result in significant seismic activity. This was despite their generally fractured nature and early indications from monitoring closure of underground openings and surface subsidence measurements that bridging of the strata was not likely occurring.

In April 1988 as a result of discussions with CANMET, a proposal was submitted to the Minister of Supply and Services by Denison-Potacan Potash Company and a contract was awarded. The title of the research project was "Hanging Wall Response to Mining of Denison-Potacan - Phase III". It was a cost shared project and total estimated costs were $150,500 subject to the Basis of Payment clause in the Contract. The work was performed under DSS Contract Serial No. 23440-8-9041/01-SQ.

The primary research objectives were to:

1. Install a microseismic system for the purpose of determining if hanging wall deformation occurring in response to mining was accompanied by seismic activity.

2. Verification of geomechanical codes GEOROC and VISCOT by comparison of output with in-situ closure and stress measurements.

The microseismic monitoring work was sub-contracted to Prugger Geophysical Services from Saskatoon, Saskatchewan, Canada. This comprised the bulk of the Phase III work. It involved a 3-month monitoring trial at the mine site.

The verification of the GEOROC and VISCOT computer programs was sub-contracted to Mraz Project Consultants Ltd. (MPC) also from Saskatoon.

1.3 Microseismic Monitoring Trial

A major concern exists in some potash mines regarding the potential for seismic activity being generated in the overlying strata with subsidence. This is because the overburden material may be mechanically strong and stiff enough to accumulate a high magnitude of stress. As subsequent apparent brittle failure or rupture of this rock which is probably associated with subsidence is thought to be the main cause of large energy magnitude seismic event(s). This is the situation of some mines in Saskatchewan, for example. In the case of the Denison-Potacan mine, it is thought that the fractured sediments comprising the hanging wall are not likely to have the capability to store strain energy such that this would occur. It was decided, however; to attempt to determine if microseismic activity was being generated in the hanging wall. As

well, little, if any documented basic research into microseismic activity had been done in potash mines with this geological setting.

A microseismic monitoring system was installed underground at the mine and data was obtained during the period January to April, 1989. It was installed on a temporary basis. The test was terminated in part due to hardware problems primarily associated with electrical interference with transducer signals from high voltage mine equipment cables and from general equipment breakdowns.

The system used single vertical-axis uni-directional type geophones connected via twisted-pair telephone cables to a central data acquisition and processing unit located underground.

The results of this trial indicated that during this period microseismic activity occurred and that it appeared to be concentrated near active mining faces. There was no indication that large magnitude of energy was associated with these events based on absence of visible damage or audible noise reported. Fifty seven (57) events were recorded. More research, including in-situ monitoring, is required in this geological setting to confirm source locations and failure mechanism associated with seismic energy release. This will entail more monitoring and analysis such as first motion studies, of vibration waveforms.

SUMMARY - PURPOSES OF THE TRIAL

1. There was some concern expressed about the eventual need for mine-wide monitoring of the design. A microseismic

monitoring system was considered likely be the best tool for this purpose. A change in stress conditions could probably be inferred through failure indicated by seismic activity.

2. As a corollary, the data from microseismic monitoring has valuable potential for use in mine design and sequencing after a dependable database has been established.

3. It was considered to have had the potential for providing preliminary information on whether seismicity of significant magnitude of energy was associated with failure of the hanging wall.

4. To a lesser degree of importance, it would provide an opportunity to evaluate monitoring hardware and software for use in the mine environment tested.

5. There was no plan to use the system as a tool for prediction of local roof falls or local pillar spalling.

SUMMARY - MAIN RESULTS OF MICROSEISMIC MONITORING TRIAL

1. The trial showed that microseismic events occurred during the test period. The average frequency of events recorded was about 1 per day. All events appeared to be of low magnitude energy.

2. The events recorded showed a concentration of activity at the

north end of Panel 11 located in the active 11360 stope mined by drill and blast method. It is likely that the events were associated with brittle fracturing which would be expected near the periphery of the opening.

3. There was only minor activity in the older mined-out areas. It may be inferred that there was no significant pillar over-stressing there at time of the survey.

4. It was determined that most events occurred close to the mining horizon in the potash or salt.

5. There was no significant correlation found between the seismic activity recorded and the following:

   (a) Output from VELMINA - a three-dimensional numerical model simulation that included: steady state shear stresses, normal stresses and steady state convergence rate;
   (b) Total surface subsidence;
   (c) Geological features - a major fold and varying interval of salt between the top of the mining horizon and overlying clastic sediments.

1.0 Sommaire administratif

1.1 L'arrière-plan technique : conception et réalisation de la mine DPPC

La mine DPPC se situe au sud-ouest de Sussex, Nouveau-Brunswick, comme le montre le schéma 2.1. Le gisement Clover Hill a été identifié en 1973, en utilisant les forages exploratoires de surface, sous la direction du Département de Ressources Naturelles du Nouveau-Brunswick.

En 1975, le gouvernement du Nouveau-Brunswick a accordé les droits exclusifs d'exploitation du gisement Clover Hill à la société International Minerals and Chemical Corporation (Canada) Limited (IMC).

IMC, utilisant le forage de surface, délimitait une ressource de 200 million de tonnes à richesse de 28% de K_2O, indiquant un des gisements potassiques les plus riches du monde.

La production de la potasse a commencé en juillet, 1985. La production prévue pour l'année 1990 est à peu près 1,1 million de tonnes.

Le gisement se trouve complètement dans le synclinorium Marchbank, la plus grande structure géologique méridionale du sous-bassin Moncton, comme le démontre le schéma 2.2. Les couches potassiques font part de la formation évaporitique de Cassidy Lake du Groupe de Windsor, comme le démontre la colonne stratigraphique du synclinorium Marchbank, schéma 2.3.

Les couches évaporitiques sont organisées en quatre zones :

1. le halite inférieur
2. le halite central
3. les couches potassiques
4. le halite supérieur

Les couches potassiques se répartissent en deux zones : la couche sylvinitique (Sylvinite Bed) et la couche inférieure gradationelle (Lower Gradational Bed).

La couche sylvinitique est composée de grains fins de sylvinite et de halite. Cinq couches distinctes peuvent être identifiées en fonction de la minéralogie, la couleur, et la teneur en matière insoluble. De la couche la plus vieille (inférieure), ils portent les lettres indicatrices A, B, C, D, et E, et les zones B et C forment le gisement principal de minerai potassique, comme le démontre le schéma 2.4.

Les couches supérieures qui couvrent la zone évaporitique Cassidy Lake sont des sédiments variés, y inclus une brèche créée par la dissolution, des grès silteux, des grès, des conglomérats, et des calcaires.

Le gisement DPPC se trouve à une profondeur de 880 m sous-surface, avec un longeur de 10 km dans la direction des couches, et une largeur maximale de 3,5 km.

L'exploitation s'accompli avec une méthode de chambres et piliers modifiée, avec le remblayage mis en place qu'après l'exploitation

complète des chambres. Des tunneliers et le forage et tir sont tous les deux utilisés pour gagner accès et pour le développement des chambres d'exploitation, ce qui est accompli avec une série de bancs horizontaux. Ces chambres sont de 20 à 30 m de largeur, d'une taille de 5 à 30 m, avec une taille moyenne de 10 à 15 m. Les piliers entre les chambres sont de 20 à 40 m d'épaisseur. Les plafonds (les toits) des chambres d'exploitation sont renforcés avec des boulons complètement résinés (full-length resined bolts). Le remblayage s'effectue avec les déchets d'halite granulaire, transportés et mis en place par des moyens hydrauliques, utilisant une saumure saturée.

Les tunnels d'accès permanent pour chaque panneau (plusieures chambres ensembles) sont créés en utilisant une méthode de relâchement de contraintes, pour protéger ces structures semi-permanentes contre les fermetures rapides.

Les convoyeurs transportent le minerai potassique des lieux d'exploitation vers les stockages souterrains, d'où le minerai est transporté vers la surface avec un ascenseur de 25 tonnes.

Un programme compréhensif de surveillance et d'essais sur place a été réalisé pendant les premières années d'exploitation pour l'évaluation du comportement en fluage des couches évaporitiques. Ces résultats ont été utilisés pour la calibration et la vérification sur chantier des modèles numériques de fluage pour la mine entière.

Des essais de comportement mécanique ont été réalisés sur des échantillons des couches évaporitiques et des couches supérieures

sédimentaires. Pour les roches évaporitiques, des essais de fluage et de résistance démontraient un comportement viscoplastique et élastoplastique, tandis que les roches sédimentaires exhibitaient un comportement élastique, suivi par l'affaiblissement soudain (rupture fragile). Les données des essais ont été adaptées dans les lois semi-empirique de fluage et les résistances dans les critères Mohr-Coulomb.

Les détails des méthodes et des données cueillies se trouvent dans les rapports des Phases I et II, entitrés "Le remblayage dans les mines de potasse du Nouveau-Brunswick", livrés à CANMET en 1985 et 1989.

En bref, les résultats nous démontrent que les évaporites possèdent une faiblesse mécanique, et ils ont la capacité de se déformer d'une façon visqueuse. Si les contraintes minimales sont faibles, la rupture fragile est typique.

Les roches sédimentaires sont plus résistantes et plus rigides que les roches évaporitiques. Leur mode de rupture est fragile, et ces roches sont aussi fissurées in situ. Ce dernier fait indique sans doute une rigidité et une résistance sur place réduites, ce qui est important dans l'estimation de la réaction du massif supérieur à la fermeture des chambres d'exploitation après l'extraction des couches potassiques.

1.2 L'arrière-plan technique : les activités de recherche Phase III à DPPC

La suite des travaux Phase I et II a été décidée comme un étude de la stabilité du plafond de la mine, en étudiant ss réaction à l'extraction minière. Une inquiétude existait concernant les couches supérieures et leur capacité pour l'accumulation de l'énergie élastique, qui pourrait peut-être déclencher un effondrement spontané, initié par la propagation incontrollable de la rupture fragile et la génération de la séismicité. Ces inquiétudes existaient malgré certaines indications que les roches au-dessus de la mine étaient suffisament fissurées pour que les contraintes ne se concentreraient pas, à cause de leur redistribution liée avec les non-linéarités élastiques et élastoplastiques. Aussi, il faut dire que la recherche précédente sur l'activité microséismique dans les couches évaporitiques n'existait pas à cet emplacement.

Au mois d'avril, 1988, après les réunions avec CANMET, une proposition de DPPC a été envoyée au Département de Services et d'Approvisionnement, et un contrat fut accordé à titre de "La Réaction Mécanique du Toit de la Mine DPPC - Phase III". Les dépenses totales prévues de $150,000 seraient partagées entre les deux organismes, et les travaux seraient accomplis sous le contract DSS N° 23440-8-9041/01-SQ.

Les buts du programme de recherche étaient :

1. L'installation d'un réseau de capteurs séismiques pour observer si les déformations dans le plafond se

manifestaient par les émissions microséismiques.

2. La vérification des logiciels GEOROC et VISCOT, utilisant les données de vitesses de fermeture et les mesures de contraintes.

Les travaux microséismiques ont été réalisés par Prugger Geophysical Services de Saskatoon, Saskatchewan, et leur contrat pour trois mois de surveillance comprenait la majorité des travaux Phase III.

La vérification des logiciels a été réalisée par Mraz Project Consultants Ltd. (MPC), aussi de Saskatoon, Saskatchewan.

1.3 Les essais de surveillance microséismique

Dans certaines mines de potasse, les ingénieurs sont inquiets au sujet de la génération d'éffets séismiques dans le toit de la mine, à cause de l'extraction des couches de minerais. Les couches supérieures sont rigides et résistantes et peuvent, en principe, accumuler l'énergie élastique, et un grand évènement séismique pourrait se produire avec la rupture fragile de ces couches, ce qui arrive dans certaines mines de potasse à Saskatchewan. Dans la mine DPPC au Nouveau-Brunswick, il est supposé que les couches supérieures sont suffisament fissurées qu'elles ne peuvent pas supporter la grande concentration de contraintes nécessaire pour générer un grand évènement séismique. Dans le but de vérifier cette hypothèse, et aussi parce que très peu d'information existait

pour les mines de potasse de ce type, un essai de trois mois de surveillance microséismique a été conçu.

Un réseau souterrain temporaire de capteurs a été installé et surveillé pendant la période janvier-avril, 1989. Les capteurs étaient de type géophone, axe vertical, liés par des fils électroniques tordus, avec un appareil d'enregistrement central. La terminaison de l'essai s'est effectuée à cause des problèmes avec l'interférence électronique dans les capteurs, lié à la présence de cables électriques à haute tension.

Les données indiquaient qu'il y avait des évènements microséismiques, localisés dans les régions d'exploitation active, et cinquante-sept (57) évènements discrets ont été enregistrés. Basé sur les observations visuelles et auditoires, il était évident qu'il n'y avait pas de stockage d'énergie en quantité, avec les relâchements brutals liés avec ces émissions microséismiques. A fin d'effectuer la localisation précise des sources séismiques dans le milieu géologique à DPPC, de déterminer les mécanismes, et de faire l'analyse fréquentielle et spatio-temporelle des émissions, il nous faut encore des efforts de recherche et de surveillance sur ce chantier.

Sommaire - Les buts des essais microséismiques

1. La surveillance de la réalisation entière de la mine était un sujet d'inquiétude. Un réseau microséismique était consideré comme la solution de choix, car les redistributions des contraintes globales pourrait-être surveillées, et au cas de ruptures, l'interprétation serait plus facile en considerant l'activité séismique.

2. De plus, les données microséismiques pourraient, en principe, contribuer à la conception et à la réalisation de l'évolution de la mine, étant donné qu'une base de connaissance se développait.

3. Le réseau aurait pu donner de l'information préliminaire sur les concentrations des contraintes compressives dans le plafond de la mine, ce qui pourrait causer de grands évènements séismiques.

4. Moins important, mais intéressant quand-même, le développement de l'expertise avec les capteurs, le réseau, et les outils d'enregistrement dans un milieu minier était à considéré.

5. L'utilisation du réseau pour prédire des chutes de toit locales ou l'instabilité des piliers n'a pas été considérée dans la conception.

Sommaire - Les résultats des essais microséismiques

1. L'essai a fait l'épreuve de l'existence des évènements microséismiques, avec une fréquence temporelle d'un par jour, et toutes d'une magnitude faible.

2. La concentration des évènements se produisait dans le panneau 11, dans le chambre d'exploitation 11360, en train d'être développée par les méthodes de forage et tir. Il est supposé que ces évènements étaient liés avec les petites ruptures fragiles qui sont toujours prévues autour d'une chambre d'exploitation.

3. L'activité microséismique dans les régions déjà exploitées était minimale, ce qui nous mêne à supposer que les piliers ne sont pas en train d'attirer les concentrations excessives de contraintes.

4. La majorité des évènements séismiques se localisait très proche de la couche d'exploitation, soit dans le sel gemme, soit dans la potasse.

5. Nous n'avons pu trouver des corrélations entre l'activité microséismique et les choses suivantes :

   a) Les résultats des calculations numériques en trois dimensions de VELMINA, y compris le niveau des contraintes normales, en cisaillement, et les vitesses de fermeture dans le régime de fluage permanent ;

b) La magnitude de la subsidence à la surface ;

c) Les conditions géologiques, y inclus la location des plis structurels, et la distance entre la zone d'exploitation et les couches sédimentaires supérieures.

En sommaire, nous devons signaler qu'il n'y avait que 57 évènements microséismiques enregistrés. Peut-être que les difficultés techniques, surtout à cause de l'interférence électronique, étaient derrière ce manque de données, et peut-être que le faible nombre est lié à un essai trop court, et peut-être qu'enfin il y a très peu d'évènements. C'est regrettable que l'importance et la rentabilité des ces résultats microséismiques soient limitées par le manque d'une suffisance de données.

SECTION 2.0

2.0 INTRODUCTION

2.1 Background to Mine Development

The Denison-Potacan Potash Company mine site is located southwest of Sussex, New Brunswick. The location is shown in Figure 2.1. The Clover Hill deposit was first identified by surface exploratory drilling conducted in 1973 under the direction of the New Brunswick Department of Natural Resources.

In 1975, the Government of New Brunswick granted International Minerals and Chemical Corporation (Canada) Limited (IMC) exclusive rights to explore and develop the Clover Hill property.

IMC subsequently conducted a surface exploration drilling program which defined approximately 200 million tonnes of potash ore grading 28% K_2O. This made this one of the world's highest grade potash deposits.

In 1979, Denison Mines Limited purchased the Clover Hill property and, in 1980, formed a partnership with the Potash Company of Canada. An extensive underground exploration program led to a decision in 1983 to develop the property with a capacity of producing about 1.3 million tonnes of product per year. Potash production commenced in July 1985. Annual production projected for year 1990 is about 1.1 million tonnes.

2.2 Stratigraphy and General Description

The Clover Hill potash deposit is confined to the Marchbank Syncline, which is the most southern major structural feature of the Moncton Subbasin. It is shown in Figure 2.2. The potash deposit is part of the Cassidy Lake Evaporite Formation of the

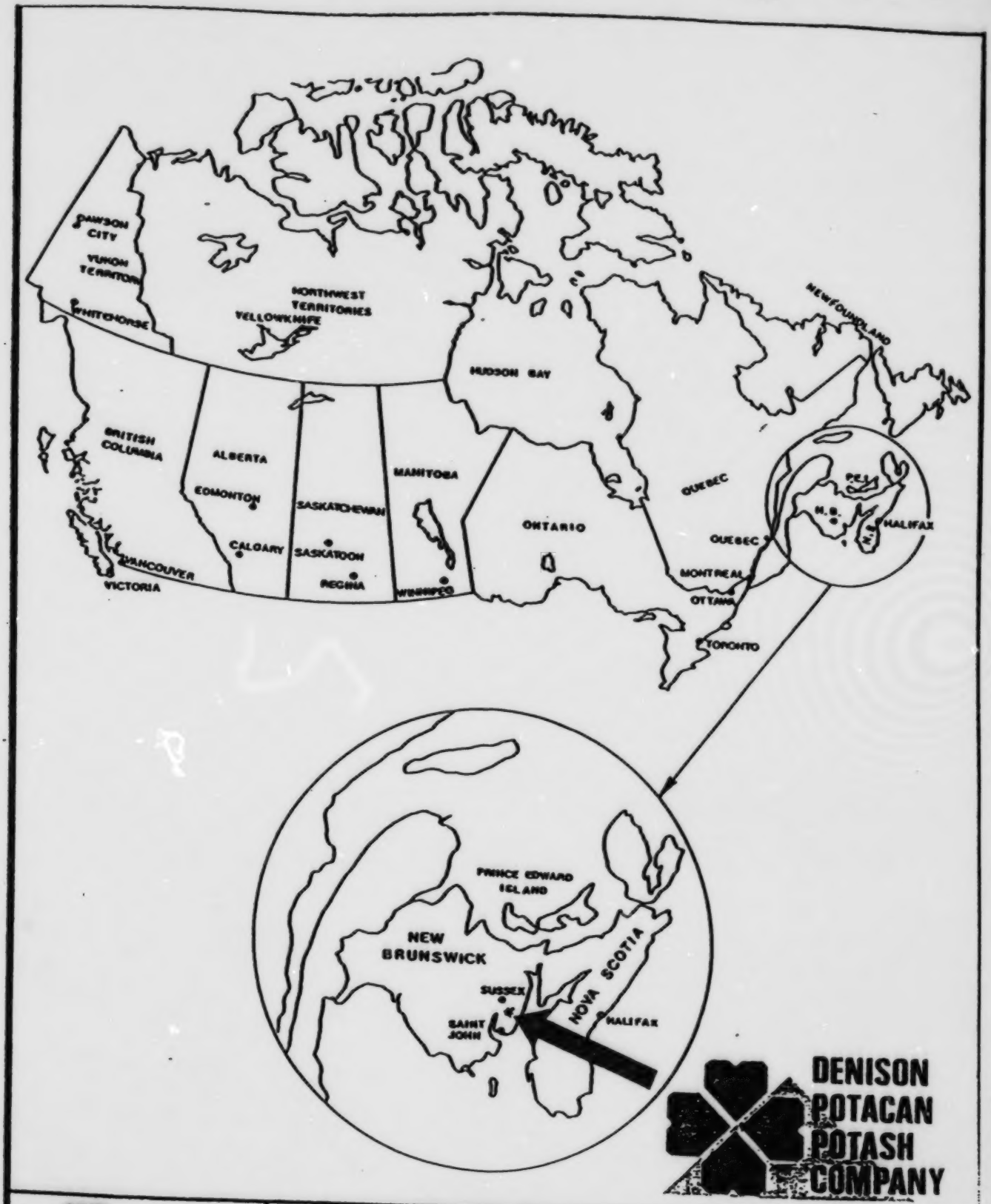

DENISON POTACAN POTASH COMPANY

DENISON POTACAN POTASH COMPANY	TITLE: LOCATION OF MINE SITE	SCALE: N.T.S.
		FIGURE: 2.1

DENISON POTACAN POTASH COMPANY

TITLE:
GEOLOGY OF THE MONCTON SUBBASIN IN NEW BRUNSWICK
(After Waugh and Urquhart, 1983)

SCALE:
N.T.S.

FIGURE:
2.2

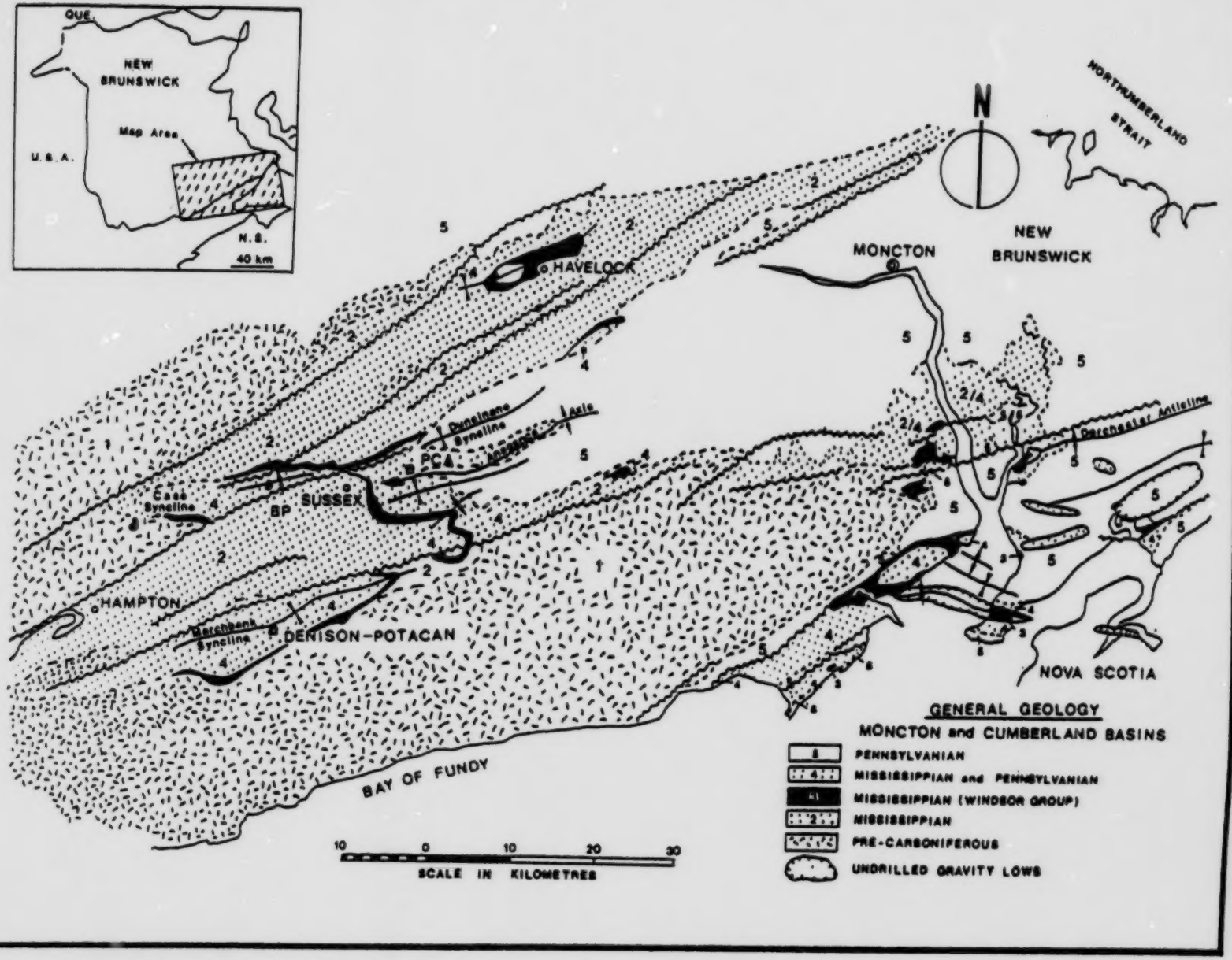

MARCHBANK SYNCLINE – STRATIGRAPHIC COLUMN

GROUP	FORMATION	MEMBER	BED		GENERAL LITHOLOGIES
HOPEWELL	Wanamaker	Fowler Brook			Grey red sandstone and siltstone numerous grey limestone nodules
		DeForest Lake			Grey red to grey brown conglomerate and sandstone
		Scoodic Brook			Grey red sandstone and siltstone
					unconformity
	Campbel Settlement				Pale red vuggy siltstone/sandstone
	Poodiac				Grey brown siltstone
					Grey to grey brown sandstone/siltstone
					Grey brown siltstone and sandstone
					Variable collapse breccia
WINDSOR	Plumweseep	Grey Clay			Green grey claystone
		Upper Salt			Not present in Marchbank Syncline
		Upper Anhydrite			Grey to bluish grey anhydrite
	Cassidy Lake	Upper Halite			Fine to medium grain orange to brown halite interbedded with numerous argillaceous and red sylvite beds and borate minerals
		Potash	Sylvinite Bed		Brick red very fine to fine grain sylvinite
			L.G.B.		Light orange halite with sylvite clusters
		Middle Halite			Light brown medium grain halite with irregular bands of dark brown to dark gray argillaceous halite
		Basal Halite			Very light grey to clear medium to coarse grain halite with irregular dark brown black argillaceous halite bands
	Upham	Upperton			Grey anhydrite
		Devine Corner			Light grey to buff limestone

DENISON POTACAN POTASH COMPANY

TITLE:

STRATIGRAPHIC COLUMN
MARCHBANK SYNCLINE
(After Waugh and Urquhart, 1983)

SCALE:
N.T.S.

FIGURE:
2.3

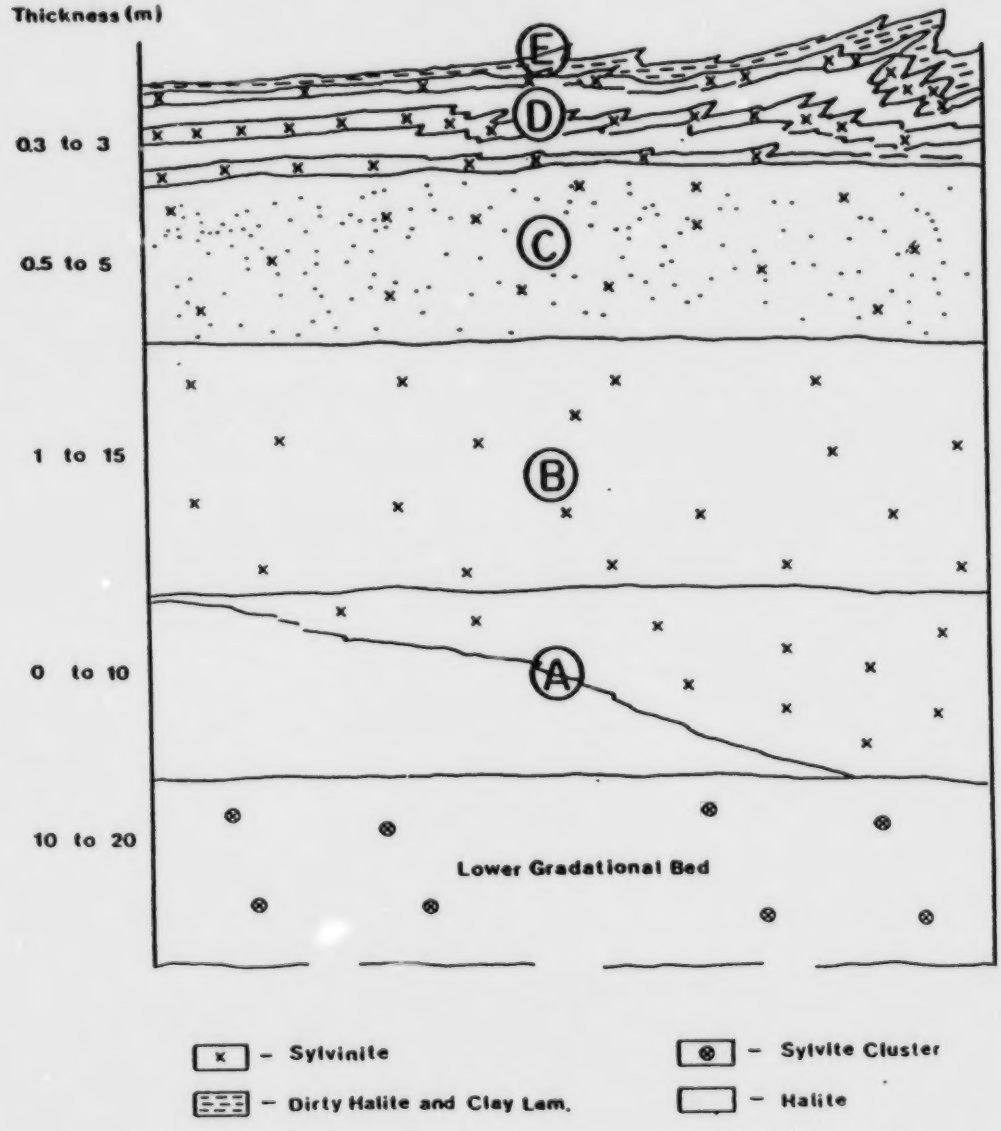

DENISON POTACAN POTASH COMPANY

TITLE:
SCHEMATIC OF CASSIDY LAKE FORMATION POTASH MEMBER
(After Waugh and Urquhart, 1983)

SCALE:
N.T.S.

FIGURE:
2.4

Windsor group as shown in the Marchbank Syncline stratigraphic column, Figure 2.3.

The evaporite interval has been subdivided into four members:

1. Basal Halite;
2. Middle Halite;
3. Potash;
4. Upper Halite.

The potash member consists of the Sylvinite Bed and Lower Gradational Bed.

The Sylvinite Bed is composed of fine-grained sylvite and halite. It is subdivided into five distinct zones based on mineralization, percent insolubles and colour. These have been designated from oldest to youngest as the A, B, C, D and E zones. The B and C zones comprise the main ore bed as shown in Figure 2.4.

The Lower Gradational Bed is composed of medium to fine-grained brown to orange halite with sylvite clusters being present.

The formations comprising the overburden overlying the potash and halite members of Cassidy Lake Formation consists of a sedimentary sequence including collapse breccia, siltstones, sandstones, conglomerate and limestone. Figure 2.3 shows details of the stratigraphic column including the lithology underlying the mining horizon at the Sylvinite Bed.

2.3 Description of Mine and Mining Methods

The Denison-Potacan Potash deposit is at a depth, on average, of approximately 880 metres below surface. It is approximately 10 kilometres in length along the strike and has a maximum plan width of about 3.5 kilometres.

A modified room and pillar method of mining with delayed backfill is used. It utilizes both cutting machines and drill and blast methods for hanging wall/footwall development and top slicing and benching in the stopes. Benching is done using cutting machines or drill and blast equipment depending on ore thickness. Stoping widths typically vary from 20 m to 30 m and stope heights range from about 5 m to 30 m with average height of 10-15 m. Pillars breadths vary from 20 m to 50 m depending on stoping height. The final stope backs are normally developed in Upper Halite and obvious visible weakness features such as clay laminae or seams and sylvite and anhydrite stringers are removed, if possible. The final stope backs are supported with full length resin-grouted rebars. Slurried tailing fill using the halite waste fraction of the ore and a saturated brine for hydraulic transport is placed in stopes after mining. It is placed for a long term ground stabilization and for tailing disposal.

Panel entries for both access and conveyor ways are mined using a stress relief layout method. As well, stoping in thinner areas with cutting machines uses a stress relief method involving sequence of extraction and a yielding pillar design.

Conveyor belt systems are used to transport ore from the mining areas to underground storage bins and then to loading pocket and

production shaft through which it is hoisted in 25 tonne skips to surface.

The ore on surface is conveyed to a mill on site where sylvite is removed as product and the waste, principally halite, is returned to underground as backfill.

A mine plan showing existing mining panels 10, 11, 12, 13 and 14 with a typical section through Panel 11 is shown as Figures 2.9 plan and 2.10 section.

2.4 Summary - Rock Mechanics Studies

2.4.1 Material and Mechanical Properties - Summary

Laboratory testing of core samples from the mining horizon and from the overburden rocks overlying the evaporite interval was conducted prior to mining. The program was largely carried out at the materials testing facility at the University of Waterloo, Ontario. The results have been used for input for numerical modelling simulations, development of a number of parameters (constants) in creep models and were fitted to brittle yield and time dependent failure criteria.

Sylvinite Bed, Upper Halite and Lower Gradational Bed

The types of tests conducted on the evaporites included:

1. Triaxial creep tests at constant strain rates;
2. Uniaxial tests;
3. Triaxial brittle yield tests at constant strain rates;
4. Brazilian tests for indirect determination of uniaxial strength.

Table 2.1 contains a summary of the mechanical properties.

The evaporites exhibit typical plastic behaviour of salt rocks. The plastic deformation or creep action is the reaction to loading providing the differences in the principal applied stress and confining stresses are sufficient.

The testing showed brittle yield indicative of elastic behaviour occurred when the differences in the principal stresses (shearing stress) was less than the limit of elasticity (creep limit, yield limit). Brittle rupture type behaviour also was confirmed when the strain rate, due to the combination of applied stresses, was excessive. In-situ brittle fracture, of the evaporites, is evident particularly on the periphery of the pillars and locally but to a lesser extent in the immediate backs of the openings. This is a concern for local ground control but it does not dominate the in-situ evaporite behaviour.

Overburden Material

Four types of testing were performed:

1. Sonic velocity measurements used for determination of the dynamic elastic constant;
2. Brazilian tests for uniaxial tensile strength;
3. Unconfined (uniaxial) compressive strength tests;
4. Triaxial compressive strength tests.

Table 2.1

Summary Mechancial Properties - Ore Zone and Upper Halite

Property	Units	Sylvinite Bed	Upper Halite Bed	Lower Gradational Bed
Density	kg/m^3	2,050	2,150	2,100
Young's Modulus	GPa	5.45	10.21	6.92
Poisson's Ratio	-	0.33	0.33	0.33
Unconfined Compressive Strength	MPa	26	29	28
Tensile Strength	MPa	1.7	2.0	1.5

Table 2.2 contains a summary of mechanical properties values of the overburden rocks that were tested.

The results of the strength tests for the overburden material were plotted as Mohr-Coloumb diagrams and are shown in Figures 2.5 to 2.7. As well, they were fitted to a parabolic failure criterion after Dusseault et al, 1987. They show substantial shear strengths are possible with increasing confinement.

Some fracturing is present in the overburden rocks except in the siltstone caprock breccia. The fracturing would be expected to reduce the rock mass strengths including the stiffness.

Backfill

Laboratory testing of granular halite backfill was also conducted. The test program was reported in some detail in the report of Phase II project to CANMET from the mine in 1989. The test program included:

a) material characterization;

b) compaction creep tests;

c) brittle strength tests.

2.4.2 In-Situ Monitoring and Testing

A considerable amount of in-situ monitoring and testing of the behaviour of entries, stopes and pillars has been carried out since early stages of mine development and it is continuing.

Rock mechanics instrumentation for measurement of closure, strain, rock stress and local movements are used. As part of the initial rock mechanics program, monitoring stations were established in a test room. It was excavated in a remote location that had probable minimum influence from adjacent mining activity.

Table 2.2

Summary Material and Mechanical Properties - Overburden Rocks

Property	Units	Poodiac Sandstone	Poodiac Siltstone	Fractured Poodiac Sandstone	Siltstone Caprock Breccia
Density	kg/m^3	2,500	2,550	2,500	2,530
Dynamic Elastic Modulus	GPa	41	47	34	17
Static Elastic Modulus (Young's)	GPa	10	24	14	0.43
Poisson's Ratio	-	0.11	0.16	0.16	0.33
Unconfined Compressive Strength	MPa	84	134	82	5
Tensile Strength	MPa	6.7	13	8.4	0.8
Cohesion	MPa	15	31	27	4.7
Angle of Internal Friction	degrees	53.5	43	24.5	32.5

FIGURE 2.5

Mohr-Coulomb diagram for Poodiac Sandstone

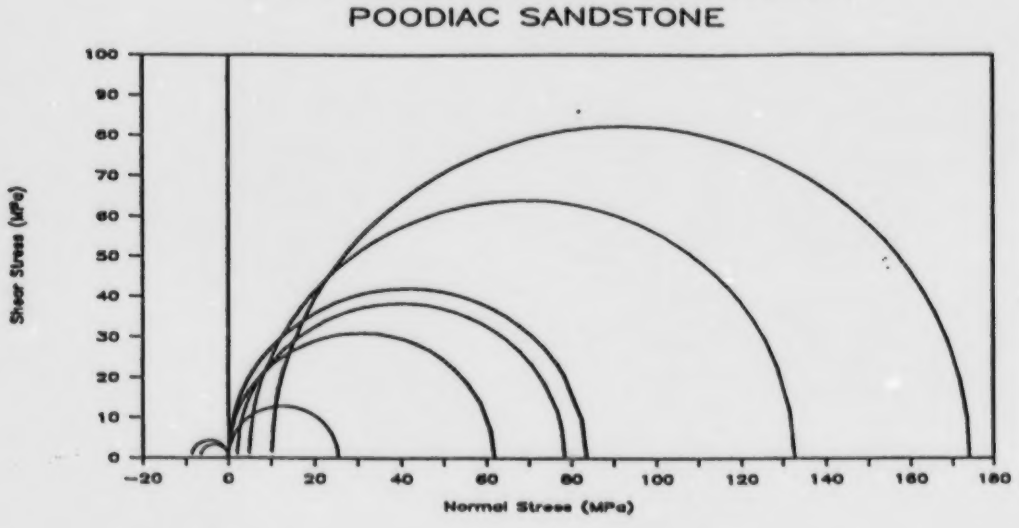

FIGURE 2.6

Mohr-Coulomb diagram for Poodiac Siltstone

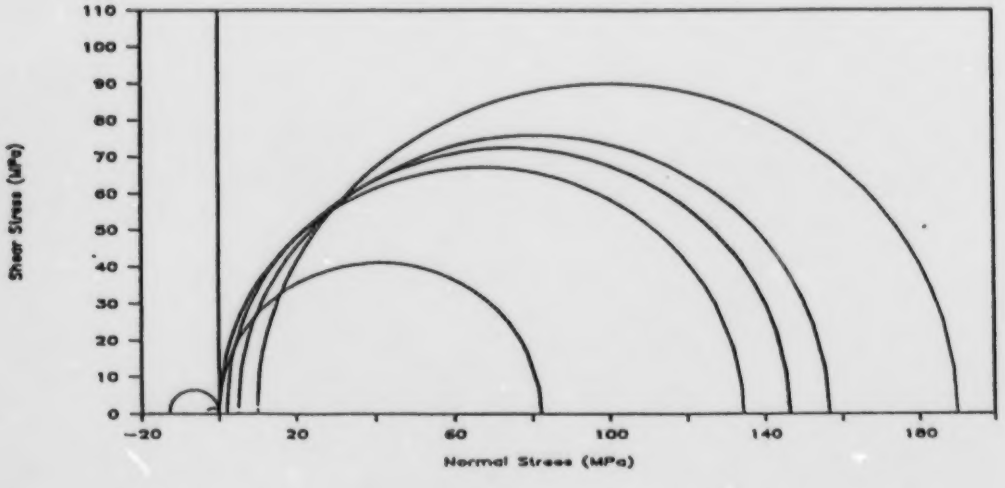

FIGURE 2.7

Mohr-Coulomb diagram for fractured Poodiac Sandstone

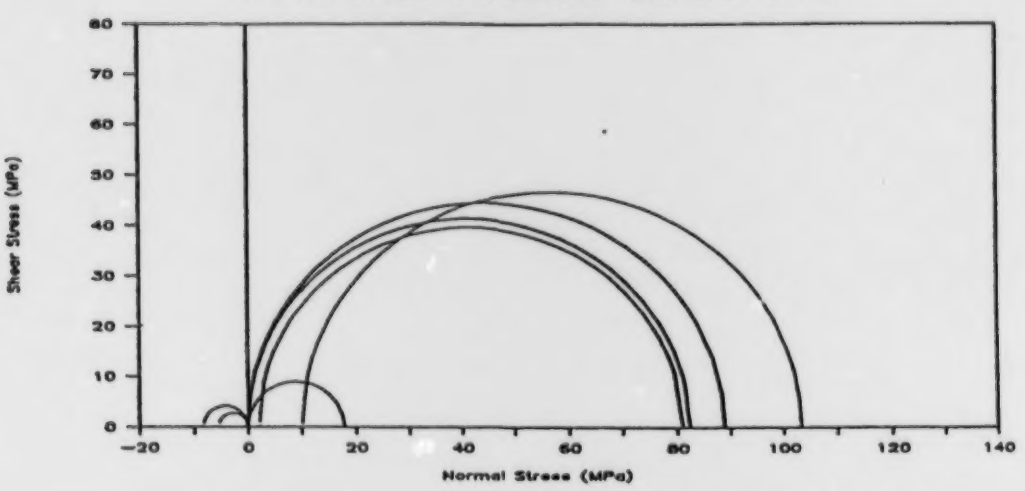

FIGURE 2.8

Mohr-Coulomb diagram for Siltstone Caprock Breccia

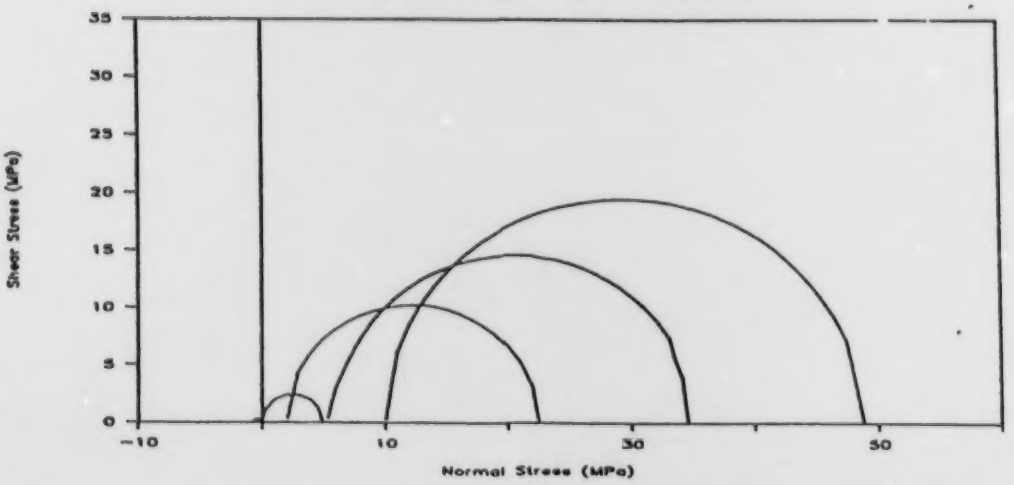

Table 2.2 contains a summary of mechanical properties values of the overburden rocks that were tested.

The results of the strength tests for the overburden material were plotted as Mohr-Coloumb diagrams and are shown in Figures 2.5 to 2.7. As well, they were fitted to a parabolic failure criterion after Dusseault et al, 1987. They show substantial shear strengths are possible with increasing confinement.

Some fracturing is present in the overburden rocks except in the siltstone caprock breccia. The fracturing would be expected to reduce the rock mass strengths including the stiffness.

Backfill

Laboratory testing of granular halite backfill was also conducted. The test program was reported in some detail in the report of Phase II project to CANMET from the mine in 1989. The test program included:

a) material characterization;

b) compaction creep tests;

c) brittle strength tests.

2.4.2 In-Situ Monitoring and Testing

A considerable amount of in-situ monitoring and testing of the behaviour of entries, stopes and pillars has been carried out since early stages of mine development and it is continuing.

Rock mechanics instrumentation for measurement of closure, strain, rock stress and local movements are used. As part of the initial rock mechanics program, monitoring stations were established in a test room. It was excavated in a remote location that had probable minimum influence from adjacent mining activity.

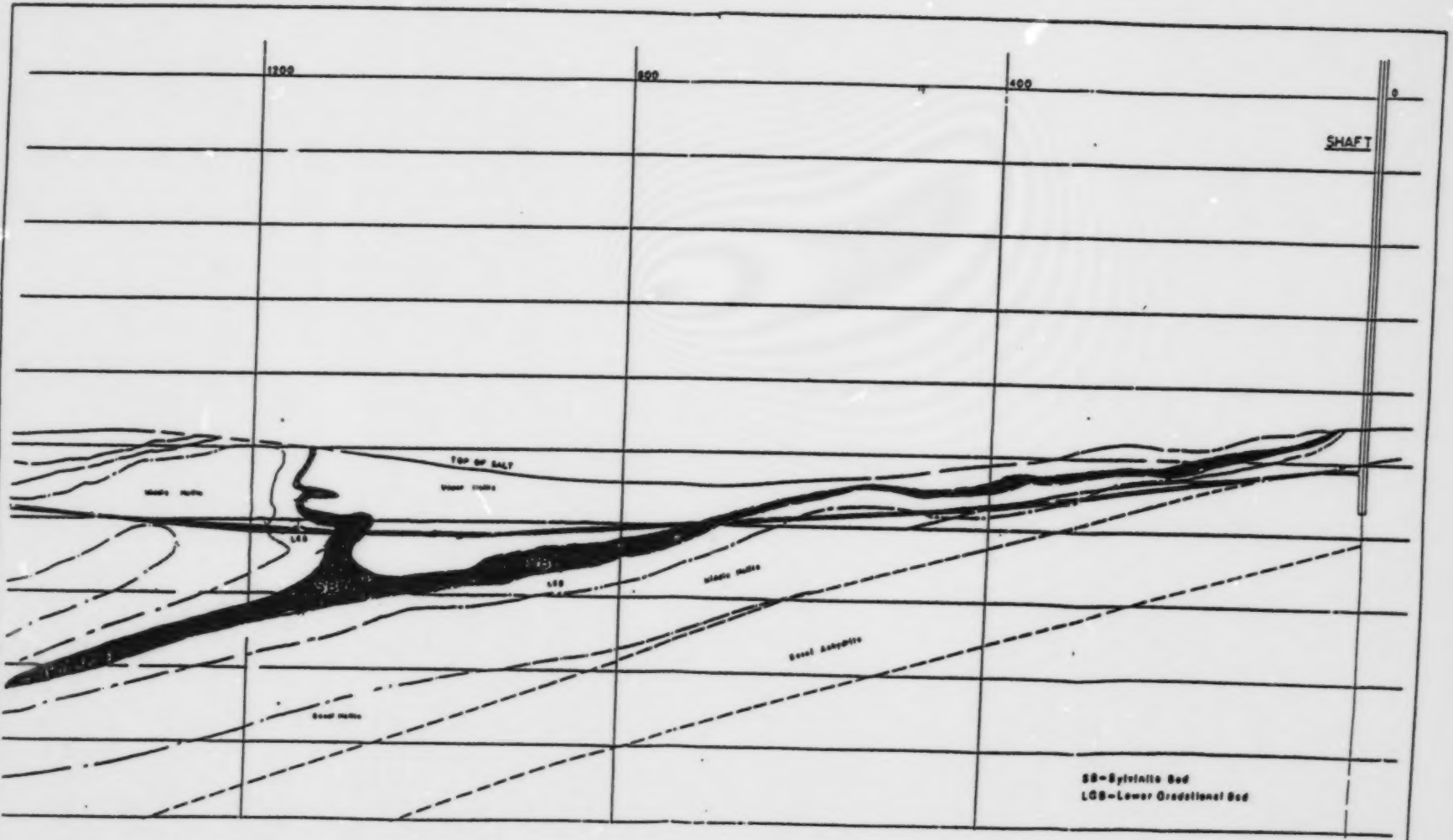

DENISON POTACAN POTASH COMPANY

TITLE:
PANEL 11
TYPICAL GEOLOGICAL CROSS-SECTION

SCALE: N T S

FIGURE: 2.10

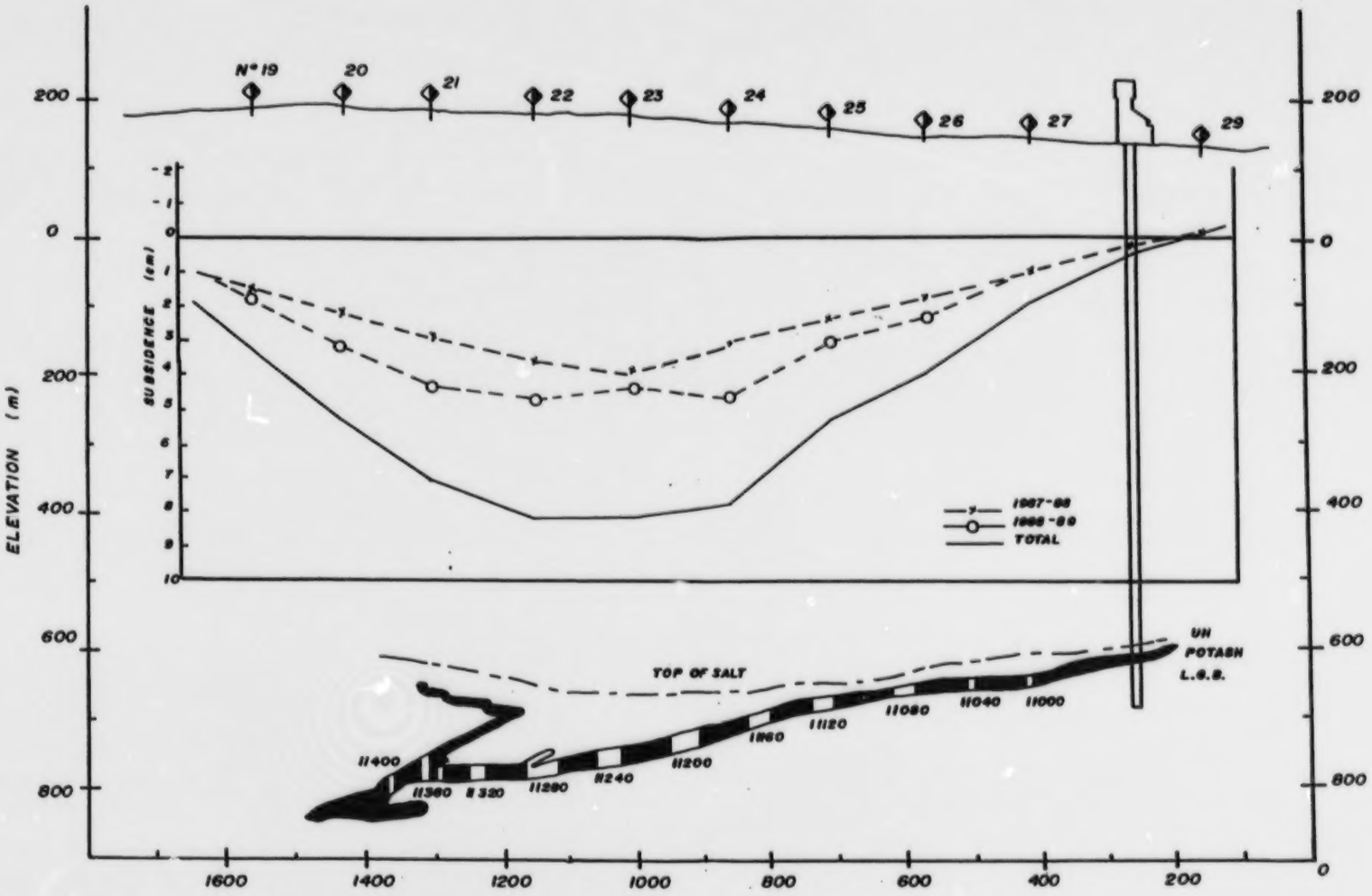

								SCALE 1:8000		DATE	DENISON - POTACAN POTASH COMPANY SUSSEX, N.B.
								DESIGNED			
								DRAWN	J. POULIN	AUG. 10, '90	
								CHECKED			
DWG NO.	REFERENCE DRAWINGS	NO.	DESCRIPTION OF REVISION	DATE	BY	CHK.	APP.	APPROVED			

TITLE: NORTH SOUTH SEC. II PANEL

DWG. NO. FIG. NO. 2.12

REV.

7 87 DPPC-ENG-058

A test stope was also selected for monitoring and rock mechanic evaluation. The cross sectional dimensions of the test site opening were 4.8 m wide by 4.8 m high and 42 m wide by 4 m high, respectively. Types of instrumentation used included: closure meters for measurement of absolute component of vertical and horizontal convergence, multi-anchor extensometers installed in backs and pillar walls for measurement of relative movements at different depths and oriented hydraulic pressure cells installed for measurement of magnitude of stress and changes in magnitude of stress with time.

The data obtained from these early measurements was used, in conjunction with results of laboratory testing of intact samples, for establishing a number of important parameters for development of a site specific behaviourial model for the evaporites. In summary, it was used for: determination of parameters to fit a creep model and a shear failure criterion, and as well for input data and for verification and calibration values for numerical analysis simulations. It was also intended as a database for the purpose of prediction and assessment of behaviour of mine openings.

The details of that work are summarized in some detail in reports of Phase I and Phase II CANMET projects conducted at the Denison-Potacan Mine and submitted in 1985 and 1989, respectively.

In addition to the test room and test stope measurement stations, fairly extensive monitoring of "stress - relief" multiple entries, single entries and various stope and pillar sizes has been done. The main thrust of this work has been to provide data on

closure and stress magnitudes for comparison with numerical analysis results, assessment of ground support systems and in stability evaluations.

Monitoring of overburden subsidence induced by the mining has been carried out since 1985. This corresponds to the pre-start of stoping. It involved installation of a grid of subsidence monuments on surface. The grid includes two lines of monuments over each mining panel. The grid has been expanded ahead of mining so that, if possible, the initial survey is at undisturbed surface. The survey is carried out yearly. The results are shown in Figures 2.9 and 2.11, plans, and 2.12, a graph of subsidence rates. They show that subsidence of the overburden strata is not apparently delayed after mining and that it appears to be occurring in an orderly fashion from the size and shape of the subsidence bowl. (Mraz et al, 1989)

Ground Control Monitoring

The monitoring of ground movements for assessment of the stability of local conditions is done largely on the basis of operations needs. The types of instruments and methods that are used include: visual check of shallow (2.5 m - 3.7 m length) observation holes drilled into the back, observation of reaction of ground support loading, closure meters and electrical read-out type ground movement monitors (GMM's) installed on mechanically anchored rockbolts.

2.4.3 Numerical Analysis

Numerical simulations have been used as an important design tool at the mine since start of stoping. Input parameters for the mechanical properties and time dependent parameters were obtained from laboratory testing of intact rock cores and in-situ monitoring of the ground behaviour.

A shear stress criterion by Von Mises was adopted. This criterion is based on distortion energy theory and involves determination of an effective stress level. The Von Mises effective stress concept is further elaborated by Farmer (1985) and by Jaegar and Cook (1979).

The reasons for adoption of this criterion and more details are described in some detail in Phase II report.

A constitutive law governing the time-dependent behaviour of the evaporites was developed for the mine. It was developed through a joint effort of Mraz Project Consultants Ltd. and the University of Waterloo as part of Phases I and II work. It was based on the rheological and stress-strain properties of the halites and sylvite found by laboratory testing of cores and in-situ monitoring in test room and test stope. It was incorporated into the numerical analysis code, Flac, developed by ITASCA Consulting Group Inc. from Minneapolis, Minnesota. ITASCA rewrote the source code to include the specific creep model for the mine.

As well, a creep law for halite backfill used at the mine was developed and incorporated by the same groups. The two laws have been referred to as the Mraz Creep Laws. This computer code has been used in most of the numerical simulations for stability analysis at the mine.

Numerical modelling programs used have been:

1. FLAC Code (ITASCA)
2. VELMINA Code (L. Rothenburg)

FLAC is a general geomechanics numerical model which uses the explicit finite difference method to solve the basic equations of motion. It is a two-dimensional model and it includes the ability to simulate large-strain plastic behaviour and time-dependent creep action.

This geometry constraint and material behaviour can be suitably applied for most situations to the Denison-Potacan Mine. As indicated above, the source code was modified to include the constitutive equations that represent the evaporites and the halite backfill behaviour.

The program has been used quite extensively to model: alternative dimensions of room and pillar layouts, multiple openings (3, 4, and 5) stress-relief panel entries and as well effect of backfill in rooms for overburden support and secondary mining has been simulated.

The results of modelling with FLAC appear to reasonably represent the actual observed and measured rock response. Most of the modelling with FLAC has been carried out by external consultants. In-house capability now exists to conduct this work.

The VELMINA code was used for three dimensional modelling. This program is reported to be a mathematical implementation of the Displacement Discontinuity method commonly used for stability analysis of geomechanics problems which exhibit visco-elastic material. Some details of this program and the modelling work done with it are described in Phase II report. It used linearly visco-elastic host rock properties outside of the mining seam and the in-seam pillars were modelled with non-linear elasto-visco-plastic properties. The behavioral laws and input parameters used were the same as those used in FLAC.

The three-dimensional modelling was very useful as it involved simulation of several mining panels on plan section taking into account variable mining heights. Simulation of the effects of interaction between stopes and blocks of stopes were predicted. As well, effect of hydraulic backfill on reduction of overburden subsidence and in pillar confinement for possible secondary mining of pillars at a later date was simulated. The model output included: normal and shearing stress magnitudes, convergence and convergence rates.

The results obtained with VELMINA were compared with measured in-situ convergence rates and output from the finite element code VISCOT. A good agreement was reported. This modelling work was conducted externally.

2.5 Phase III Work - Background

The results of the earlier work in Phases I and II CANMET sponsored projects related to the use of delayed backfill for planned selective pillar recovery. The project titles were "Use of Backfill In New Brunswick Potash Mines". The conclusions of the studies showed that pillar mining should be possible within 10 to 15 years after fill placement based on predicted backfill compaction rates. They also showed that convergence rates during "secondary" mining would be similar to that measured in Panel 11 at primary mining stage. These indicate that hanging wall loads induced by mining would be transferred through the fill. The study also showed both predicted and actual measured subsidence rates at the time were comparable and that extensive bridging of the overburden strata was unlikely to be occurring. As well, this previous work addressed: fill placement density requirements, alluvial sand addition for possible improved early strength, effect of low fractional density (less than 0.7) on unconfined compressive strength and a fit of the fill brittle strength data to a Mohr-Coulomb shear failure criterion.

As a follow-up to the work done in Phases I and II, it was decided that a study should be conducted to assess the hanging wall response to mining. This was based on some concern that the overburden rocks may be capable of storing sufficient strain energy

that may result in release of large magnitude seismic energy in the case of a sudden brittle failure. This was despite their generally fractured nature and early indications that bridging of the overlying strata was not occurring and so that a sudden rupture with release of seismic energy was unlikely. The main purpose of this follow-up study was to assess the response of the hanging wall to mining by microseismic monitoring. As well there was an interest in determining if significant microseismic activity was occurring in the pillars and immediate host rock.

In April 1988 as a result of discussions with CANMET, a proposal was submitted to the Minister of Supply and Services by Denison-Potacan Potash Company and a contract was awarded. The title off the research project was "Hanging Wall Response to Mining of Denison-Potacan - Phase III". It was a cost shared project and total estimated costs were $150,500 subject to the Basis of Payment clause in the Contract.

The Statement of Work, from the Contract, Appendix A, provided the research objectives. It was:

> Verify and refine the results of the Phase I study on use of backfill in New Brunswick Potash Mines by monitoring hanging wall deformation and seismic events occurring in response to mining to determine optimum mining sequence and backfill placement to achieve second stage mining in the pillars at Denison-Potacan in a safe and economic way.
>
> (a) Install and operate a microseismic monitoring system and carry out complimentary deformation measurements as required.
>
> (b) Determine roof, wall and floor convergence and stresses in a backfilled room in comparison to an empty mining room suitable to verify numerical modelling results from the programs GEOROC and VISCOT.

(c) Prepare and conduct a technology transfer seminar in Fredericton, New Brunswick on work performed at Denison-Potacan under Phase I, II, and III.

The microseismic monitoring trial that was carried out to meet the first objective was contracted to a sub-contractor. The Company retained Prugger Geophysical Services from Saskatoon, Saskatchewan, Canada to carry out the work. This comprised the bulk of Phase III research.

The second objective involved verification of two numerical analysis codes with in-situ measurements of convergence and stress magnitude in a backfilled room compared to an empty room. The codes checked were GEOROC and VISCOT. The Company retained Mraz Project Consultants Ltd. from Saskatoon to conduct this study. Details of that study are reported in attached Appendix B.

The following report is a Final Report of the work performed under DSS Contract Serial No. 23440-8-9041/01-SQ.

SECTION 3.0

3.0 MICROSEISMIC MONITORING TRIAL

3.1 Introduction

Microseismic activity induced by mining has been detected at most mines where either local microseismic or regional systems installed on surface have been used. The origin of seismic activity, in geological material, is thought to be related to the processes of deformation and failure which are accompanied by a sudden release of strain energy. These processes involve yielding and fracturing. In the case of salt or potash, there are studies that suggest acoustic emissions occur at the immediate pre-yield and post-yield stress regime regions (Hardy et al). The yield strength for salt or potash may be defined as the differential stress magnitude at which plastic behaviour is initiated. It would also be expected that seismic activity would be associated with sudden shear or tensile type brittle fracture.

In the case of potash mines, a major concern exists regarding the potential for seismic activity being generated in the overlying strata. This has been experienced in some Saskatchewan potash mines as well as in Germany, for example. This is because overlying strata in these examples, particularly in case of Saskatchewan, has a high stiffness modulus, and responds elastically to loading. It also possesses high mechanical strengths. It would hence be expected to be capable of storing substantial strain energy. A failure of this material when over stressed would likely result in a component of the strain energy being released as seismic energy. The concept of energy balance (Cook, 1967) and (Salamon, 1974, 1984) provides an explanation of

seismic energy in relation to released energy and stored strain energy for elastic conditions. It can be expressed as:

$$Er = Em + Es \qquad E_2\ 3.1$$

where
Er = released energy
Em = stored strain energy
Es = seismic (Kinetic) energy

It is the seismic energy which is recorded by mine microseismic systems.

In contrast, salt and potash deforms by massive plastic deformation (creep action) when subjected to a differential stress in excess of its yield strength or creep limit. Stresses are imposed on the overburden strata as a consequence of closure of the mine openings which is primarily by creep action, as well as bed separation and fracturing of the salt and potash. Subsidence of the overlying strata normally occurs in response to this closure. The rate of subsidence may vary from the rate of mine opening convergence depending upon whether "bridging" of the overburden occurs. It is thought that "bridging" of the overburden strata over the openings results in the delay between excavation closure and subsidence of the surface. This apparently is the major source of seismic energy in the case of potash mines when brittle failure of it occurs.

The overburden strata above the evaporites at the Denison-Potacan Mine consists mainly of consolidated clastic sediments

ranging from siltstones to conglomerates which are classified based on grain size. Some fracturing occurs within the sequence. The potential for hang-up and delay in subsidence with mine opening closure is not considered to be great because of the fracturing.

In contrast, at a potash mine in Saskatchewan studied for seismicity, the immediate overburden consisted of a thick (425 m) sequence of relatively competent carbonate rock (D. Gendzwill et al, 1981). The seismic events recorded were attributed to brittle failure or sudden rupture (presumably normal faulting) of this rock associated with subsidence of the mine overburden. A number of the recorded events were reported to be of earthquake magnitude.

Other factors such as depth of mining, extraction rate, aerial extraction ratio and sequencing of stoping were not compared between the two mining districts. These would be anticipated to influence rate of subsidence.

A microseismic monitoring system was installed at the Denison-Potacan Potash Mine during the period January to April 1989. It was installed on a temporary basis to determine the frequency and location of microseismic events, if they were occurring. There had been no previous indication that the mine was active. The trial was terminated in part due to system hardware problems after a 3-month period.

The results of this short trial indicated that during this period induced microseismic activity was occurring and that it appeared to be concentrated near active mining faces. There was no indication that large magnitude of energy was associated with these events based on lack of visible damage or audible noise. More

research, including in-situ monitoring, is required in this geological setting to confirm source locations and failure mechanism of seismic activity.

The details of the monitoring trial and results are in Appendix A. It was prepared by A. Prugger, Consultant. This Section is a summary of that work.

3.2 PURPOSES OF THE MONITORING TRIAL

There was some concern for seismicity associated with subsidence of the hanging wall. It was considered to be of low potential because of the general apparent fractured nature of the overburden rocks. However, it was subsequently decided that monitoring should be conducted to determine if seismic activity was being generated by hanging wall movements. As a secondary reason, it was also decided that a monitoring system should be investigated for the purpose of determining location of failure areas and possible changes in location of failure areas as mining progressed. The second purpose as a mine wide monitoring tool may be of greater significance. Following is a summary of the main purposes of the trial:

1. It would have potential for providing, at least, preliminary information on whether seismicity of significant magnitude of energy was associated with failure of the hanging wall in this geological setting.

2. There was some concern about the eventual need for mine-wide monitoring of the response of the pillars and hanging wall to mining. Microseismic monitoring would indicate locations of brittle type failures associated with seismic energy release. Excessive stress conditions could be inferred from this seismic activity. A change in locations of seismicity could be used to possibly evaluate a pattern of failures related to the mine design.

3. As a corollary, the data from microseismic monitoring has valuable potential for use in mine design and sequencing after a dependable database has been established.

4. To a lesser degree of importance, it would provide an opportunity to evaluate monitoring hardware and software for use in this mines environment.

5. There was no plan to use the system as a tool for prediction of local roof falls or local pillar spalling.

3.3 SUMMARY - DETAILS OF MONITORING TRIAL

3.3.1 Location and Equipment

An array of 11 geophones was installed around panel 11. Figures 2.9 and 2.11, plans, shows locations of the geophones. Figure 2.10 provides geological section through panel 11. The geophones were velocity gauge type and unidirectional (single axis). They were mounted vertically on the surface of salt or sylvinite backs in panel entry drifts. The sensors used were manufactured by Mark Products and had flat frequency response of 4.5 to 250 Hz. The spacing of the geophones ranged from 200 m to 400 m. Figure 2.10 plan shows location of geophones and mining at time of the trial. The geophone array network was connected to centrally located data acquisition and processing unit via two-pair twisted unshielded telephone cables. The processing unit consisted of: differential amplifiers, filters, A-D convertor, storage buffer. It also consisted of software for: event recognition, source location determination and signal processing. The processing system and software were supplied by Microseis from Saskatoon, Saskatchewan.

The processing unit and software performed satisfactorily.

3.3.2 Event Recognition and Source Location Techniques

1. The recognition of seismic events was done using software employing a real-time STA/LTA algorithm. This method has been reportedly used for detection of seismic signals in potash mines elsewhere with good success.

   It is designed to trigger on signals with a fairly sudden on-set such as seismic events but to reject signals induced by heavy mine equipment, for example.

   It was also possible to discriminate between vibrations induced by blasting and microseismic events. This was done by analysis of frequency spectra. A central blasting method is also used at the mine so that blast times are known accurately and isolation of blasting caused "events" was easier.

   As well, the system was programmed to trigger as an event only if 4 or 5 transducers were hit within a selected time frame and the vibration was within a selected frequency band.

2. The event source determination technique used an earthquake location method. It utilized the Simplex stepping procedure in the software algorithm. This method is described in some detail in a paper by Prugger and Gendzwill (1988).

   The method involved a computer software (automated) selection of the co-ordinates (x, y, z) of the source of the event. This is done by evaluating the minimum difference in observed and calculated arrival times of the signal at each phone to get a "best fit" location solution. The best solution is that in which the statistical difference between the two arrival times is minimum for the geophones affected in the array.

   In this trial, accurate source location was impaired to some degree by two factors:

   1. Difficulty in picking arrival times of signals at some of the geophones. This was because of very significant electrical interference caused by high voltages cables in proximity of the telephone cables. This resulted in 60 Hz "noise" on geophone signal cables. Software filters were applied with some success in attempt to overcome this. This probably resulted in a number of actual microseismic event being missed due to the interference.

2. The vertical location of events was poorly constrained because most of the geophones were at approximately the same elevation.

   Source location accuracy for the trial was estimated to be 50 - 200 m vertically.

   Source location verification was done with a blast at a selected location. The horizontal distance error from the computer solution was 5 m and vertical error was 9 m and the calculated velocity of 4725 m/sec was consistent with salt P-wave propagation velocity. The calibration was considered reliable.

In case of a future installation, the following deficiencies in the trial system would be addressed: (1) The system should be resistive against induced electrical current by use of proper shielding and grounding measures; (2) A constant voltage source should be used; (3) An expanded array of geophones should be installed including an attempt to account for elevation so that the system be more sensitive to small energy events, and better reliability for vertical source determination be achieved, respectively.

3.4 SUMMARY - MAIN RESULTS OF TRIAL

1. The trial showed that microseismic events occurred during the test period. The average frequency of events recorded was about 1 per day. All events appeared to be of low magnitude energy.

2. The events recorded showed a concentration of activity at the north end of Panel 11 in the active 11360 stope mined by drill and blast method. It is likely that the events were associated with brittle failure which would be expected near the periphery of the opening.

3. There was little activity in the older mined out areas. It may be inferred that in these areas there was no pillar "over-stressing" at time of the survey to the extent that seismic energy was released with sudden fracturing.

4. It was determined that most events occurred very close to the mining horizon in the potash or salt.

5. There was no significant correlation found between the seismic activity recorded and the following:

   (a) Output from VELMINA three-dimensional simulation that included: steady state shear and normal stresses and steady state convergence rate;
   (b) Total surface subsidence;
   (c) Geological features - major fold and interval between top of mining horizon and overlying clastic sediments.

In summary, it should be noted that there were only fifty-seven (57) microseismic events recorded. This may be due in part to events being missed because of hardware problems mainly associated with induced electrical "noise" interference. It is also due to the short term trial. This small number of events would hence reduce somewhat the significance of some of the results.

APPENDIX A

RESULTS OF MICROSEISMIC MONITORING AT THE DENISON-POTACAN POTASH MINE AT CLOVER HILL, NEW BRUNSWICK IN THE PERIOD JANUARY 24, 1989 THROUGH APRIL 7, 1989

FINAL REPORT (DRAFT COPY)

June, 1990.

Arnfinn F. Prugger, M. Sc.
Geophysicist
Prugger Geophysical Services
1040 Aird Street
Saskatoon, Saskatchewan (S7N-0T1)
CANADA.
(Tel. 306-652-7511 or 306-933-8682)

Contents :

1. MICROSEISMIC MONITORING IN A MINE : WHAT IS IT AND HOW IS IT USEFUL ? 3

2. BACKGROUND TO SEISMICITY IN POTASH MINES 6

2.1 Large-Scale Seismicity (Noticeable Earthquakes) 6

2.2 Microseismicity in Potash Mines 9

3. SEISMIC MONITORING METHODOLOGY 14

3.1 Event Recognition 15

3.2 Picking Arrival Times 16

3.3 Source Location 18

4. MICROSEISMICITY AT THE CLOVER HILL MINE, 1989 22

4.1 Blast Records 22

4.2 Microseismic Events 24

4.3 Discussion 27

5. REFERENCES 30

6. FIGURE HEADINGS 31

Figures ..... 32 - 46

RECURSIVE OR FEEDBACK DIGITAL FILTERS ..... 47 - 73

DISCUSSION OF ELECTRICAL INTERFERENCE PROBLEMS ENCOUNTERED DURING SEISMIC MONITORING, JANUARY - APRIL 1989, AT THE CLOVER HILL MINE, NEW BRUNSWICK ..... 74 - 78

SUMMARY OF SEISMIC EVENT LOCATIONS, CLOVER HILL POTASH MINE, NEW BRUNSWICK ..... 79 - 90

REFERENCE PAPERS

1. MICROSEISMIC MONITORING IN A MINE : WHAT IS IT AND HOW IS IT USEFUL ?

The purpose of studying mine-induced seismicity is to accurately quantify how the "hostrock" reacts geomechanically to the cutting of rooms during mining. From the mine operator's point of view an understanding of these processes is useful in predicting and comprehending hazards, and in evaluating the overall "performance" of a mine design, (ie.- how successfully rock stress and stress concentrations have been managed). Monitoring seismicity on a continuous basis in a mine gives observational information of rock-failure in the vicinity of the mine. When rock breaks in a brittle manner seismic waves, or vibrations, are emitted into the surrounding rock. Thus when a mine seismologist observes a microseismic event he is seeing a direct effect of rock breaking : a seismic wiggle-trace is an information-preserving "mapping" of rock fracture (which might have occurred some distance from the sensor - from a few tens of metres to many kilometres).

At present, analysis of seismic signals tells the mine operator WHEN and WHERE rock is breaking in the vicinity of the mine, and gives an estimate of the size of the failure zone. This information can be used, along with other rock mechanics observations :

1. As a safety tool in reaction to a large rock-failure event : the mine operator will know where to go to inspect for damage, or for rescue purposes, and will have a measure of the size, or energy release, of the event.
2. To quantitatively evaluate the day to day performance of a mine design and to interpret ground stability in the mine. In this context seismic

monitoring can be used as a forward planning and mine design tool to give the immediate observed response of the rock to any changes in the mining pattern, or to any unusual geological or tectonic situation that the operator might be cutting in to. The long term goal would be to use the observed pattern of seismicity to spot areas of umusually high rock failure, and eventually gain enough understanding of these observations to predict roof-falls and other hazards.

3. As a means of evaluating the rock mechanics model of the mine ; if rock is observed to be breaking in areas where a finite element model fails to predict high shear stresses then the model is demonstrably incorrect.

The information provided by seismic monitoring gives observational confirmation of the success or failure of the management of rock stress and stress concentrations in the mine.

Monitoring seismicity is an integral part of the long-term ground-control and rock mechanics program at some mines. Engineering staff able to determine when, where, and on what scale rock is breaking in the vicinity of their excavation, (24 hours a day, day after day, year after year using sensors placed some distance from a failure zone), will have a better understanding of mining effects on the surrounding hostrock than engineers without access to such data. In many mines there is a real possibility of generating an earthquake of substantial energy release, usually by activating a pre-existing fault near the mine. Full-time seismic monitoring is the only way to "keep an eye" on such potential problem zones. Roof-falls are a serious safety hazard in any mine, and there is unfortunately no mechanical device, data acquisition system,

computer system, etc. that can reliably predict when and where a roof-fall will occur. While it is unlikely that the results of seismic monitoring alone could predict a roof-fall, microseismic data may provide key information to the thinking engineer who, using all of the information at his disposal, will predict any such hazard. Monitoring seismicity gives a set of specific, systematic observations of the set of circumstances associated with a rock-failure hazard, (such as a roof-fall), which can be analysed in detail in the context of other similar observations.

Small-scale seismic events are common at underground mines, occurring regularly whether the operator is aware of them (through some monitoring program) or not ; they are free, they cost nothing. Why not use the information provided by this seismicity to gain some understanding of how mining is affecting the rock about the mine ?

2. BACKGROUND TO SEISMICITY IN POTASH MINES :

It is probably true that there is some seismicity associated with EVERY underground mining operation. While noticeable earthquakes and/or "rock-bursts" occur at some mines, microseismicity has been observed at every underground mine where monitoring instruments have been set up. Events strong enough to be noticed by persons living in the vicinity of potash mines have occurred in Germany, Brazil, the USSR and Saskatchewan. These "large-scale" events, in the Richter magnitude range +1.0 to +5.6, are outright earthquakes. Microseismic events, typically in the Richter magnitude range -4.0 to -1.0, are not generally noticeable by anything but sensitive seismic monitoring instruments.

2.1 Large-Scale Seismicity (Noticeable Earthquakes) :

In Saskatchewan noticeable earthquakes have occurred at five of the ten potash mines operating in the province. These events, first noticed in the fall of 1976, have been in the Richter magnitude range +1.5 to +3.7, (as shown in the accompanying Table, compiled by Gendzwill, 1990, University of Saskatchewan). The proximity of these earthquakes to mines, in areas where previous seismicity was unknown, led to initial speculation, followed by the inevitable conclusion, that all events are induced by the mining activity. Noticed effects have ranged from "I thought a truck ran into the house", or "It felt like the furnace blew up", to (in very few cases) cracked wall plaster. The largest earthquake seen at a Saskatchewan mine was a magnitude +3.7 event near Esterhazy on February 18, 1988. This event caused no apparent damage to the mine (which remains in full produc-

tion), and although residents in nearby farming communities noticed the earthquake, structural damage was minimal. These observed effects are typical of all mine related earthquakes in the province : to date damage caused by mine-induced noticeable earthquakes in Saskatchewan has been minimal.

The fact that only low levels of apparent damage are observed time after time is somewhat puzzling : earthquakes generated in similar geological settings in other mining areas, and in the magnitude range seen at Saskatchewan potash mines, have been very destructive. Earthquakes and rockbursts in the deep gold mines of South Africa have produced devastating results, killing mine workers and causing regions of mines to be shut down ; an event of Richter magnitude +3.0 or +4.0 is considered a very serious hazard in these mines. In Canada a "bump", or severe ground disturbance, occurred in the working area of a Springhill, Nova Scotia coal mine in October 1958 claiming the lives of 75 mine workers and resulting in closure of the mine. And more recently, an earthquake of magnitude +3.9 (i.e.- of only slightly greater energy release than the largest Saskatchewan mine-induced event) occurred at one of the Falconbridge nickel mines near Sudbury, Ontario in mid-June 1984 causing failure of portions of backfilled sections of the mine which trapped and killed four mine workers. The Falconbridge mine was closed as a result of the earthquake. While large events that claim lives always receive a great deal of attention it should be noted that mining-induced seismicity at all scales has been observed across Canada for many years, and continues to be of concern in coal, metal and potash mines (see for example, the review paper by Hasegawa et al., 1989 enclosed in the Appendix).

The only serious damage that may be attributable to induced earthquakes in Saskatchewan potash mines are a water inflow into the Gerald (IMC-K2) mine near Esterhazy, which was noticed shortly after a magnitude +2.6 event on December 25, 1985, and small water seepages at the PCS-Cory mine, which have occurred in the vicinity of prior earthquakes.

The largest mining induced seismic event in history occurred at a potash mine. Pillar failure in a potash (carnallite) mine in Werra, East Germany in June 1975 resulted in a magnitude +5.6 earthquake that caused extensive damage to buildings in nearby villages. The event was caused by the sudden failure of all support pillars over a 3.35 square kilometre area in the mine. Concrete foundations and buildings in the nearby village of Sunna were extensively damaged and shaking was felt on surface for hundreds of km. Another magnitude +5.5 event, apparently triggered by "planned mine blasting", resulted in severe damage to "80 % of buildings" in nearby Volkershausen, East Germany in March, 1989 ; a 6 square km region of the village dropped 60 cm.

In general terms, the geomechanical in Werra, of a brittle and competent sandstone in the immediate hanging wall taking up much of the stress created by mining, is similar to the situation in Saskatchewan of a brittle and competent limestone over the mine taking up stress created by mining. Mines in both regions operate at similar depths (1000 m), and there is no unusual lithostatic stress pattern in either area. An important difference between the two mining camps is that large pre-existing faults are common in East Germany, while there are no active faults (in the usual sense of the word) in the Phanerozioc cover near the Saskatche-

wan mines. The largest East German seismic events occur when stress-change due to mining activates slip on pre-existing faults. In potash mining areas of Saskatchewan, potentially active faults are generally restricted to solution collapse zones ; mining near such regions is avoided in all but the most unusual circumstances. So unless Saskatchewan mine operators change their strategy of staying well clear of collapse zones it is unlikely that events of magnitude much larger than those already observed should occur. However, given the proximity of old fault systems to mines recently opened in New Brunswick, there is some possibility that they might generate larger, fault-related earthquakes as workings expand with time. The north shore of the Bay of Fundy in New Brunswick has a long history of sporadic, but significant seismic activity. Events up to Richter magnitude +5 were noted as early as the seventeenth century by the first European settlers to the area ; this trend has continued to the present (see paper by Basham et al., 1979 enclosed in the Appendix). To date none of the observed seismicity has been attributed to movement on any of the fault systems near the Clover Hill mine ; (this statement must be tempered by the fact that location accuracy for events in this area has always been poor due to limited regional seismograph coverage). While no event greater than magnitude +5 has occurred in the region in historic time, the Fundy area has been assigned a fairly high "seismic risk" factor.

2.2 Microseismicity in Potash Mines

While noticeable earthquakes of Richter magnitude +1.5 to +3.7 have occurred sporadically (once or twice per year) at only a few mines in

Saskatchewan, small-scale microseismicity (Richter magnitude -2.0 to -4.0) was observed at every potash mine where instruments were set up. Temporary seismic monitoring projects similar to the one carried out at the Clover Hill mine have been run at many Saskatchewan potash mines ; a set of frequency of occurrence histograms for data from five mines is given in Figure 1. The variability in these results is striking : mines with a thick hanging wall salt cover (IMC-Esterhazy, PCS-Rocanville) experience 1 - 2 microseismic events per WEEK while about 10 events were seen per DAY (with as many as 25 events on some days) at the Cominco-Vanscoy mine, which is deeper than the rest and has a very thin salt cover. As well, high levels of seismicity have been observed in association with major brine inflows at both the Esterhazy IMC-K2 and the PCS-Rocanville mines. At present the two IMC mines near Esterhazy, (Yarbo-K1 and Gerald-K2), and the PCS-Cory mine have permanent seismic monitoring systems in place ; PCS plan to install additional systems at their Lanigan mine this summer, and at Rocanville in the fall.

Contrary to initial expectations, no relationship was found between the large earthquakes and the microseismic events. The small events were generally located within salts near the mining level, while the large events appear to be the result of sub-horizontal shear failure in hanging-wall limestones ; for more discussion of some of these results see papers by Gendzwill (1983 & 1984), Gendzwill and Prugger (1988) and Prugger and Gendzwill (1988) enclosed in the Appendix. Analysis of seismogram waveforms of the small events allowed a number of possible modes of failure within the salts to be proposed ; (i.e. - rock fracture that would give

rise to the observed waveforms). Most microseismic events occurring near potash mine openings were the result of slab delamination in either the roof or in the floor, within a few metres of mine rooms. In essence, these events were caused by the formation of horizontal tension cracks as horizontal stresses were locally redistributed about mine rooms. This mode of failure is illustrated in Figure 2. Many seismic traces showed clear evidence that the crack-rupture propagation was a complex, heterogenous process. Virtually none of the small seismic events showed any indication of true shear failure. The types of failure indicated by analysis of seismic waveforms is in good agreement with the modes of small-scale failure that is observed during a visit to a Saskatchewan potash mine.

One of the more interesting microseismic event case histories was presented in a paper by Vance and Mottahed (1985, enclosed in the Appendix). In November 1984 a major brine inflow occurred at the Rocanville mine. A production room cut into a pre-existing collapse structure, where salts of the Prairie Evaporite had been dissolved and overlying material had dropped into the solution cavity, as shown in Figure 3 . In December 1984 a microseismic monitoring system was installed underground about the inflow point at Rocanville. The system was put in place to monitor rock failure on a day-to-day basis that might be occurring in areas of the mine not easily accessed, and so provide information about the extent of the area affected by the brine inflow. On encountering the brine at Rocanville it was not known how much of the geologically anomalous area was affected by the water entering the mine. The map of observed seismic events showed a ring pattern of rock failure distributed over a large area

within the anomaly (Figure 4). The operator interpreted this "to imply that the area affected and weakened by dissolution during the water inflow was fairly large in extent" (Vance and Mottahed, 1985). The pattern of seismicity shown in Figure 4 could be interpreted as the aftershock sequence following a larger event that had occurred earlier near the center of the ring, the failure which connected hanging wall aquifers to mine openings. In March 1985 valves in a concrete plug were closed and the brine flow was shut off. As soon as the inflow was stopped the seismic event rate dropped from about 1 per day to none. From this the operator concluded "that relatively stable conditions were obtained once the dynamics of large brine flow rates were stopped" (Vance and Mottahed, 1985). A similar pattern of a ring of microseismic events about an area of a marked absence of any activity was seen during a major brine inflow that started in December 1985 and is still being dealt with at the Gerald (IMC-K2) mine ; (oral paper presented by Ellinger and Vance at the 11th District 4 Meeting of the CIM September, 1988, Saskatoon, Canada). Ongoing monitoring of seismic event patterns is used to check effects of grouting and other efforts to control this inflow, and to "follow" the water as it breaks-in to different points in the mine.

Revised May 13,1988Table 2: Mining induced earthquakes in Saskatchewan
R = location based on regional seismic network, accuracy 20 km.
No symbol where regional location is not available.
S = location based on isoseismal survey, accuracy 1 km.
M = location based on microseismic system, accuracy 100 m or better.

	Location	Date	G.M.T.	Lat.	Long.	Mag.	Ref.
1	I.M.C. K-1	1976, Nov 7	12:27:15	50.69	101.94R	3.0	GSC
2	I.M.C. K-1	1978, Nov 4	01:23:52	50.70	101.90R	3.1	GSC
3	Cory	1979, Nov 18	23:02:13	52.10	106.92S	2.4	GSC
4	Cory	1980, Feb 29	19:41:41	52.12	106.93S	3.0	GSC
5	Cory	1980, Mar 18	00:31:51	52.08	106.90S	2.8	
6	Cory	1980, Aug 6	05:23:53	52.11	106.93S	2.3	
7	I.M.C. K-1	1981, Jan 27	06:13:11	50.70	101.90S	2.9	
8	I.M.C. K-1	1981, Jan 27	19:34:09	50.70	101.90S	2.7	
9	I.M.C. K-2	1981, Apr 13	03:28:21	50.66	101.85S	3.2	
10	Cory	1981, May 11	14:50:09	52.11	106.91S	2.3	
11	Cory	1982, Jan 8	16:46:16	52.11	106.93M	2.4	
12	I.M.C. K-1	1982, Sep 28	07:17:49	50.72	101.95S	3.4	
13	Cory	1983, Jan 6	02:35:04	52.12	106.93S	2.7	GSC
14	C.C.P.	1984, Feb 20	01:19:23	51.95	105.77S	2.4	GSC
15	I.M.C. K-2	1984, Sep 27	08:48:10	50.65	101.89S	3.5	GSC
16	I.M.C. K-2	1984, Oct 25	13:00:18	50.65	101.89R	2.5	GSC
17	I.M.C. K-1	1984, Nov 2	10:24:21	50.68	101.90R	3.0	GSC
18	I.M.C. K-2	1984, Nov 9	02:11:41	50.61	101.83S	2.7	DJG
19	Cory	1985, Apr 6	19:43:39	52.11	106.93R	2.9	GSC
20	I.M.C. K-2	1985, May 15	10:39:03	50.70	101.80R	3.0	GSC
21	I.M.C.	1985, Nov 29	19:27:35			2.5	DJG
22	I.M.C. K-2	1985, Dec 25	15:50:--	50.65	101.88S	2.6	DJG
Note: Event 22 occurred coincidentally with arrival of surface waves from a M = 5.7 Northwest Territories earthquake. It was felt but instruments were saturated with the NWT event.							
23	I.M.C. K-2	1986, Jan 6	08:--:--				DJG
Note: Event 23 was felt but not recorded on instruments							
24	Cory	1986, Jan 29	18:02:36	52.11	106.93R	1.5	DJG
25	I.M.C. K-2	1986, May 18	16:20:13	50.74	101.85R	2.9	DJG
26	Cory	1986, Dec 6	14:51:18	52.11	106.93R	2.1	DJG
27	P.C.A.	1987, Jul 3	11:28:43	52.06	106.34S	2.1	DJG
28	P.C.A.	1987, Jul 21	08:06:40	52.06	106.34M	2.7	GSC
29	I.M.C. K-2	1987, Jul 30	14:33:19	50.66	101.84S	3.3	GSC
30	I.M.C.	1987, Oct 22	04:34:29			3.4	DJG
31	I.M.C. K-2	1988, Jan 7	09:57:05			2.7	DJG
32	I.M.C. K-1	1988, Feb 18	05:27:13	50.71	101.95S	3.6	DJG
33	I.M.C. K-2	1988, Mar 25	22:14:19	50.65	101.89M	3.7	DJG
34	I.M.C. K-1	1988, Nov 7	14:28:20	50.72	101.89s	3.5	DJG
35	I.M.C. K-2	1989, Jan 20	15:56:10			2.7	DJG
36	Cory	1989, Mar 29	04:10:30	52.12	106.95S	2.2	DJG
37	Cory	1989, Jun 5	12:43:05	52.12	106.95S	2.6	DJG

3. SEISMIC MONITORING METHODOLOGY

The basic observational information in the study of seismicity is the set of ground vibration records measured at a number of stations about the area of rock failure. Typically 6 to 12 vibration sensors are set up to form an array covering much of the mine. The goal is to strive for asymmetry in the array - my "rule-of-thumb" is to try to position sensors so that no three lie along a straight line. This may, of course, not be possible, depending on ease of access to various regions of the mine. Sensors are generally spaced 300 - 600 metres apart.

The transducers used most successfully in potash mine seismic studies to date have been geophone sensors with a flat frequency response from 4.5 Hz to 250 Hz. These are mounted vertically to the mine roof using HILTI bolts shot into the rock. The Mark Products model L-1 (1480 ohm) or model L-15 (380 ohm) geophones have been found to work well ; (any similar 4.5 Hz geophone would do). Unamplified geophone signals are then carried some distance (up to 3 km) on light, two-pair twisted cable (22 gauge telephone wire, or similar) to a set of differential amplifiers at a central instrument site. Amplifiers are commonly run at run at gain settings ranging from 60 db to 78 db (1000 x to 8000 x) with high-cut filters set at 50 Hz, 100 Hz, 200 Hz, or 300 Hz, depending on the degree of electrical interference encountered, and the digital sampling rate used ; (i.e.- DON'T set high-cut filters above the Nyqvist frequency, which is equal to 1 over 2 times the sampling interval). Geophone voltages can be converted to the speed of particle displacement at the station (metres / sec in the vertical direction) using the calibration factor of the geophone manufac-

turer. Signals should be digitized at a sample rate no lower than 0.005 s immediately after amplification ; (0.002 s or 0.001 s would be better if data storage is not a problem). Corresponding Nyquist high-frequency cutoffs are then 100 Hz, (or 250 Hz, or 500 Hz). The set of digitized seismic signals from all sensors comprising the geophone array are buffered and fed into a computer based recording system which monitors seismic activity continuously, but only saves incoming traces when an event is "recognized" by the controlling program. Recognized events are written from the memory buffer to a permanent storage device, (now either to a computer hard disk or to solid state memory modules - in the past to cassette tape).

Specific monitoring systems are in a continuous state of development as the workers who create software respond to improvements in instrumentation and (especially) computer hardware. For a good discussion of the a state-of-the-art system used in South Africa see the paper by Green (1988) endclosed in the Appendix.

3.1 Event Recognition

Step one in any seismic monitoring system is to record ground vibration signals for every legitimate seismic event that occurs. The controlling computer must begin recording just before a rock failure event occurs (using a pre-event buffer system), and stop when signals die down to background levels ; (for an in-depth discussion see, for example, the textbook by Lee and Stewart, 1981, listed in the references). The most successful, and thus the most common, real-time event recognition algo-

rithms are variations of the "STA/LTA" method. Average absolute values of signal amplitudes are calculated over a short time-window (short-term average amplitude = STA) and a long time-window (LTA), and recording is triggered when the STA/LTA ratio exceeds a pre-specified value. This simple algorithm is designed to trigger on signals with a fairly sudden onset, such as a seismic event, but reject signals that build up more slowly to high levels, such as a passing train or a truck. Modern versions of the STA/LTA event recognition method often include the improvements that a certain number of channels have to be hit within a reasonable time window, and/or that the incoming energy must be within a certain frequency band.

By trial-and-error it was determined that to trigger on microseismic events in potash mines (using recording parameters described above) the STA should be calculated over 0.3 to 0.6 s , the LTA should be calculated over 5.0 to 10.0 s , and an event is recognized when the STA/LTA ratio is 1.5 to 2.5 . For the small events signal codas rarely last more than 1 s, so a recording window length of 5 s was always sufficient to pick up the entire signal at all sensors. The STA/LTA method has consistently worked well for seismic events in potash mines.

3.2 Picking Arrival Times

Since seismic energy travels at finite velocities through rock, vibration signals will in general arrive at different times at different geophones (ie.- earlier at the near sensors, later at the far sensors). The differences in arrival times at the sensors are used to compute the location

of the rock failure. To achieve a good source location calculation, the arrival_time of seismic energy at each station must be picked accurately from plotted seismograms of each event. This can be a difficult task : for small events the rock noise signals are so weak that ambient interference will all but obliterate the ground vibration signal. This problem of a low signal-to-noise ratio is obvious in the plot of the seismograms shown in Figure 5. Although weak, the seismic signal can be made out on most channels, coming in at about 2.7 - 3.2 s , (this is what the STA/LTA algorithm triggered on), but exact arrival times are impossible to pick, especially on channels 3 and 4.

However, as long as the monitoring program recognized and recorded the event signal there are numerous mathematical filtering procedures that can be used to "clean up" noisy traces. It is often useful to look at the frequency spectrum of the noisy trace, then decide by visual inspection which frequency components constitute "signal" and which constitute "noise". Appropriate digital filters are then applied, trace by trace as required, to give a set of seismograms where the rock-noise is much easier to discern. Frequency filtering using recursive methods is discussed in a technical note included in the Appendix, (FORTRAN subroutines to carry out high-cut, low-cut, and notch filtering operations are also included). Picking accuracy is further improved by interactively adjusting the vertical scale amplification and by expanding the horizontal scale and "stretching" the signal trace. Filtering and scaling the seismograms in Figure 5 results in the traces shown in Figure 6 ; notice how much easier it is to distinguish exact arrivals on this record once filters are applied. Event arrival times are then picked

interactively with a cursor on the set of seismograms plotted on a computer screen.

The major noise problem in mines is electrical interference from the many power systems that are in use, especially when thyristor controls have been implemented. In instances where electrical interference occurs at many harmonics of 60 Hz, frequency-filtering can attenuate a significant portion of the micro-earthquake energy in the process of removing undesired "noise". For events like the one shown in Figure 7 the more sophisticated noise-adaptive filter of Anderson and McMechan (1988, enclosed in the Appendix) was found to work extremely well in cleaning up the noisy signal. The procedure is to compute a Fourier transform over a "noise" window before the first arrivals, then a second transform later in the record over a "signal + noise" window, subtract the amplitude spectrum of the "noise" from the amplitude spectrum of the "noisy data", and compute the inverse Fourier transform. This spectral subtraction algorithm is highly effective in attenuating stationary noise from seismic data, as shown in Figure 8.

3.3 Source Location

The strategy of all seismic event location methods is to find that point in the Earth for which a set of calculated seismic travel times matches the set of arrival times measured from seismogram records. In other words, choose a model to describe how vibrations travel from source to receiver, then search for a point in space for which the DIFFERENCE between observed and calculated travel times is a MINIMUM. This idea is

illustrated in the plot of the "errormap", a contour drawing of the statistical difference between calculated and observed travel times in the region about the geophone array. Contours in the errormap are lines of equal residual time misfit for a given event ; the minimum in the contour plot gives the best-fit location solution. Figure 9 is a typical errormap of residual times for one microseism. Figure 10 shows the detail of the residual misfit right around the solution point. The event occurred near the center of the white ellipsoid at 100250m E, 103450m N, and 350m Z (approximately). In Figure 10 all points within the white area have an average residual misfit of 5 msec or less per geophone. In other words, the calculated arrival time at each geophone differs from the observed arrival time by less than 0.005 s, (so average differences between calculated and observed times are within one digital sample at all sensors, which is a very good fit). The minimum error point near the center of the white ellipsoid has a residual of 3.9 msec per geophone. The vertical location is poorly constrained because all geophones are placed in the roughly horizontal plane of the mine level. Nevertheless, the best-fit location can be determined unambiguously, (at least to a certain degree of accuracy), as shown by the clear single minimum in the errormap plot.

Location programs directly find the minimum-error location (the center of the white ellipsoid) using less computer time than it takes to generate the errormap plot. The optimization scheme I use to rapidly home in on the best-fit location solution involves a Simplex stepping procedure ; this method of source location is fully described in the paper by Prugger and Gendzwill (1988) enclosed in the Appendix. Tests using

synthetic data and dynamite blasts show that the location scheme works well provided :

1. That both calculated and observed arrival times are normalized to their respective mean values ; in other words, the mean observed arrival time is subtracted from all observed arrival times, and the mean calculated arrival time is subtracted from all calculated arrival times. This leads to two sets of values which can be statistically compared to one another with much more consistency than data that are normalized to some single reference geophone, (as shown in Prugger and Gendzwill, 1988).
2. That the starting value, or initial guess, for the iterative location calculation be reasonably close to the final solution. In practice this simply means choosing the geophone with the earliest arrival as the starting point, (or use some other, more sophisticated method of coming up with a rough first-estimate of the starting location).
3. That the L1 rather than the L2 error statistic is minimized. The L1 misfit estimator E is given by

$$E = \frac{1}{n} \sum_{j=1}^{n} \P\ TO_j - TC_j \P$$

where TO_j is the observed arrival time at geophone 'j' of 'n' sensors, TC_j is the corresponding calculated arrival time from the trial source location, ¶ ¶ denotes absolute value, and E is the function to be minimized. This "E" is the misfit parameter that is contoured in the errormap plots. Using the L1 norm tends to de-emphasize effects of a few large time-pick errors on the location solution. This results in a more robust, more accurate location solution.

4. That seismic propagation speed V-velocity be treated as an unknown, along with X-east, Y-north, and Z-depth, in the source location calculation when absolute first-arrived energy cannot be picked with certainty. If coherent late-phase arrival times are used as input to the location program - reasons for doing this are discussed in section 4.1 - velocity must be considered as an unknown quantity in the calculation. This step requires the assumption that all sensors are getting energy with the same mode of source to geophone travel path, whatever that travel path might be.

For the microseismic data collected at Clover Hill it was found that a uniform-Earth, or straight-ray, velocity model adequately described source to geophone travel paths. The data sets, (which were all recorded at the mining level with no more than 10 vertical component sensors), did not warrant a more sophisticated velocity model. Additional constraints on the locations are that Z-depth not lie above the Earth's surface, and that V-velocity be a realistic value (ie.- in the range 2000 - 7000 m/s, which spans the propagation speeds possible for rock in the vicinity of the potash zone in New Brunswick).

4. MICROSEISMICITY AT THE CLOVER HILL MINE, 1989

An 11 channel seismic monitoring array was installed underground at the Clover Hill potash mine near Sussex, New Brunswick on January 24, 1989, and kept running until April 7, 1989. Eleven vertical component geophones were set up to cover a one square kilometre area in the central "Panel 11" region of the Clover Hill mine. Geophones were located in "quiet" drifts (i.e.- away from conveyor belts and main travelways) whenever possible, in a pattern designed to cover most of Panel 11. This project was undertaken as part of a long-term ground-control and rock mechanics program at the mine. While seismic monitoring projects of a similar nature have been carried out at potash mines in Saskatchewan, this was the first such project to be carried out at a New Brunswick potash mine. Results of this initial period of monitoring were intended to be used to assess the feasability of undertaking a permanent seismic monitoring program at the mine.

4.1 Blast Records :

In 74 days of passive monitoring at Clover Hill 57 rock-failure events and numerous blasts were recorded. Seismograms from dynamite blasts are usually very easy to distinguish from rock-fracture events with a little experience. A dynamite shot generates seismic energy that vibrates over a broad band of frequencies, including high frequency energy that sometimes "overdrives" the Teledyne amplifiers that were used at Clover Hill. This results in a seismogram with a characteristic large, low-frequency oscillation dominating the high frequency vibrations that are also present,

as shown in Figure 11. Seismograms from a rock-failure tend to be less complicated and limited to a narrower, often lower frequency band (recall Figure 6).

Throughout the Clover Hill seismic monitoring study, production blasts were recorded at 08:00 and 20:00 every day. Unfortunately the production blasts were usually set up to detonate in more than one location at a time, so the resulting seismograms were too complicated to be used for anything but testing whether or not the recording system was functioning. A program of collecting simple blast data was therefore initiated, and a few small blast events were recorded, (some shots were set up specifically to provide test data for the seismic monitoring project, and some blasts were shot to bring down loose ground). An example of these small blast data is event 1989/58/20:01:41, which was recorded on only 5 of 11 channels because damage to many of the geophone cables (Figure 11). The calculated location put this event at (2115 m E, 6219 m N, 307 m Z, and speed 4725 m/s), as shown in the errormap plot, Figure 12 ; the surveyed location (reported one month after the calculated position had been worked out) was at (2110 m E, 6220 m N, 316 m Z). Horizontal distance error was about 5 m, vertical error was 9 m, and the calculated speed of 4725 m/s was consistent with salt P-wave velocity measured on core samples from the mine. This worst-case event (with fewer than half of the geophones functional) indicates how accurately event locations can be determined for most events.

4.2 Microseismic Events :

As discussed in section 2.1, no large scale seismicity is known to have occurred near the two potash mines in New Brunswick. However, since there are old faults in the vicinity of the Clover Hill mine, there is a distinct possibility that a mining-induced earthquake of appreciable magnitude will occur during the life of the mine. In 74 days of passive monitoring at Clover Hill 57 rock-failure events were recorded. These results are summarized in Figure 13, a plot of the number of seismic events observed per day. For comparison, recall the plot of similar data from Saskatchewan potash mines, Figure 1. Ambient electrical "noise" in the mine interfered with the seismic monitoring system throughout the survey. The recording efficiency was therefore generally quite poor, and many rock-failure events were no-doubt missed because they happened to occur during times of increased electrical interference. For example, no seismicity was observed in the period March 17 through 27, when electrical interference was increased because of problems with the power sled near the instrument site. Seismograms from all of the recorded events had to be filtered to bring out rock-fracture signals clearly. Based on the observations during days of low-noise recording (February 8 through March 5), rock-failure events occurred at an average rate of 1 - 2 events per day at the Clover Hill mine during the Spring of 1989, with as many as 5 events on March 5. Suggestions for eliminating electrical interference problems at Clover Hill are discussed in a technical note included in the Appendix.

A histogram of calculated seismic speeds is given in Figure 14. For

comparison, laboratory measurements on core specimens give P- and S-wave velocities of :

- 4700 m/s and 2700 m/s for the hanging wall claystone ("Caprock"),
- 5200 m/s and 3000 m/s for mine level salts ("Middle Halite"),
- 5950 m/s and 3450 m/s for anhydrites in the footwall ("Basal Anhydrite").

Energy from most of the microseismic events came across the array (of vertical component geophones) at the salt or anhydrite shear wave, (2800 m/s to 3600 m/s), a substantial number (about one third) show that P-wave energy was picked. This is in marked contrast to results from all Saskatchewan potash mines where P-waves are rarely seen using a similar instrument setup. The implications of these observations are not yet clear. Calculated propagation speeds might be useful in working out specific failure mechanisms in the future (i.e.- as more better quality data are collected and added to this Figure).

Calculated seismic event locations for the 57 rock-failure events are plotted on a mine map in Figure 15. Locations are estimated accurate to better than 50-100 m horizontally and 50-200 m vertically. Location uncertainty is greater for the microseisms than for the blasts (recall section 4.1) since seismic event arrival times were always difficult to pick with confidence. Most events occurred at, or very close to the mine level. In an attempt to correlate the pattern of small-scale rock failure of Figure 15 the following data for Panel 11 were studied :

- model-calculated steady-state shear stresses,
- model-calculated steady-state normal stresses,
- model-calculated steady-state convergence rate,

- total surface subsidence (elevation change) measured on surface,
- measured ore thickness contours,
- geological data, including a cross-section.

There was no significant correlation between the seismic observations and any of the the model-calculated values. Highest steady-state shear stresses, along with the highest closure rates, are predicted to occur near the center of Panel 11, close to rooms 11160 and 11200 ; this is roughly coincident with the maximum elevation change measured on surface. Most of the seismic activity, however, occurred in room 11360 to the north, near two areas that were being mined during the survey (near 1600E & 6600N, and near 1950E & 6850N). There were relatively few events in older areas of the mine. Indications are thus that brittle failure about mine rooms tends to occur as rooms are being cut, with far less failure in older rooms. More events occurred at the "edge" of the mine workings than near the center of the mined-out region ; this implies that there was virtually no "pillar crushing" associated with room closure near the center of Panel 11 at the time of the seismic survey. In Figure 15 there is a tendency for events to occur along one or two "lineaments" aligned in a north-north-west / south-south-east direction ; (see, for example, the events trending from 2200E, 5900N north-west to 1200E, 6400N). Dominant structures seen in the mine, however, including the fold hinge of a major isoclinal fold ("Bauer" fold), tend to be aligned roughly perpendicular to this trend ; (i.e. - north-east / south-west, in the direction of most mine rooms in Panel 11). This lack of correlation between the pattern of rock failure and other data for Panel 11 (except areas of active mining) may be the result of having too few seismic events to allow any statistically convincing inferences

to be drawn at this time.

An interesting feature of the microseisms recorded at Clover Hill was that they generally had larger signal amplitudes than the events seen at Saskatchewan potash mines. For 50 typical events (chosen at random), the average maximum peak particle velocity was 6.4 micro-m/s at Vanscoy (1988) and 14.1 micro-m/s at Clover Hill. The largest events at Clover Hill had maximum peak particle velocities of over 30 micro-m/s, while the corresponding values at Vanscoy were just over 14 micro-m/s. The same equipment and instrument setup were used in both mines, and travel path distances were similar for both data sets, so differential attenuation should not be a factor. For whatever reason, seismic events at Clover Hill tended to be of higher peak particle velocity than similar events seen at Saskatchewan potash mines.

4.3 Discussion

The most interesting result of this study was the observation that microseismicity is common at the Clover Hill mine. Small-scale rock-failure events occur regularly, at an average rate of at least 1 - 2 per day, (and note that 5 events were picked up on March 5). The seismic patterns were not easy to explain, but this is a fairly common occurrence, especially early on in a survey program, and should not discourage Denison-Potacan from further effort in this field. The fact that brittle failure occurred where stars are marked on the map during the survey period is irrefutable. The results plotted in Figure 15 are based on observation, not on a concept, or model of what and where failure should be occurring in the vici-

nity of the mine. Unfortunately 57 events are not a large enough statistical sample on which to base robust general conclusions. With enough seismic event data you should be in a very strong position to assess whether or not your finite element model is predicting high shear stresses accurately ; (here I am assuming that the highest degree of small-scale rock failure would occur in areas of highest shear stress).

One of the most important benefits of a permanent seismic monitoring program is to identify areas of anomalous patterns of rock failure in the mine. Unusual seismic patterns might be used to quickly spot, and possibly predict, problems, specifically roof-falls and water inflows. Study of the event location map presented here shows how complex the specific pattern of rock failure is ; the results raise more questions than they answer at the moment. It will take more than a short-term monitoring project to nail down what patterns of seismicity are "normal" and which indicate, or are evidence of, some specific hazard. By monitoring seismicity you determine when, where, and on what scale rock is breaking in the vicinity of the mine (using sensors placed some distance from the failure zone), 24 hours a day, day after day, year after year. As mentioned in Section 2., there is a real possibility of generating an earthquake of substantial energy release by activating a pre-existing fault near the mine. Full-time seismic monitoring is the only way to "keep an eye" on such potential problem zones.

There are, no doubt, many technical difficulties that will have to be addressed and overcome, on a problem by problem basis, before the results of seismic monitoring can be usefully employed, (to predict roof-falls or other underground hazards for example), at the Clover Hill mine. But

none of these problems is insurmountable ; all that is required to get a permanent seismic monitoring system going at Clover Hill is a will and a commitment to accomplishing this task. Once observational rock-failure data become available on an ongoing and routine basis, your understanding of how mining is affecting the hostrock around the mine will be dramatically improved.

5. REFERENCES :

Anderson, R. G. and G. A. McMechan (1988). Noise-adaptive filtering of seismic shot records. Geophysics, 53, pp. 638-649.

Basham, P. W., D. H. Weichert, and M. J. Berry (1979). Regional assessment of seismic risk in eastern Canada. Bulletin of the Seismological Society of America, 69, pp. 1567-1602.

Basham, P. W., D. H. Weichert, F. M. Anglin and M. J. Berry (1985). New probabilistic strong seismic ground motion maps of Canada. Bulletin of the Seismological Society of America, 75, pp.563-595.

Ellinger, E. and J. Vance (1988). Microseismic monitoring system at IMC Canada, Esterhazy. Abstracts of the Eleventh District 4 Meeting of the Canadian Institute of Mining and Metallurgy (CIM), Saskatoon, Canada, p. 21.

Gendzwill, D. J. (1983). A theory for the source mechanism of the Cory mine earthquakes. Proceedings of the first International Potash Technology Conference, Potash '83, pp. 197-202.

Gendzwill, D. J. (1984). Induced seismicity in Saskatchewan potash mines. Rockbursts and Seismicity in Mines, South African Institute of Mining and Metallurgy Symposium Series 6, 131-146.

Gendzwill, D. J. and A. F. Prugger (1988). Seismic activity in a flooded Saskatchewan potash mine. Second International Symposium of Rockbursts and Seismicity in Mines (preprinted papers), University of Minnesota, Minneapolis, pp. 139-148.

Green, R. W. E. (1988). Instrumentation networks for observation of mine-induced seismicity. Second International Symposium of Rockbursts and Seismicity in Mines (Keynote Papers), University of Minnesota, Minneapolis, pp. 142-156.

Hasegawa, H. S., R. J. Wetmiller, and D. J. Gendzwill (1989). Induced seismicity in mines in Canada - an overview. Pure and Applied Geophysics, 129, pp. 423-453.

Lee, W. H. K. and S. W. Stewart (1981). Principles and Applications of Microearthquake Networks. Academic Press, New York.

Prugger, A. F. and D. J. Gendzwill (1988). Micro-earthquake location : a non-linear approach that makes use of a simplex stepping procedure. Bulletin of the Seismological Society of America, 78, pp. 799-815.

Prugger, A. F. and D. J. Gendzwill (1988). Results of microseismic monitoring at the Cory mine, 1981-1984. Second International Symposium of Rockbursts and Seismicity in Mines (preprinted papers), University of Minnesota, Minneapolis, pp. 317-326.

Vance, J. B. and P. Mottahed (1985). AE/MS applications to potash mining problems. Acoustic Emissions / Microseismic Activity in Geological Structures and Materials, Proceedings of the Fourth Conference, pp. 275-286.

Young, R. P., M. Bostock, D. A. Hutchins, P. Mottahed (1987). Geotomographic imaging of collapse/solution structures in potash mines using seismic methods. Proceedings of the 29th U. S. Symposium on Rock Mechanics, Tucson, pp. 19-27.

6. FIGURE HEADINGS :

1. Microseismic event frequency of occurrence at Saskatchewan potash mines.

2. Mode of small-scale failure seen in Saskatchewan potash mines that best describes observed seismic waveforms.

3. Model of the Rocanville water inflow 1984 - 1985 (from Young et al., 1986). Distances are in metres.

4. Pattern of microseismic events during the Rocanville water inflow 1984-1985 (from Vance and Mottahed, 1989). Distance is in feet, seismic events are plotted as stars, underground geophones are plotted as triangles, and the circle marks the water inflow point.

5. Example of a set of noisy seismograms, (noise is due to 60 Hz electical interference).

6. Seismograms shown in Figure 5. after application of a 60 Hz digital notch filter and a scaling function.

7. Example of extremely noisy seismograms, (noise is due to complex electrical interference involving many harmonics of 60 Hz).

8. Seismograms shown in Figure 7. after application of the Anderson-McMechan noise-adaptive digital filtering operation.

9. Errormap for a microseismic event. Geophones are plotted as white dots (with one sensor located to the north, just off the map). Contours are of the L1 time residual error per sensor, in seconds.

10. Detail of the errormap shown in Figure 9. close to the best-fit location solution point.

11. Example of seismograms from a small dynamite blast recorded at Clover Hill.

12. Errormap for blast event.

13. Number of microseismic events observed per day at Clover Hill, January - April, 1989.

14. Calculated velocity histogram, Clover Hill, 1989.

15. Microseismic event location map, Clover Hill, 1989. Distance is in metres, seismic events are plotted as stars, underground geophones are plotted as triangles, and shaded areas indicate mine rooms.

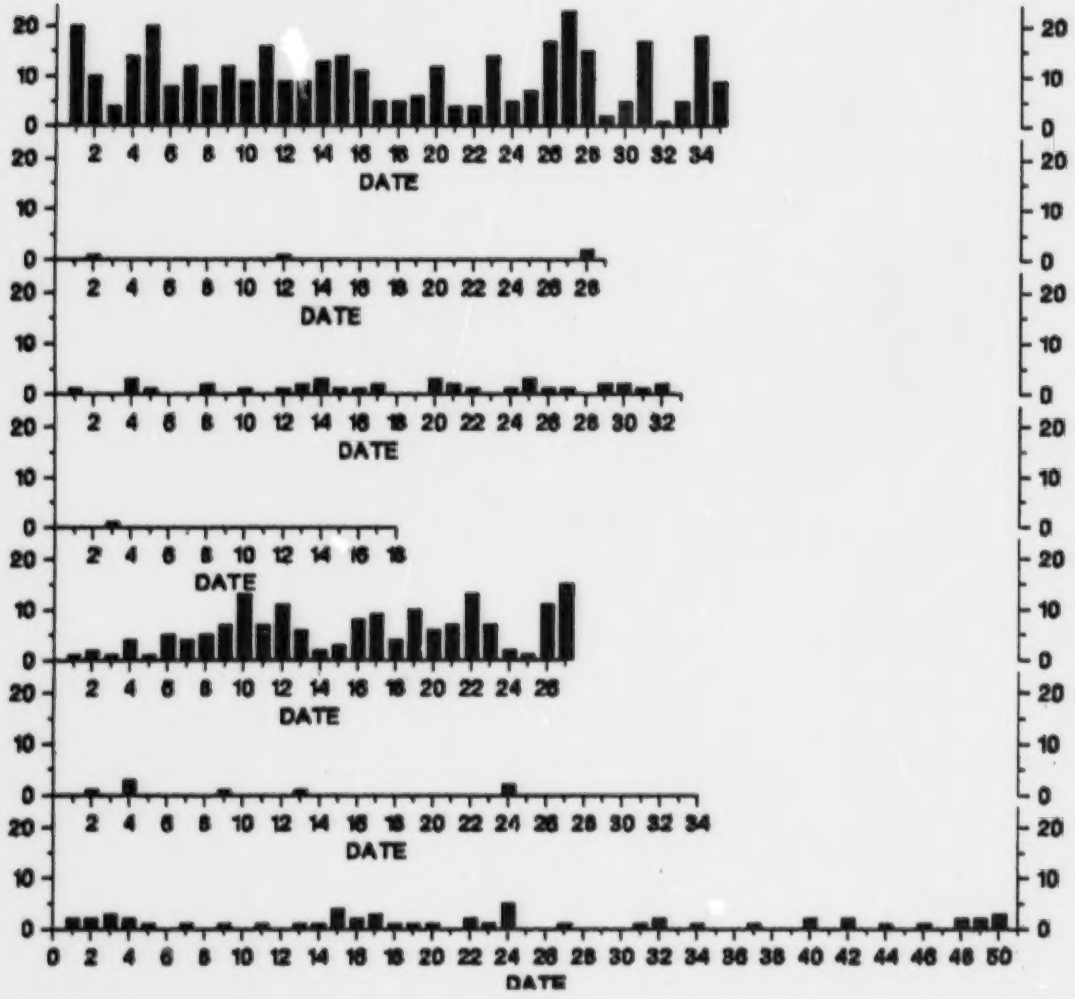

VANSCOY/COMINCO
OCT - DEC, 1985
EVENTS PER DAY = 10.4

ROCANVILLE/PCS
JUL & OCT, 1987
EVENTS PER DAY = 0.1

LANIGAN / PCS
NOV - DEC, 1987
EVENTS PER DAY = 1.1

GERALD / IMC-K2
DECEMBER, 1987
EVENTS PER DAY = 0.1

VANSCOY/COMINCO
FEB - MAR, 1988
EVENTS PER DAY = 6.1

CORY / PCS
JUN - JUL, 1988
EVENTS PER DAY = 0.2

CLOVER HILL NB.
JAN - APR, 1989
EVENTS PER DAY = 1.1

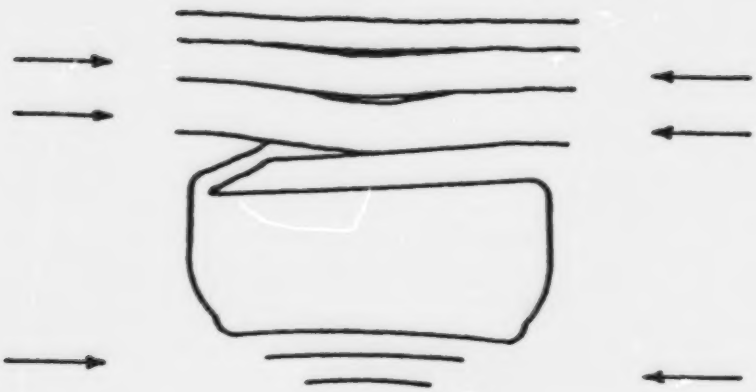

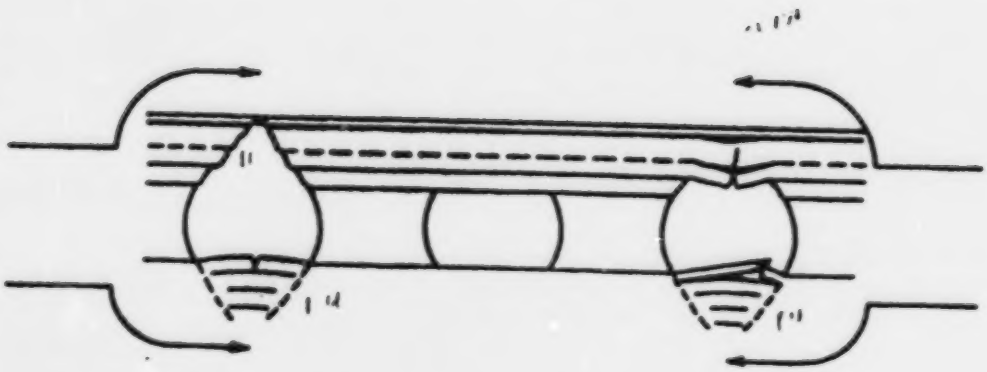

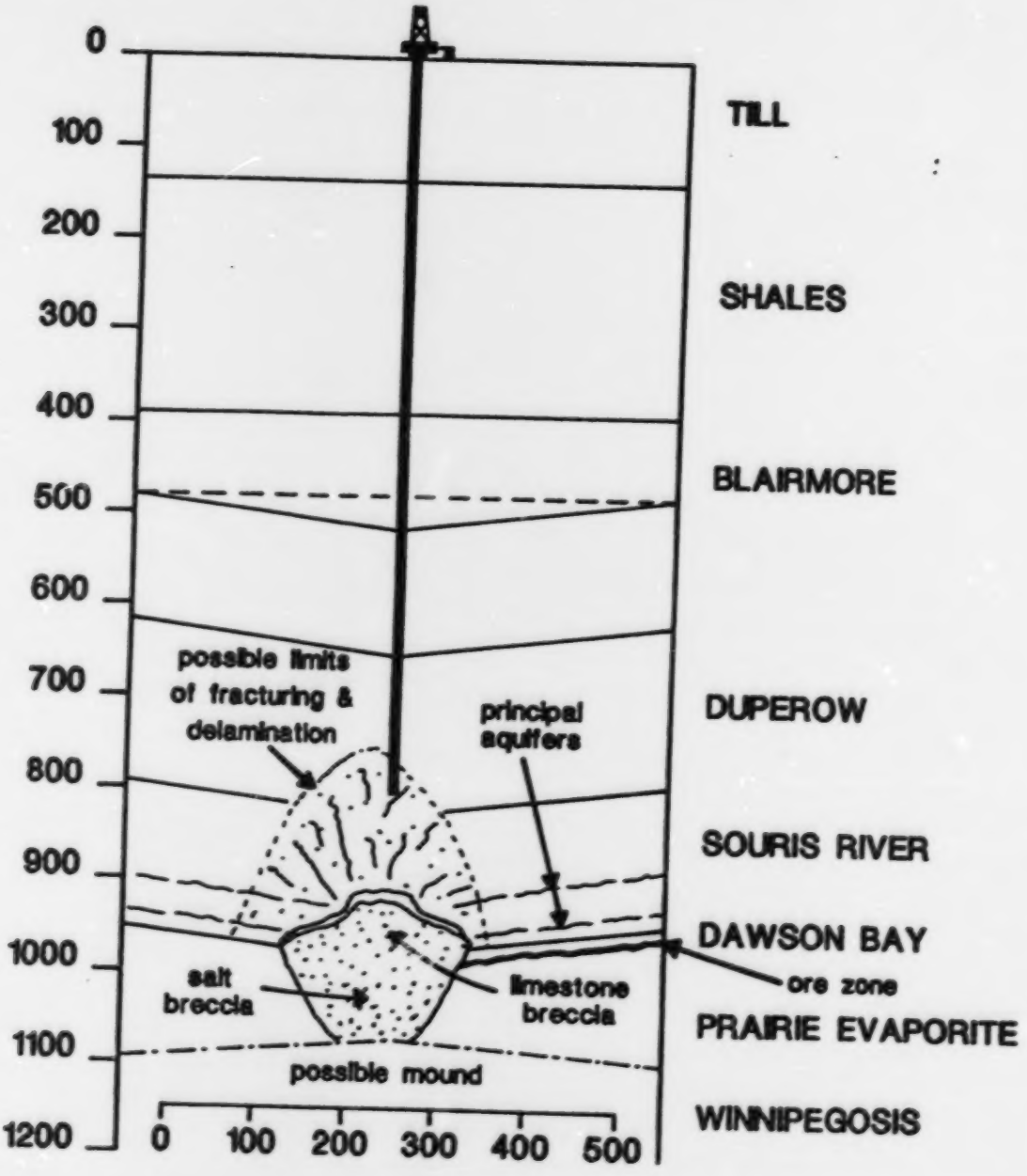
0
100
200
300
400
500
600
700
800
900
1000
1100
1200
0
100
200
300
400
500
TILL
SHALES
BLAIRMORE
DUPEROW
SOURIS RIVER
DAWSON BAY
PRAIRIE EVAPORITE
WINNIPEGOSIS
possible limits of fracturing & delamination
principal aquifers
ore zone
salt breccia
limestone breccia
possible mound

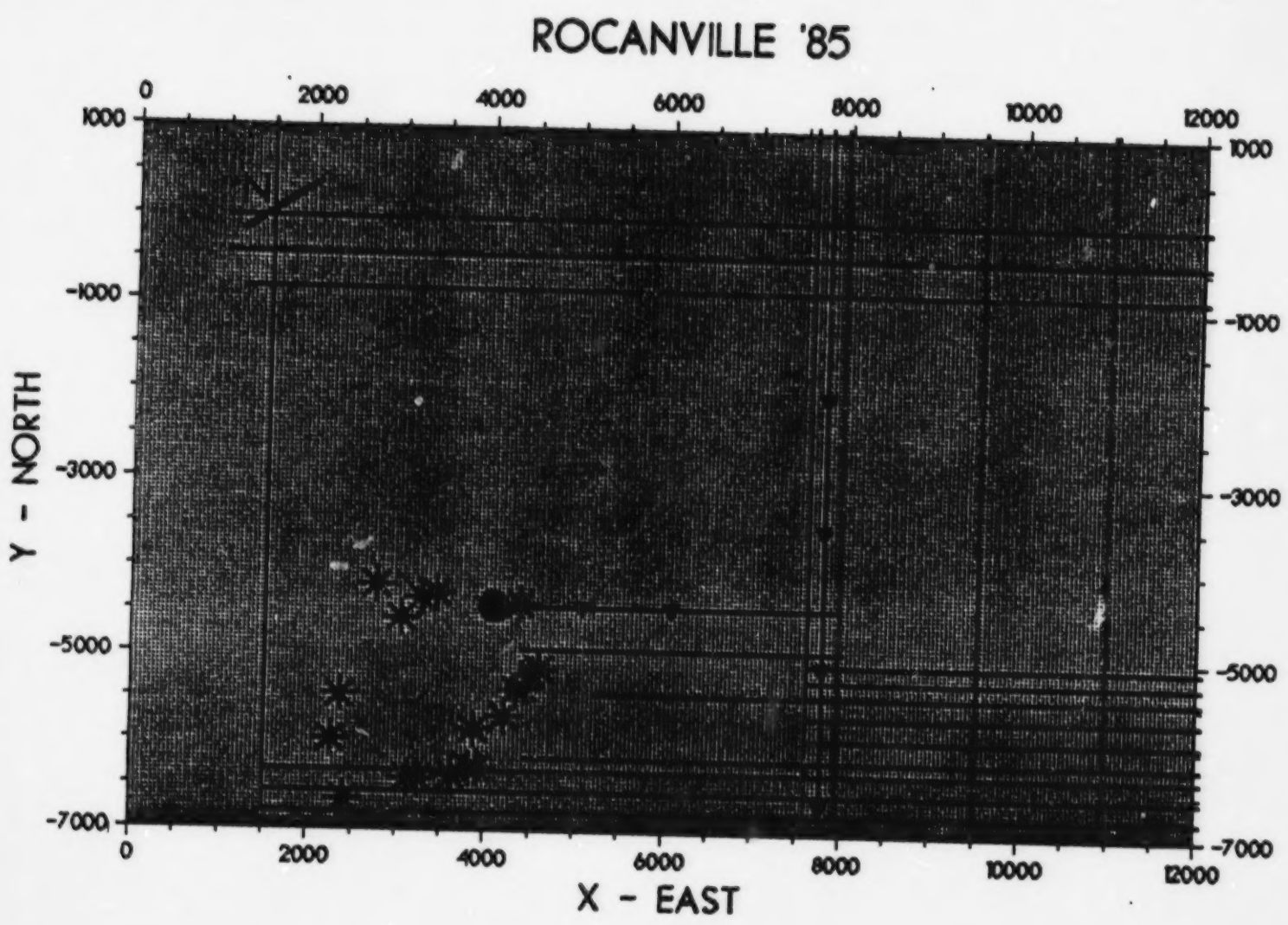
ROCANVILLE '85
0
2000
4000
6000
8000
10000
12000
1000
-1000
-3000
-5000
-7000
Y - NORTH
X - EAST

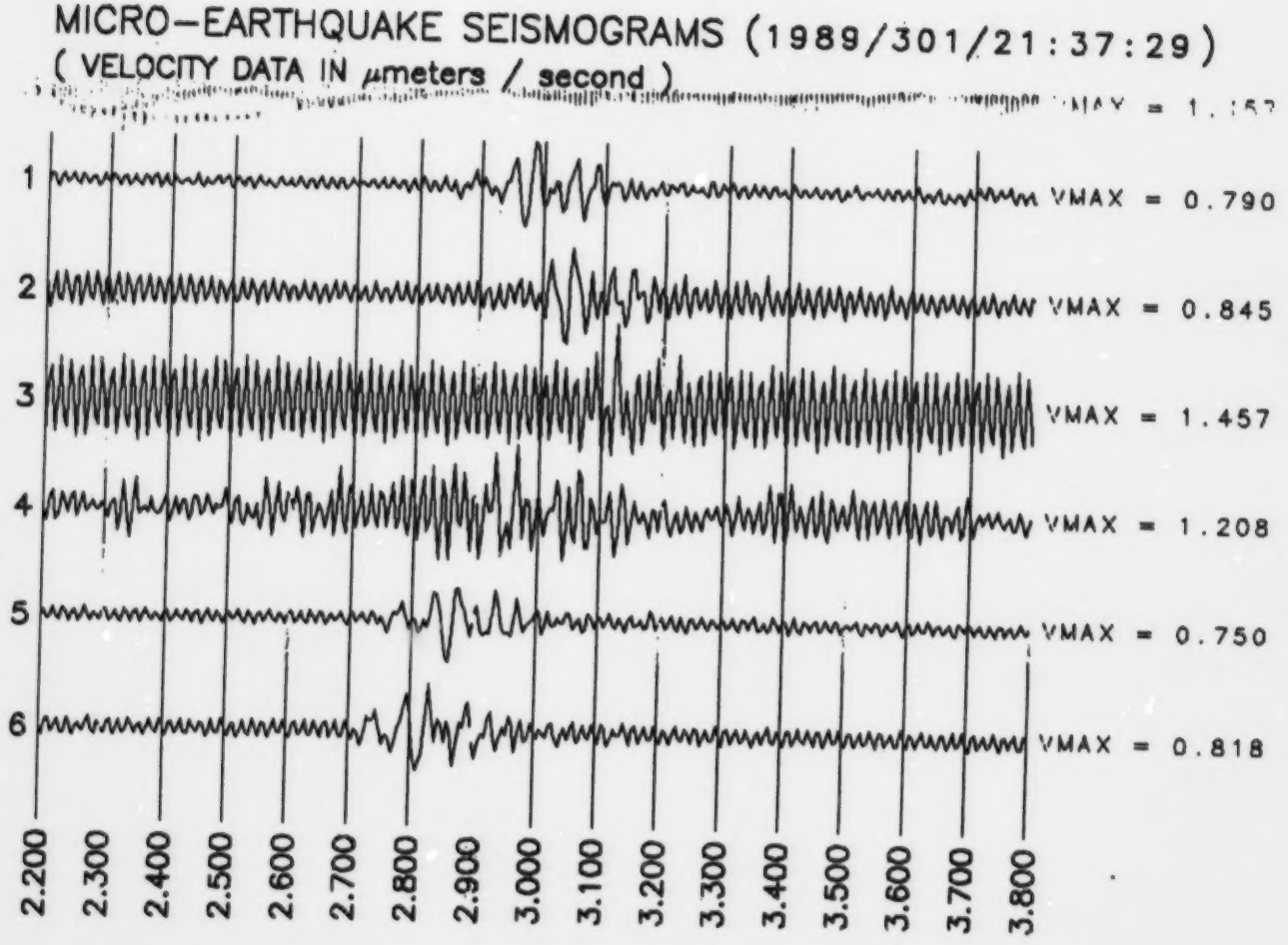
MICRO–EARTHQUAKE SEISMOGRAMS (1989/301/21:37:29)
(VELOCITY DATA IN μmeters / second)
1
2
3
4
5
6
VMAX = 0.790
VMAX = 0.845
VMAX = 1.457
VMAX = 1.208
VMAX = 0.750
VMAX = 0.818
2.200
2.300
2.400
2.500
2.600
2.700
2.800
2.900
3.000
3.100
3.200
3.300
3.400
3.500
3.600
3.700
3.800

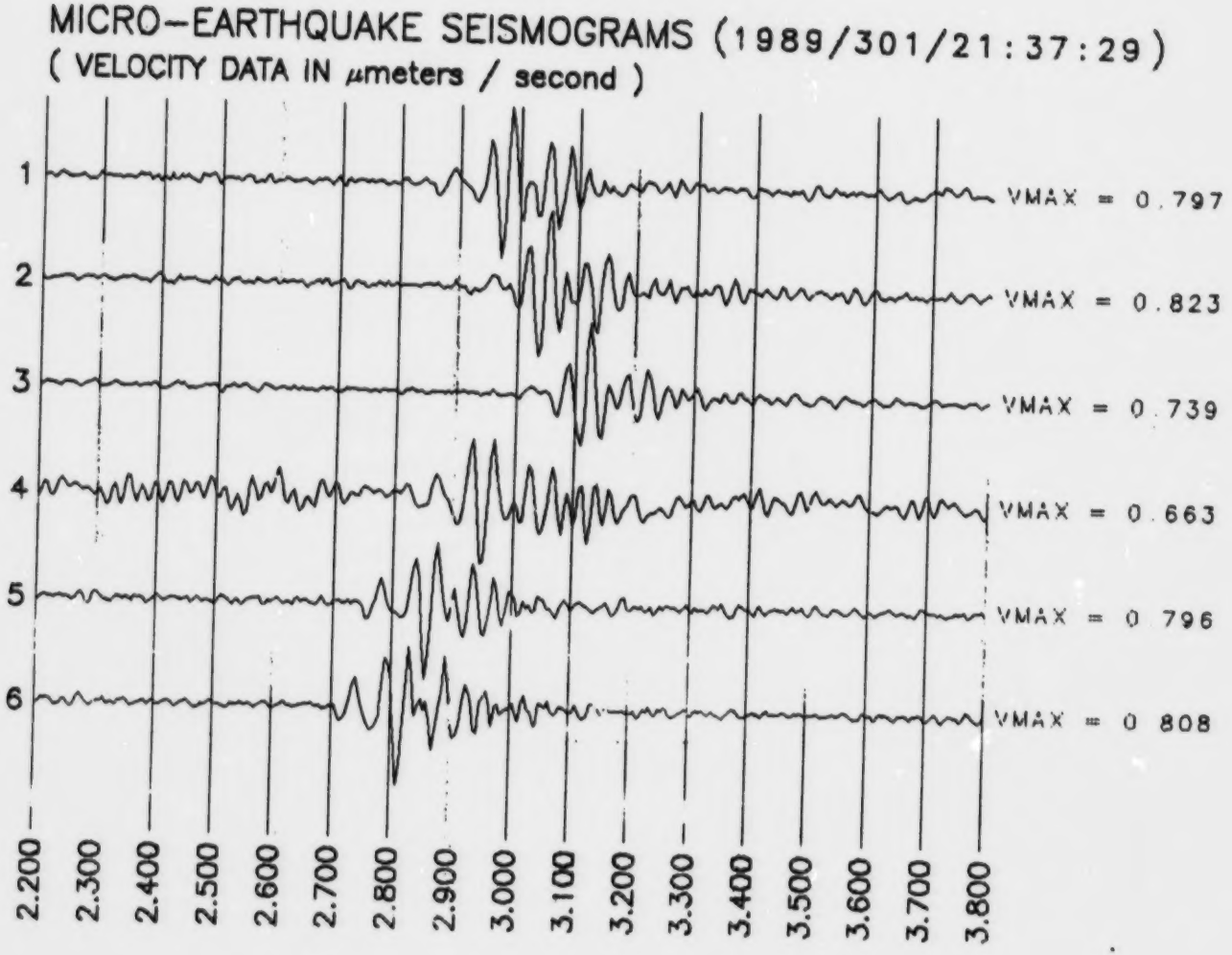
MICRO–EARTHQUAKE SEISMOGRAMS (1989/301/21:37:29)
(VELOCITY DATA IN μmeters / second)
1
2
3
4
5
6
VMAX = 0.797
VMAX = 0.823
VMAX = 0.739
VMAX = 0.663
VMAX = 0 796
VMAX = 0 808
2.200
2.300
2.400
2.500
2.600
2.700
2.800
2.900
3.000
3.100
3.200
3.300
3.400
3.500
3.600
3.700
3.800

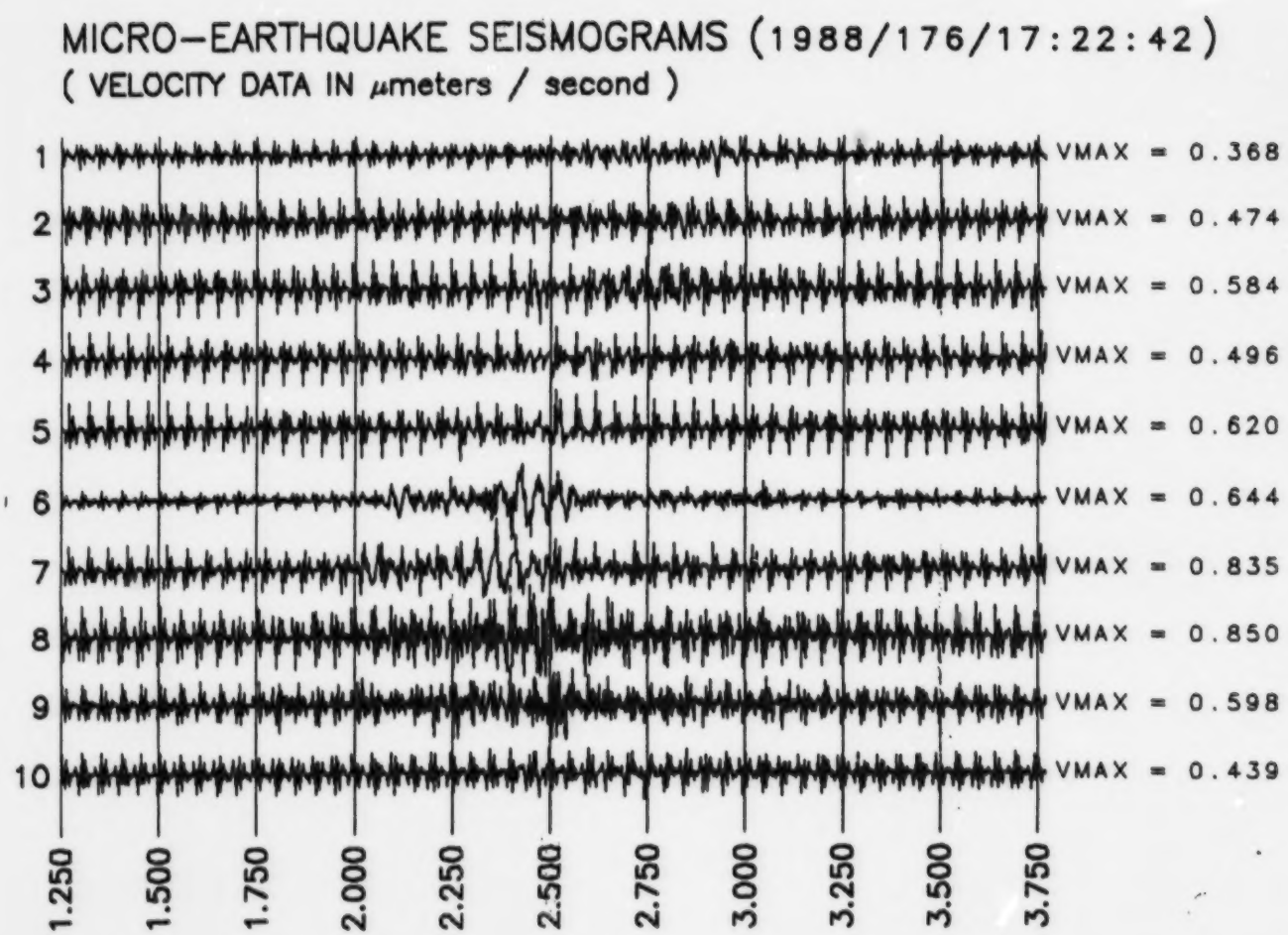
MICRO–EARTHQUAKE SEISMOGRAMS (1988/176/17:22:42)
(VELOCITY DATA IN μmeters / second)
1
2
3
4
5
6
7
8
9
10
VMAX = 0.368
VMAX = 0.474
VMAX = 0.584
VMAX = 0.496
VMAX = 0.620
VMAX = 0.644
VMAX = 0.835
VMAX = 0.850
VMAX = 0.598
VMAX = 0.439
1.250
1.500
1.750
2.000
2.250
2.500
2.750
3.000
3.250
3.500
3.750

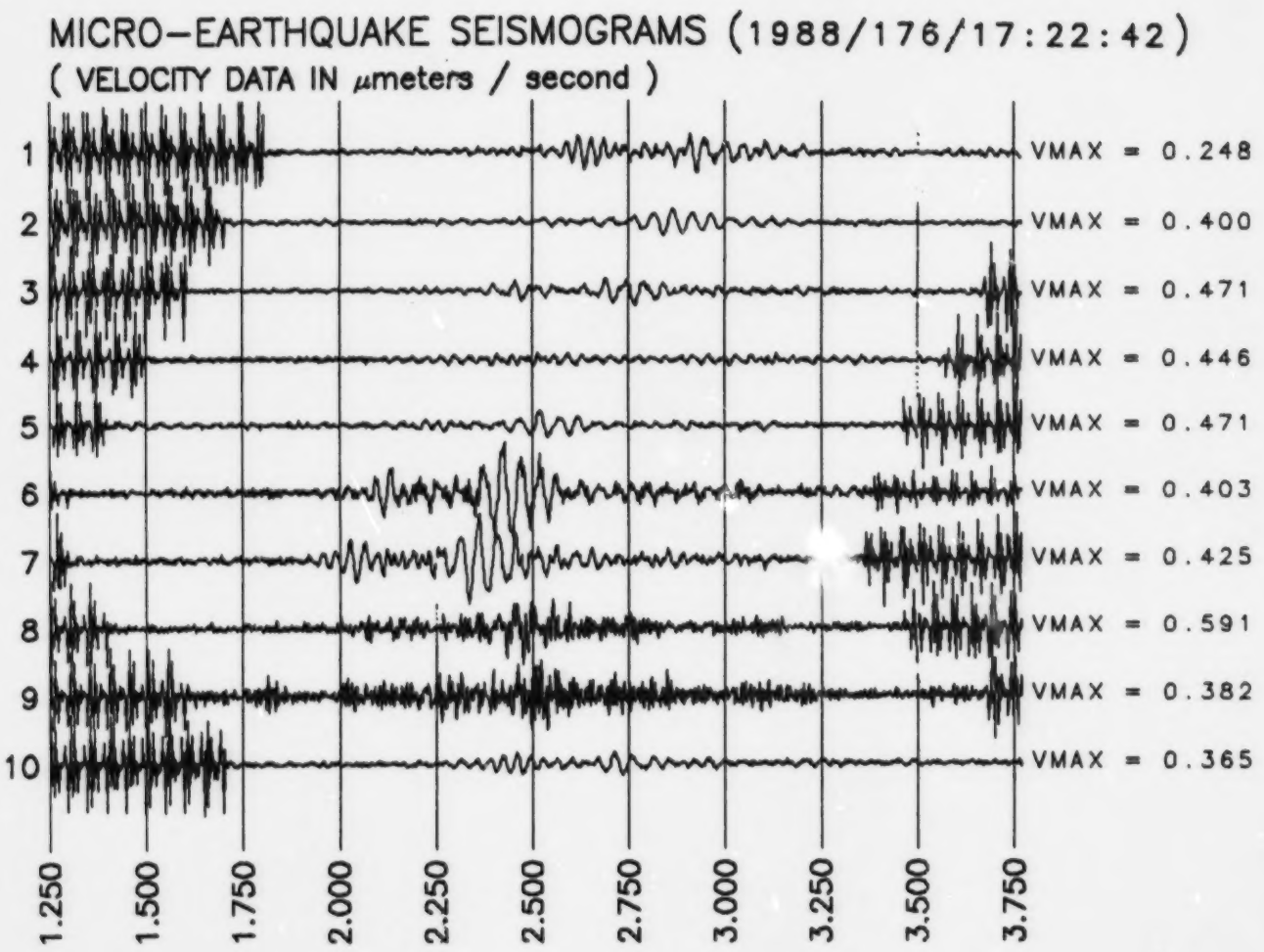
MICRO–EARTHQUAKE SEISMOGRAMS (1988/176/17:22:42)
(VELOCITY DATA IN μmeters / second)
1
2
3
4
5
6
7
8
9
10
VMAX = 0.248
VMAX = 0.400
VMAX = 0.471
VMAX = 0.446
VMAX = 0.471
VMAX = 0.403
VMAX = 0.425
VMAX = 0.591
VMAX = 0.382
VMAX = 0.365
1.250
1.500
1.750
2.000
2.250
2.500
2.750
3.000
3.250
3.500
3.750

UNIFORM EARTH ERRORMAP FOR EVENT 1988/55/7:39:50

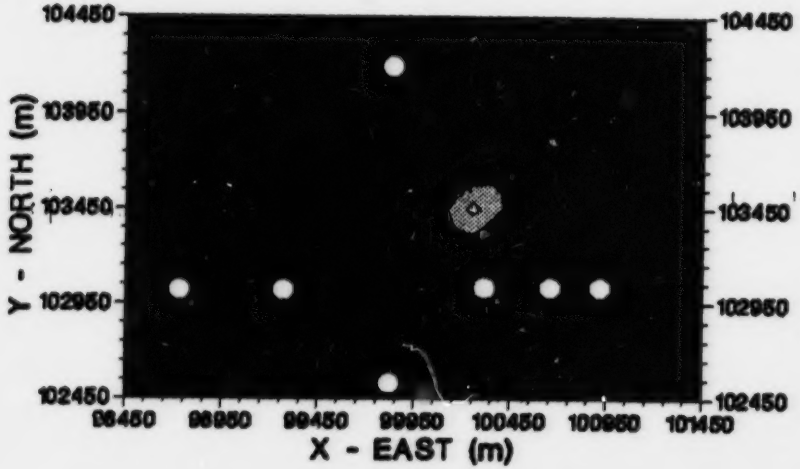

L1-norm SOLUTION
VELOCITY = 2700 m/sec

HORIZONTAL SECTION IS AT
350 m VERTICAL (Z)

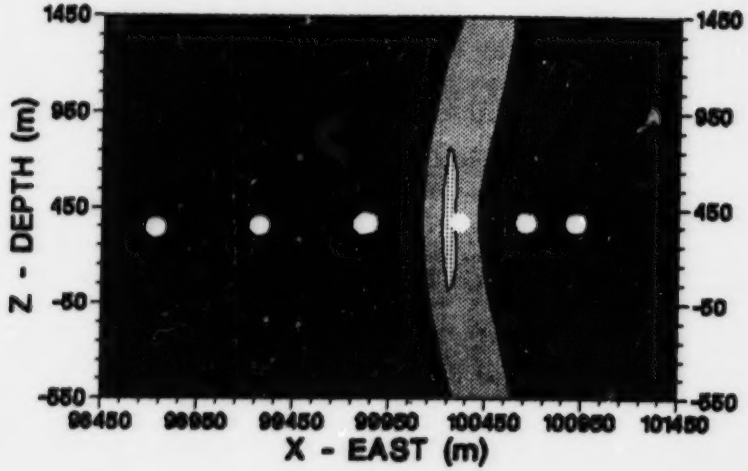

VERTICAL SECTION ALONG
103450 m NORTH (Y)

ABOVE 190
170 - 190
150 - 170
130 - 150
110 - 130
90 - 110
70 - 90
50 - 70
30 - 50
10 - 30
BELOW 10

UNIFORM EARTH ERRORMAP FOR EVENT 1988/55/7:39:50

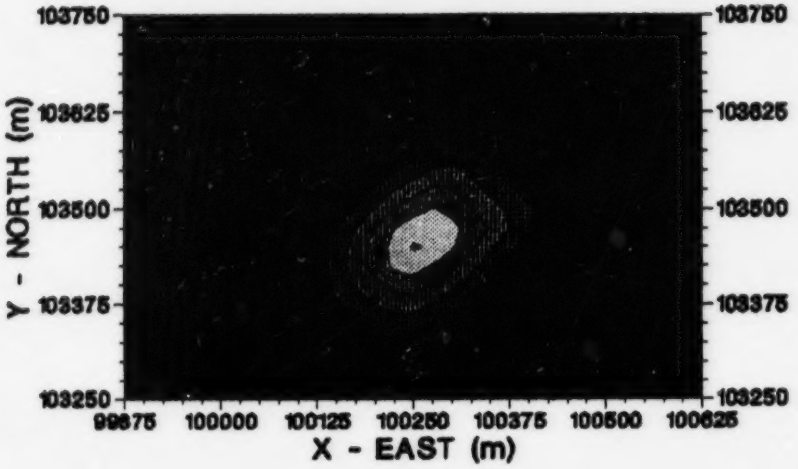

L1-norm SOLUTION
VELOCITY = 2700 m/sec

HORIZONTAL SECTION IS AT
350 m VERTICAL (Z)

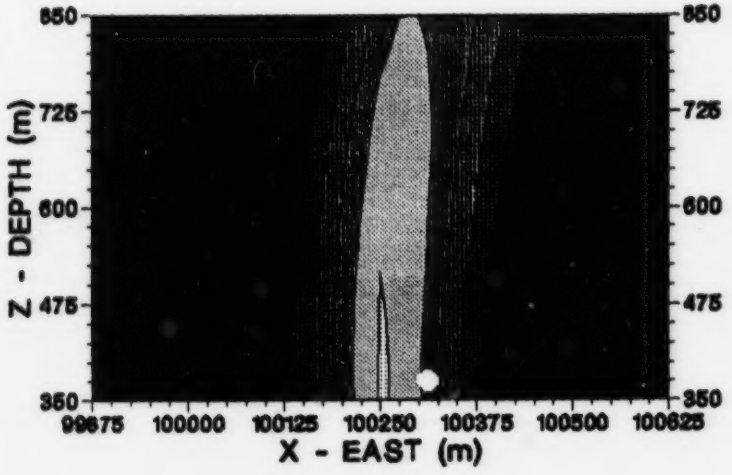

VERTICAL SECTION ALONG
103450 m NORTH (Y)

	ABOVE 50
	45 - 50
	40 - 45
	35 - 40
	30 - 35
	25 - 30
	20 - 25
	15 - 20
	10 - 15
	5 - 10
	BELOW 5

MICRØ-EARTHQUAKE SEISMØGRAMS (1989/58/20: 1: 41)

(VELOCITY DATA IN μmeters / second)

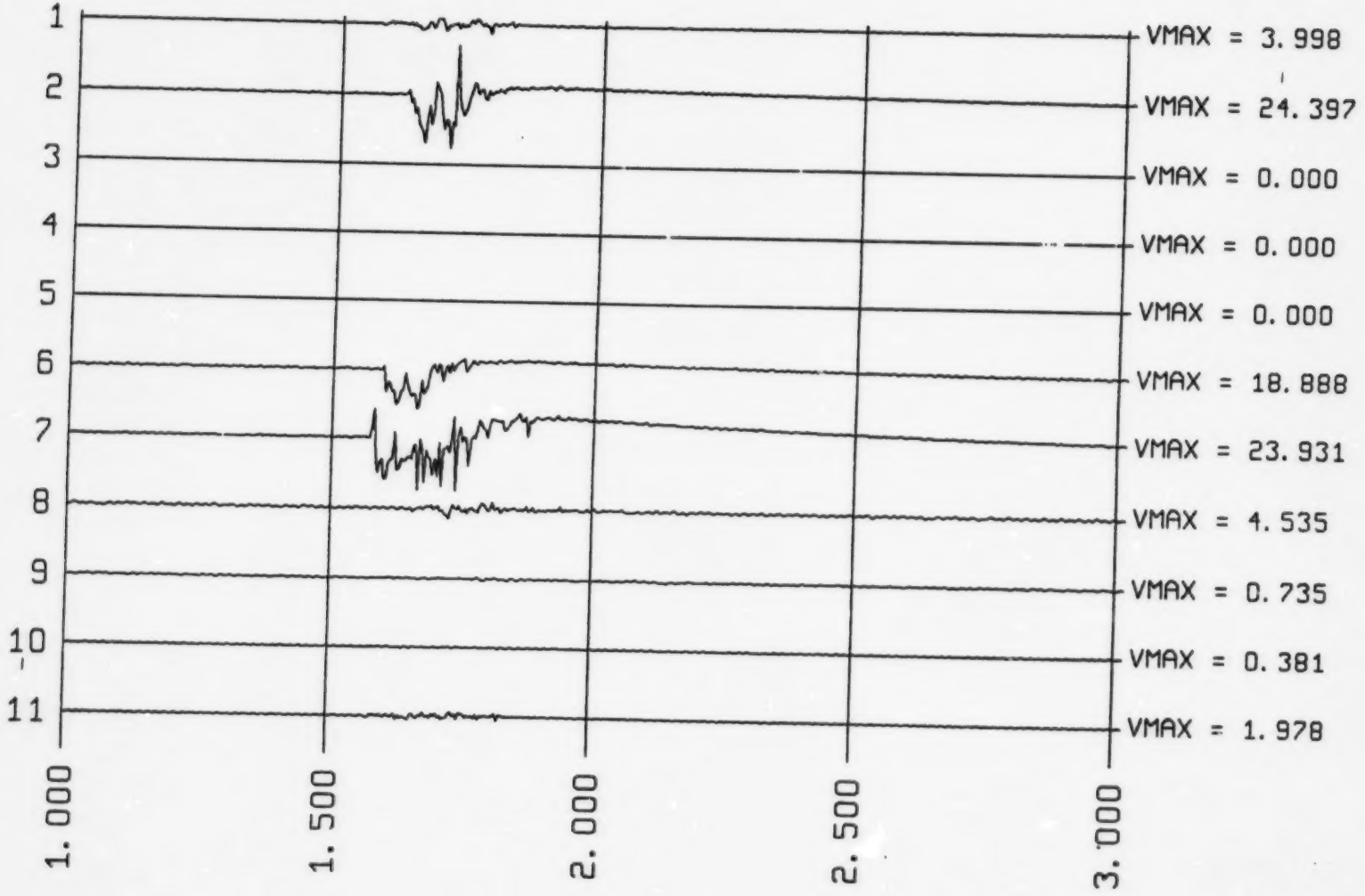

UNIFORM EARTH ERRORMAP FOR EVENT 1989/58/20:1:41

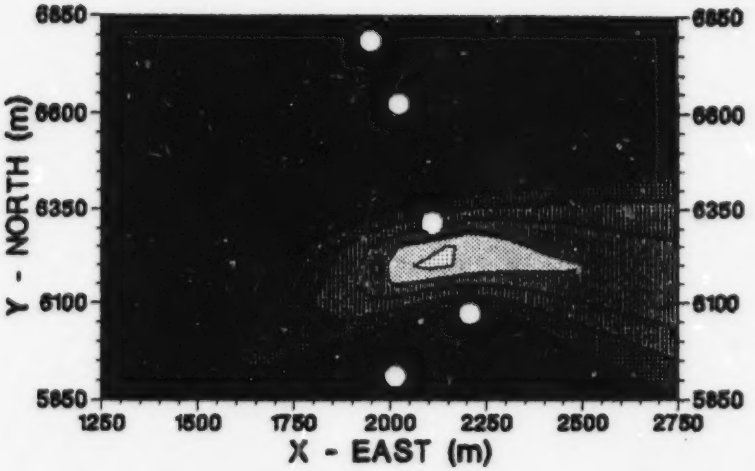

L1-norm SOLUTION
VELOCITY = 4725 m/sec

HORIZONTAL SECTION IS AT
300 m VERTICAL (Z)

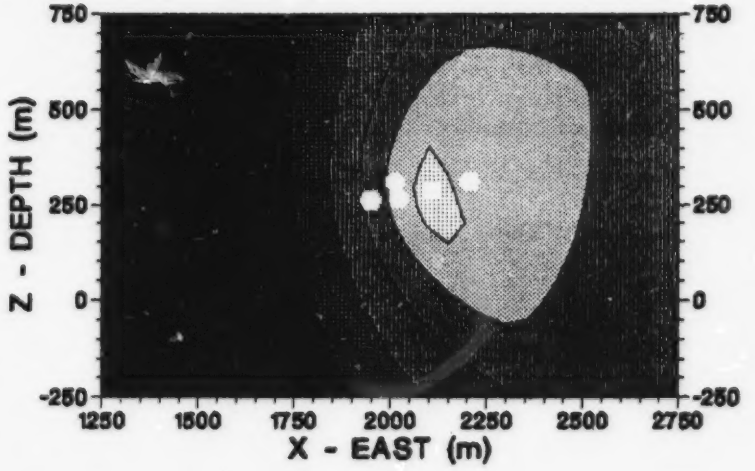

VERTICAL SECTION ALONG
6200 m NORTH (Y)

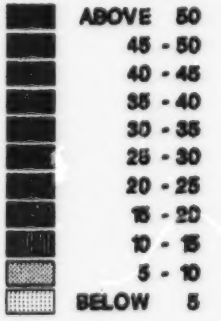

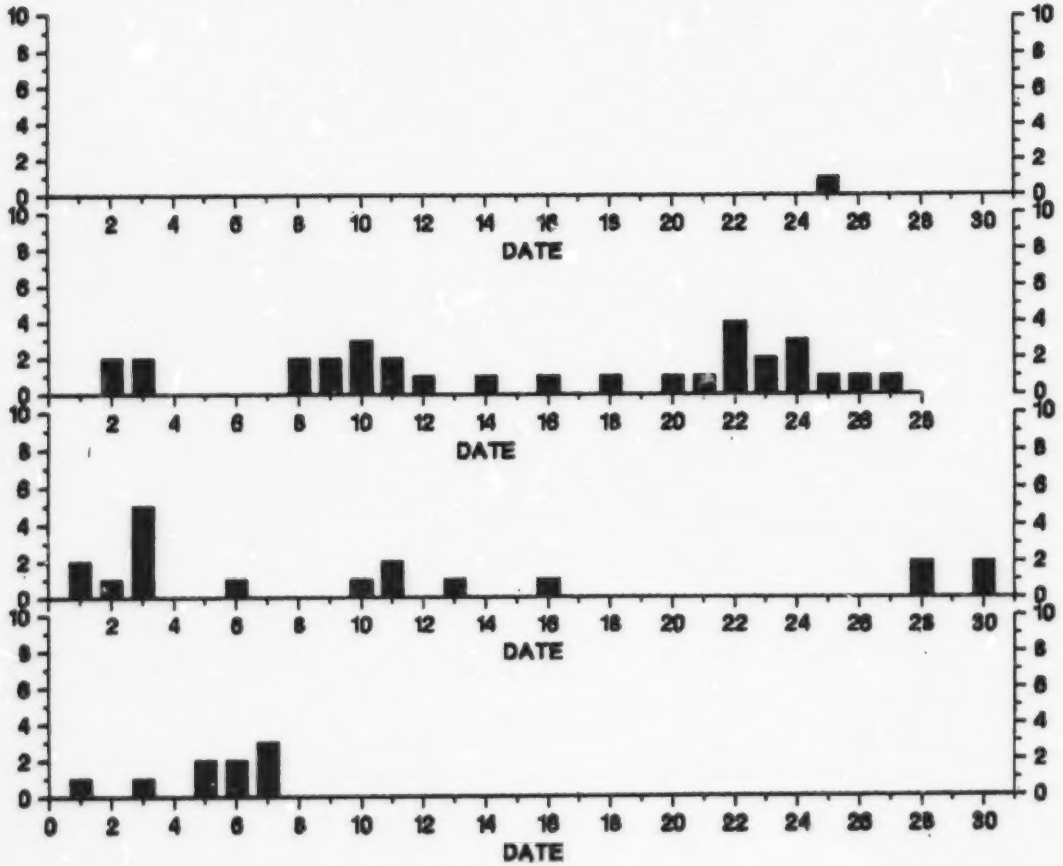

CLOVER HILL NB.
JANUARY 1989
EVENTS PER DAY = 0.1

CLOVER HILL NB.
FEBRUARY 1989
EVENTS PER DAY = 1.1

CLOVER HILL NB.
MARCH 1989
EVENTS PER DAY = 0.8

CLOVER HILL NB.
APRIL 1989
EVENTS PER DAY = 1.1

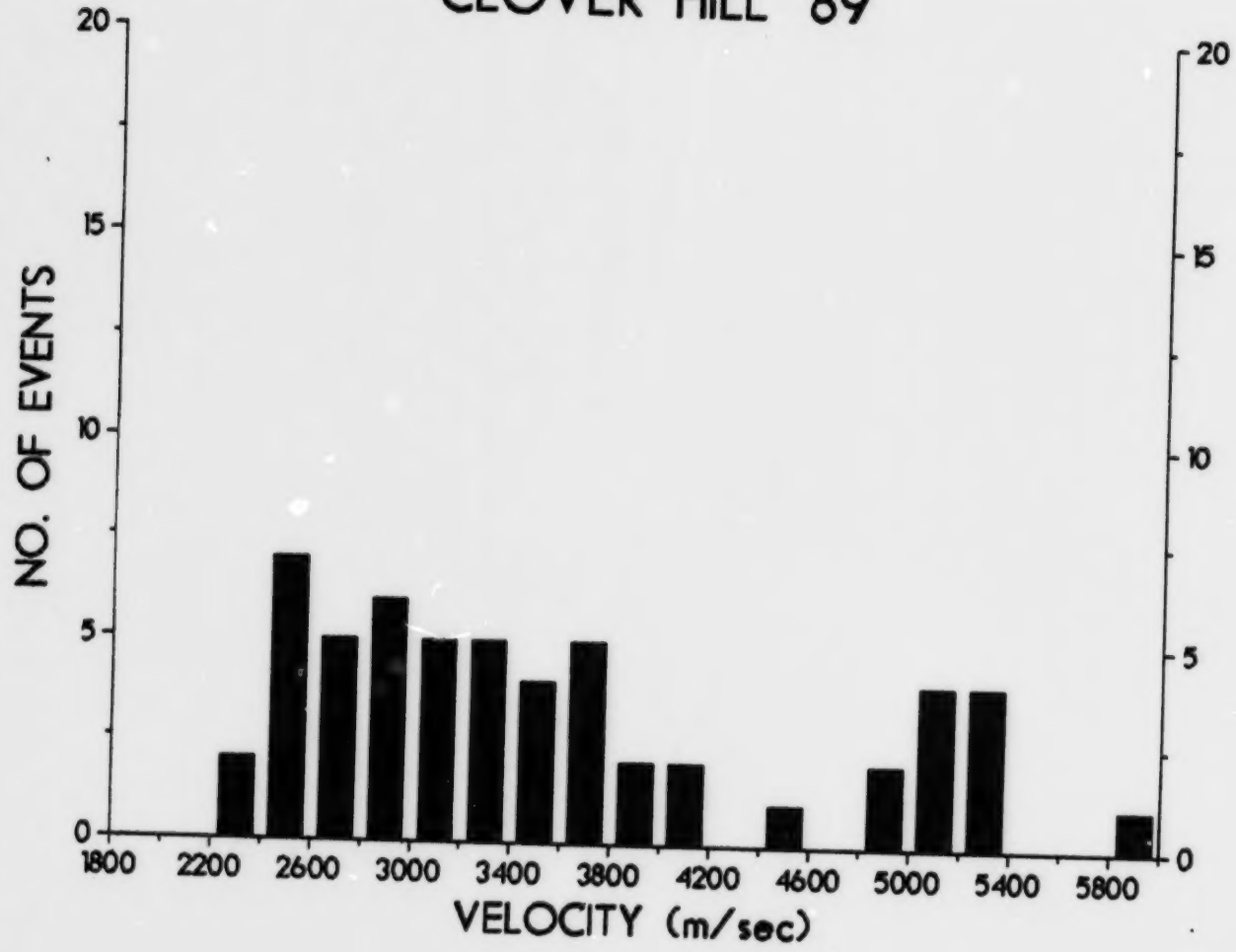
CLOVER HILL '89
NO. OF EVENTS
0
5
10
15
20
1800
2200
2600
3000
3400
3800
4200
4600
5000
5400
5800
VELOCITY (m/sec)

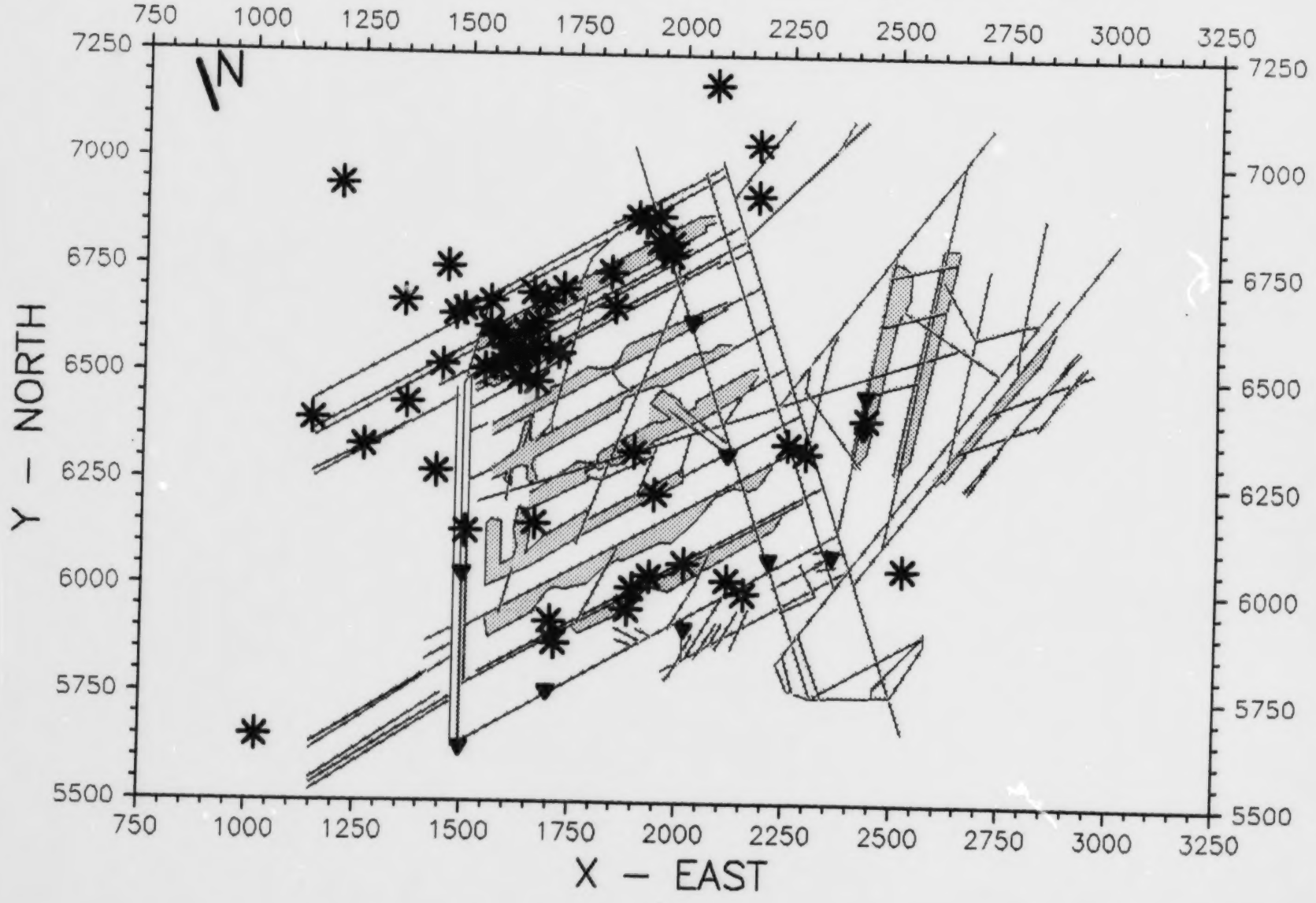
CLOVER HILL: 25/01 – 07/04, 1989
N
750
1000
1250
1500
1750
2000
2250
2500
2750
3000
3250
7250
7000
6750
6500
6250
6000
5750
5500
Y – NORTH
X – EAST

RECURSIVE OR FEEDBACK DIGITAL FILTERS

Arnfinn Prugger, Dept. of Geological Sciences
University of Saskatchewan, Saskatoon (S7N-0W0).

For some recorded seismic events high background noise levels of one kind or another can completely obliterate the incoming seismic signal. This makes the accurate picking of arrival times next to impossible, (which leads to incorrect source locations), and hampers spectral analysis and other source mechanism studies. The predominant noise problem seen in mine environments is powerline interference of 60 Hz and/or harmonics of 60 Hz. Other noise might consist of low frequency amplifier drift, high frequency vibrations from machines, high frequency powerline harmonics, high or low frequency electrical transients, and so on. But as long as an event was recognized and the seismic signals were recorded, many types of noise can be eliminated by applying an appropriate digital filter to the recorded seismic signal.

The purpose of this appendix is to discuss in simple terms a fast method of digital filtering. Methods of deriving the various filter coefficients are not covered, only the final equations are presented : this is a practical guide rather than an exhaustive analysis (which can be found in Beauchamp and Yuen, 1979, or in Kanasewich, 1981, for example). The basic strategy for working out specific filter coefficients is to represent the desired convolution in terms of complex poles and zeros in the s-plane via the Laplace transform, then apply the z-transform operator to get a set of polynomials in z (where z is the delay operator). These final z-transform equations give the recursive filter coefficients. FORTRAN subroutines to carry out the various operations are included at the end of the Appendix. The algorithms are well suited to implementation on a micro-computer.

I wish to thank Dr. K. V. Paulson and Mr. P. R. Kosteniuk, (both of the Cybernetics Laboratory in the Department of Physics at the University of Saskatchewan in Saskatoon, Canada), for teaching me the basics of time-series analysis, including the techniques presented in this Appendix. The basis of what I present here comes from unpublished course notes of K. V. Paulson.

A.1 Background :

A seismic wiggle trace, or seismogram, is a record of ground vibration amplitude varying in the time domain. Filtering these signals usually involves the removal of certain frequency components, so it is advantageous to view seismic data in the frequency domain. This is achieved by computing the Fourier transform of the seismic wiggles, to change vibration amplitudes varying in time to vibration amplitudes varying as a function of frequency ; (for a clear and in-depth discussion of the Fourier transform see Brigham, 1974).

Digital filtering is essentially a running, weighted-averaging process (convolution) applied to the original seismogram to give the desired "filtered" output. The key is to work out the appropriate filter coefficients (the numbers we multiply the original data by) to give the desired response. Unfortunately, convolution filters require a great deal of computational effort, and are thus often too slow to be implemented on smaller micro-computers. For example, if a seismic trace is made up of N = 1000 data points an ideal convolution filter to remove the 60 Hz interference from the trace would require 2(N**2) = 2,000,000

multiplications and 2N(N-1) = 1,998,000 additions. A more practical filter that requires less computation is the "recursive", or "feedback" filter developed by Shanks (1967). A recursive filter is one where elements of the filtered trace are "fed back" and used, along with the unfiltered trace elements, to calculate the next element in the filtered trace. The most recently determined element is used to determine the next element in the filtered sequence, and so on until the entire trace is filtered. The general recursive filter relation is :

$$y(t) = \sum_{s=0}^{m} a_s\, x(t-s) \;-\; \sum_{s=1}^{n} b_s\, y(t-s) \qquad (A.1)$$

where "a" and "b" are the filter coefficients, "x(t)" is the unfiltered input sequence (original seismic trace), and "y(t)" is the filtered output sequence. Output y(t) depends on former values of y(t), hence the name feedback, or recursive.

As an example, consider the filtering operation :

$$y(t) = [\, a_0 x(t) + a_1 x(t-1) + a_2 x(t-2) \,] - [\, b_1 y(t-1) + b_2 y(t-2) \,] \qquad (A.2)$$

where (a_0, a_1, a_2) are filter coefficients applied to the original unfiltered seismic trace and (b_1, b_2) are filter coefficients applied to previous samples of the filtered trace. Application of this filter results in a y(t) that is somewhat distorted (ie.- the trace will be phase shifted). To keep the filtered output zero phase (ie.- no artificial phase shift added to the filtered trace) the filter must be applied twice : first forward ("from left to right"), then backwards

("from right to left") along the trace. The filter strategy is then :

1. apply the recursive filter given in (A.2) to the data set x(t) to form y(t);
2. reverse y(t) to form y'(t);
3. apply the recursive filter to y'(t) as in step 1 to form z(t);
4. reverse z(t) to form z'(t), (as in step 2) ; z'(t) is then the zero-phase filtered version of x(t).

On a seismic data trace of 1000 samples this set of steps to remove 60 Hz interference from the trace takes 12N = 12,000 multiplications and 8N = 8,000 additions. This is far less work for the computer than the convolution filter, which takes 200 times as much effort.

Derivation of the filter coefficients "a" and "b" depends on whether you want to remove a narrow band about a single frequency (NOTCH), all frequencies above a certain frequency (HIGH-CUT), or all frequencies below a certain frequency (LOW-CUT), as well as on the digital sampling interval "T" and the "order" of the filter (explained in section A.4). Each of these operations is addressed separately.

A.2 NOTCH Filtering :

To remove a narrow band about a single frequency the filter operator in (A.1) becomes :

$$Y(t) = GMLT\ [\ a_0X(t) + a_1X(t-1) + a_2X(t-2)\ ]\ -\ [\ b_1Y(t-1) + b_2Y(t-2)\ ] \qquad (A.3)$$

where : T = digital sampling interval in seconds
FREQ = frequency you want to remove in Hertz (Hz)
PI = 3.141593
FNQ = 1.0 / (2.0 * T) = Nyqvist Frequency
OMEGA = FREQ * PI / FNQ
GMLT = 1.0 / 1.01 = gain

a_0 = 1.00000
a_1 = -2.0 * cos(OMEGA)
a_2 = 1.00000

b_1 = GMLT * -2.0 * cos(OMEGA)
b_2 = GMLT * GMLT

The recursive algorithm for removing a 60 Hz notch was tested on input of a time domain unit spike (Figure A1), which has a flat amplitude response across all frequencies in the frequency domain (Figure A2). In each of these figures trace 1 is the original, unfiltered trace and trace 2 is the filtered version of trace 1. Note the attenuation of the trace 2 signal at 60 Hz in Figure A2, which is what we wanted. If greater attenuation of the frequency is needed, the notch filter should be applied two or three times in succession to the trace ; this process of applying a filter numerous times is called "cascading".

Seismic data from a six channel recording system operated at the Cory potash mine is shown in Figure A3, with corresponding Fourier transforms of these wiggle traces in Figure A4. Note the 60 Hz powerline interference, weak on channel 2 and severe to the point of obliterating the seismic signal on channel 6. The result of applying the recursive 60 Hz notch filter to channels 2 and 6 is shown in Figures A5 and A6. The filter works extremely well : a signal similar in character to that of the other geophones has "emerged" on channel 6 ; note the reduction in amplitude at 60 Hz in Figure A6 (filtered) compared to Figure A4 (original

unfiltered data), while other frequency components remain relatively unchanged by the filtering procedure.

A.3 The Butterworth Filter :

A convenient type of filter for removing a frequency band is the "Butterworth" filter, described in any textbook on time-series analysis; (see, for example, Kanasewich, 1981, pp. 252-277). In the frequency domain the HIGH-CUT (low-pass) Butterworth filter is defined by the amplitude response :

$$\P\ H(f)\ \P \;=\; \frac{1}{[\ 1\ +\ (\ f\ /\ FC\ )^{**}2N\ ]\ **\ 1/2} \qquad (\ A.4\ )$$

where :
- f = frequency
- ¶ H(f) ¶ = signal amplitude as a function of frequency
- FC = "corner" frequency
- N = "order" of the filter

The "corner" frequency FC is the frequency at which the input amplitude will be diminished by 50% (-3 db), and the "order" of the filter dictates how sharp the cut-off is above FC . This is illustrated in Figure A7, a plot of amplitude response (¶ H(f) ¶ of equation A.4) versus frequency (f). It is important to note the following :

¶ H(f) ¶ = 1 for f << FC

¶ H(f) ¶ = 1 / 2 for f = FC

¶ H(f) ¶ = (FC/f) for f >> FC

In other words, frequencies below the corner frequency are not really affected by the Butterworth filter, while frequencies above FC are significantly reduced (especially for the high order filter). There

is a corresponding equation A.4 (and Figure A7) for the LOW-CUT (high-pass) Butterworth filter.

A.4 HIGH-CUT (low-pass) Filtering :

To remove all frequencies HIGHER than the corner frequency with a second order Butterworth Filter, use the recursive relationship A.3, where :

```
T     =  digital sampling interval in seconds
PI    =  3.141593
FNQ   =  1.0 / ( 2.0 * T ) = Nyqvist Frequency
FC    =  corner frequency in Hertz (Hz)
WA    =  tan( PI * FC * T )
N     =  2  =  order of the filter
PHI   =  PI * ( 2 + N - 1 ) / ( 2*N )
      =  PI * 3 / 4
GMLT  =  1  /  (WA**2 - 2.0*WA*cos(PHI) + 1)                    ( A.5 )

a0 =  WA**2
a1 =  2.0 * WA**2
a2 =  WA**2

b1 =  GMLT * 2.0 * (WA**2 - 1)
b2 =  GMLT * (WA**2 + 2.0*WA*cos(PHI) + 1)
```

Note that filter coefficients a_S and b_S, and gain GMLT in equation A.3 have changed.

Once the equation for a SECOND ORDER LOW-PASS filter has been worked out, the best way to create a higher order EVEN filter is to "cascade" the second order filter (equation A.5) often enough to give the desired attenuation above FC . "Cascading" a filter simply means "to apply an operator numerous times in succession" to the input data. It is simpler to do this than it is to derive the required lengthier and more complicated set of high-order filter coefficients. Furthermore, cascading small filters is generally preferable to applying single, long operators, since this helps avoid roundoff

errors inherent in the computer application of the technique.

For example, if you want to apply an eighth order filter to a signal trace, you should apply the second order filter (equation A.5) four times in succession. The only term in A.5 that changes for higher order (EVEN) filter operators is PHI, (s-plane "pole" locations), which is given by :

$$PHI(i) = PI * (2*i + N - 1) / 2*N \quad , \quad i = 1, N/2 \qquad (A.6)$$

So then for the example of an eighth order filter (i.e.- 4 x 2nd order), we would have i = 1, 2, 3, 4 giving :

$$\begin{aligned} PHI(1) &= PI * (2*1 + 8 - 1) / 2*8 = PI * 9 / 16 \\ PHI(2) &= PI * (2*2 + 8 - 1) / 2*8 = PI * 11 / 16 \\ PHI(3) &= PI * (2*3 + 8 - 1) / 2*8 = PI * 13 / 16 \\ PHI(4) &= PI * (2*4 + 8 - 1) / 2*8 = PI * 15 / 16 \end{aligned}$$

where i = 1 for the first pass of the filter, i = 2 for the second pass, and so on.

The recursive algorithm for removing frequencies above 75 Hz with an eighth order Butterworth filter was tested, (as for the NOTCH filter in section A.3), on input of a unit spike (with a flat amplitude response across all frequencies). Data are plotted in the time domain in Figure A8 and in the frequency domain in Figure A9 ; once again, in each figure trace 1 is the original, unfiltered trace and trace 2 is the filtered version of trace 1. Note the attenuation of the trace 2 signal above 75 Hz in Figure A9, which is what we wanted. And of course, to get a steeper attenuation at 75 Hz a higher order filter should be used.

Seismic data from a six channel recording system operated at the Vanscoy mine is shown in Figures A10 and A11. Note the strong powerline interference apparent on most channels and virtually obliterating the seismic signal on channel 5. But now many traces, notably 1, 3, and 6, are further degraded by significant high frequency noise (most of this noise came from faulty amplifiers, along with some 60 Hz harmonic interference). The result of applying both a recursive high-cut filter (eighth order, with a corner frequency of 100 Hz), along with a 60 Hz notch filter to all channels is shown in Figures A12 and A13. The results are obvious : seismic signals that were tough, if not impossible, to discern are now much clearer. (One might argue that we should have gone even further, filtering down to 50 or 60 Hz, but this is incidental to what is being presented here).

A.5 LOW-CUT (high-pass) Filtering :

To remove all frequencies LOWER than the corner frequency with a second order Butterworth Filter, again use the recursive relationship A.3, where :

```
T     =  digital sampling interval in seconds
PI    =  3.141593
FNQ   =  1.0 / ( 2.0 * T ) = Nyqvist Frequency
FC    =  corner frequency in Hertz (Hz)
WA    =  tan( PI * FC * T )
N     =  2  =  order of the filter
PHI   =  PI * ( 2 + N - 1 ) / ( 2*N )
      =  PI * 3 / 4
GMLT  =  1  /  (WA**2 - 2.0*WA*cos(PHI) + 1)
```

(A.7)

$a_0 = 1.0$
$a_1 = -2.0$
$a_2 = 1.0$

b_1 = GMLT * 2.0 * (WA**2 - 1)
b_2 = GMLT * (WA**2 + 2.0*WA*cos(PHI) + 1)

Note that equation A.7 is the same as the HIGH-CUT filter equation A.5 except for filter coefficients a_s and b_s.

As with the HIGH-CUT filter, the best way to create a higher order EVEN LOW-CUT filter is to "cascade" the second order filter of equation A.7 often enough to give the desired attenuation below FC, as discussed in section A.2 . The only term in A.7 that changes for higher order EVEN filter operators is PHI, (s-plane "pole" locations), given by equation A.6 .

The recursive algorithm for removing frequencies below 25 Hz with an eighth order Butterworth filter was tested, (as for the examples in section A.3 and A.4), on input of a unit spike, with a flat amplitude response across all frequencies. Data are plotted in the time domain in Figure A14 and in the frequency domain in Figure A15 ; once again, in each figure trace 1 is the original, unfiltered trace and trace 2 is the filtered version of trace 1. Note the attenuation of the trace 2 signal below 25 Hz in Figure A15, which is what we wanted.

Seismic data from a six channel recording system operated at the Cory mine is shown in Figures A16 and A17. Note the strong low frequency pulse, (some sort of electrical transient), at about 3.0 seconds visible on all channels. The transient completely dominates all frequency spectra, and would obviously corrupt any spectral analysis of these signals. But once a recursive low-cut filter (eighth order, with a corner frequency of 10 Hz) has been applied to all channels, as shown Figures A18 and A19, things look much better.

A1 Trace 1 is a unit spike at 2.5 s and trace 2 shows the time-domain effect of applying a 60 Hz notch filter to trace 1.

A2 The above traces plotted in the frequency domain.

A3 Seismograms for event 1983/285/08:03:32 (unfiltered).

A4 Spectra of seismograms for event 1983/285/08:03:32 (unfiltered) plotted in the frequency domain.

A5 Seismograms for event 1983/285/08:03:32 after application of the 60 Hz notch filter.

A6 Spectra of seismograms for event 1983/285/08:03:32 after filtering.

A7 Frequency-domain ampitude response of the Butterworth high-cut filter.

A8 Trace 1 is a unit spike and trace 2 shows the time-domain effect of applying a 75 Hz high-cut filter to trace 1.

A9 The above traces plotted in the frequency domain.

A10 Seismograms for event 1988/090/10:27:34 (unfiltered).

A11 Spectra of seismograms for event 1988/090/10:27:34 (unfiltered).

A12 Seismograms for event 1988/090/10:27:34 after application of the 75 Hz high-cut filter.

A13 Spectra of seismograms for event 1988/090/10:27:34 after filtering.

A14 Trace 1 is a unit spike and trace 2 shows the time-domain effect of applying a 25 Hz low-cut filter to trace 1.

A15 The above traces plotted in the frequency domain.

A16 Seismograms for event 1983/164/08:15:45 (unfiltered).

A17 Spectra of seismograms for event 1983/164/08:15:45 (unfiltered).

A18 Seismograms for event 1983/164/08:15:45 after application of the 25 Hz low-cut filter.

A19 Spectra of seismograms for event 1983/164/08:15:45 after filtering.

MICRO-EARTHQUAKE SEISMOGRAMS (1988/182/12/30/59)
(VELOCITY DATA IN μmeters / second)

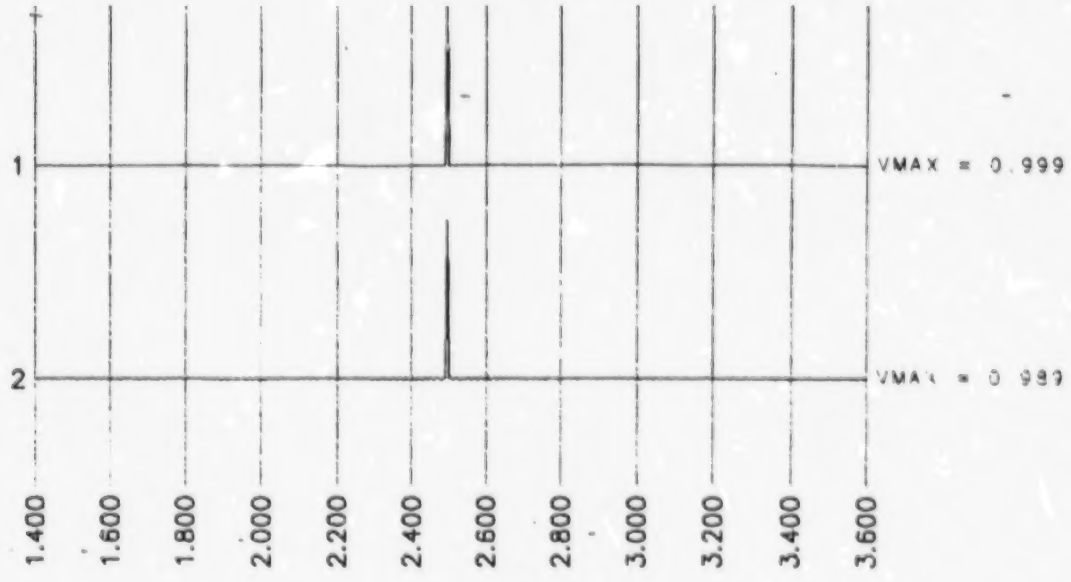

EVENT : 1988/182/12/30/59
1024 POINT FFT OF VELOCITY (μmeter/sec) DATA

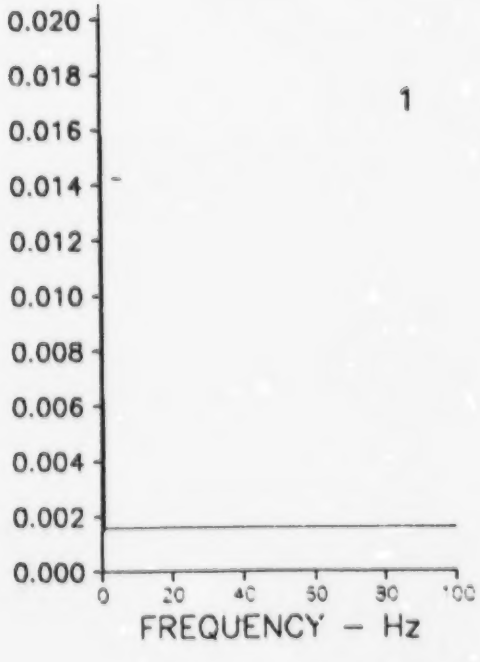

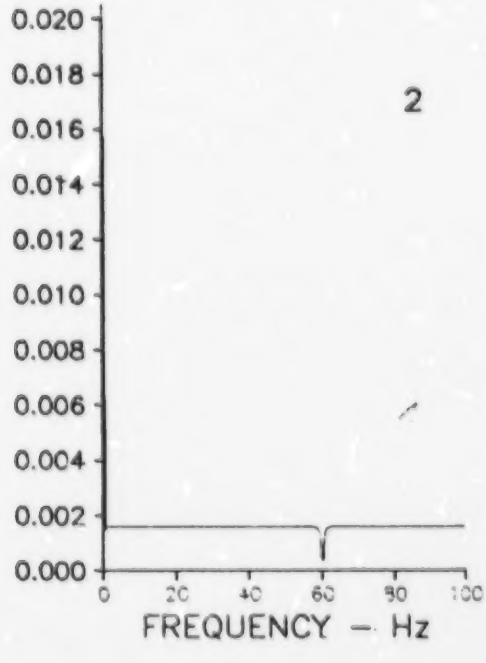

MICRO–EARTHQUAKE SEISMOGRAMS (1983/285/8/3/32)

(VELOCITY DATA IN μmeters / second)

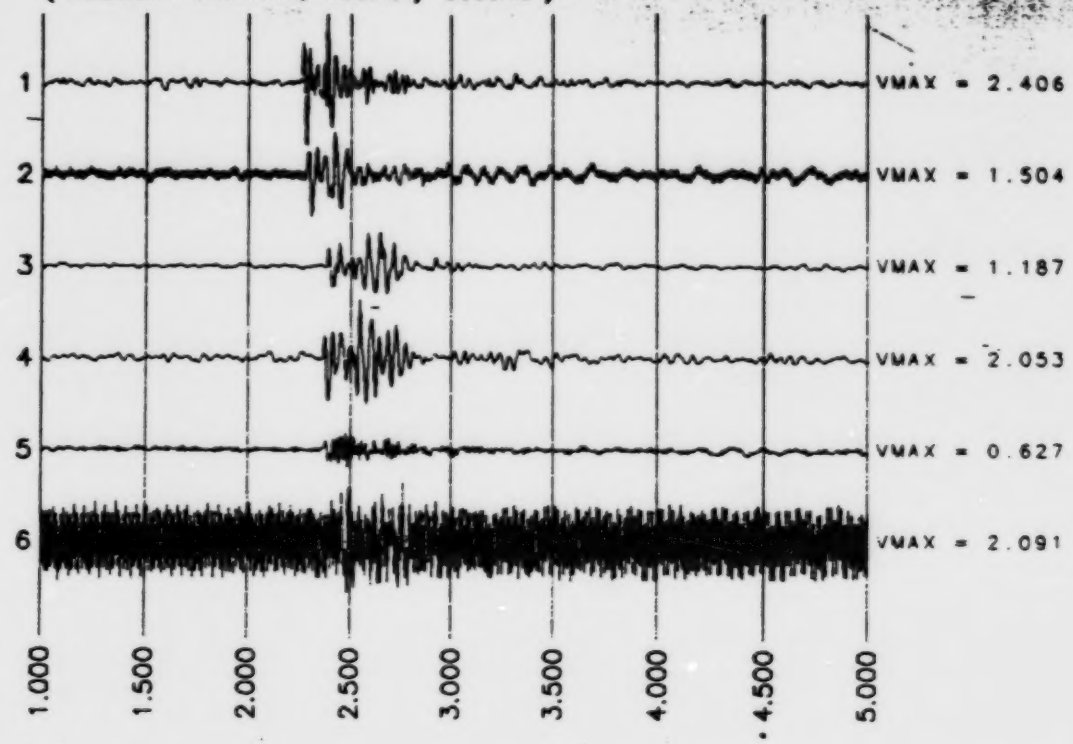

EVENT : 1983/285/8/3/32

256 POINT FFT OF VELOCITY (μmeter/sec) DATA

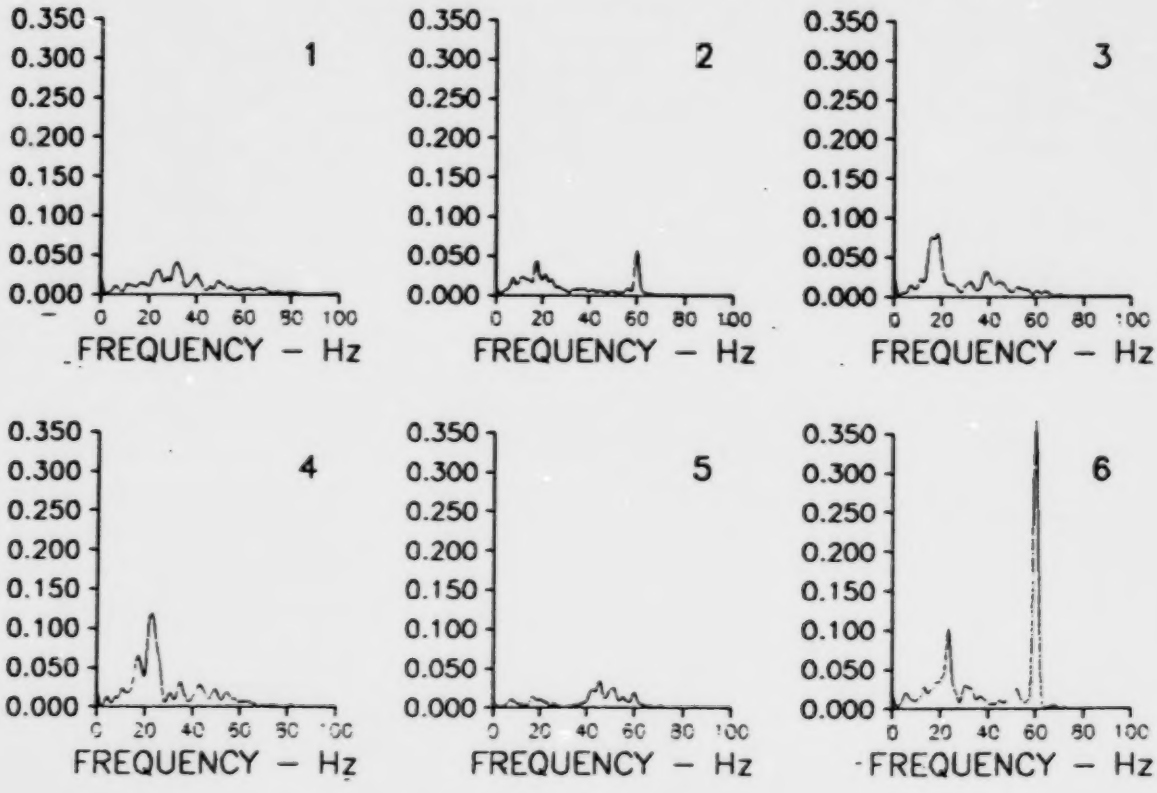

MICRO-EARTHQUAKE SEISMOGRAMS (1983/285/8/3/32).

(VELOCITY DATA IN μmeters / second)

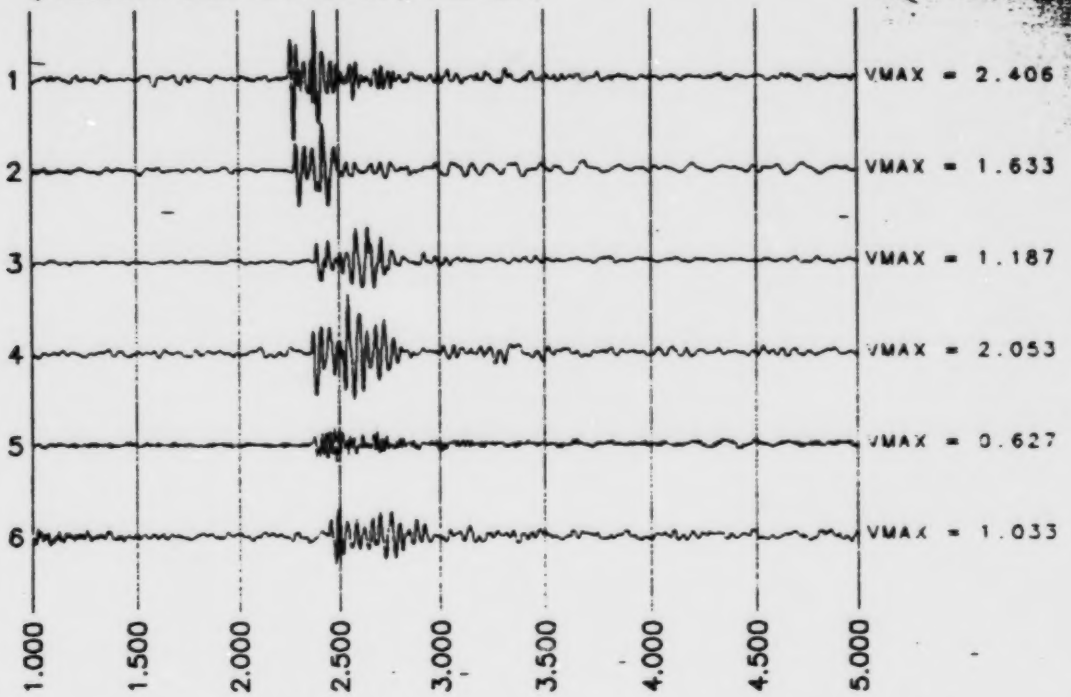

EVENT : 1983/285/8/3/32

256 POINT FFT OF VELOCITY (μmeter/sec) DATA

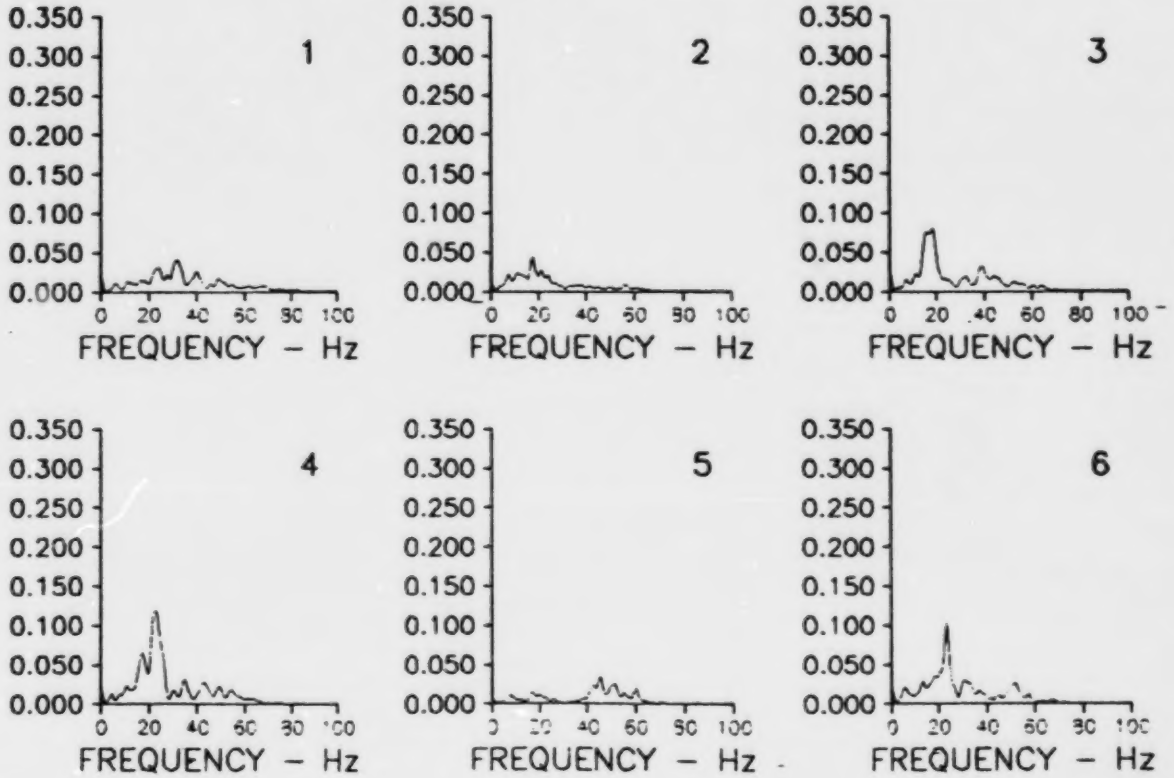

BUTTERWORTH HIGH-CUT FILTER

for N = 2, N = 4, and N = 8

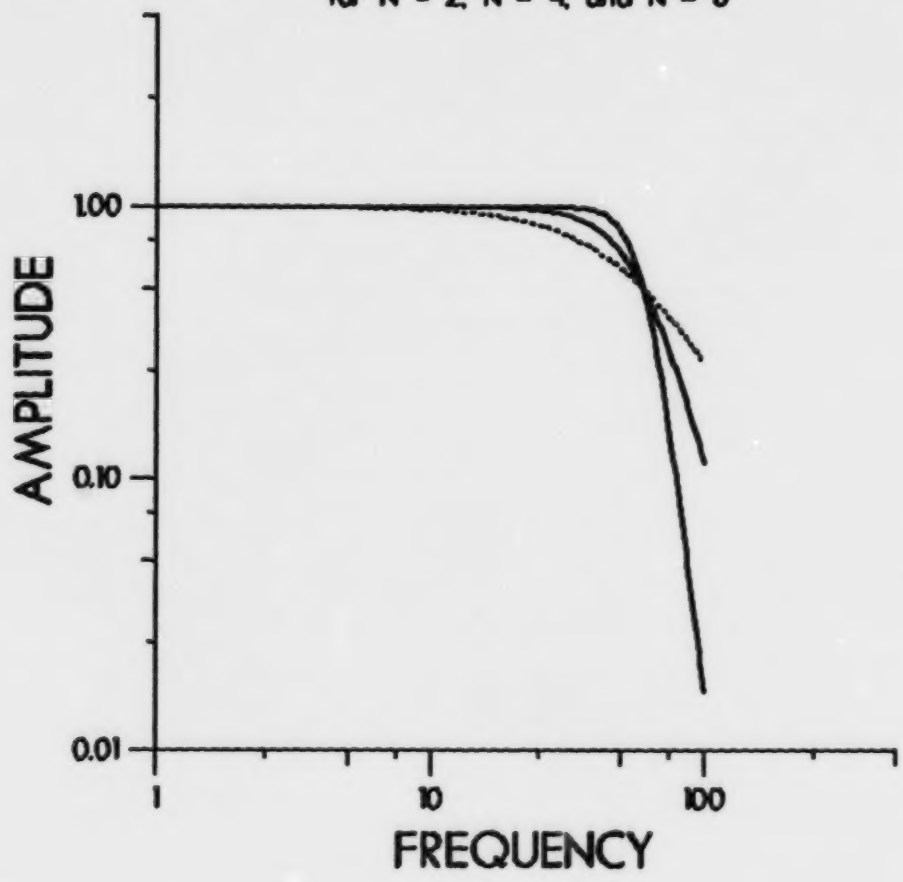

MICRO–EARTHQUAKE SEISMOGRAMS (1988/182/12/30/59)

(VELOCITY DATA IN μmeters / second)

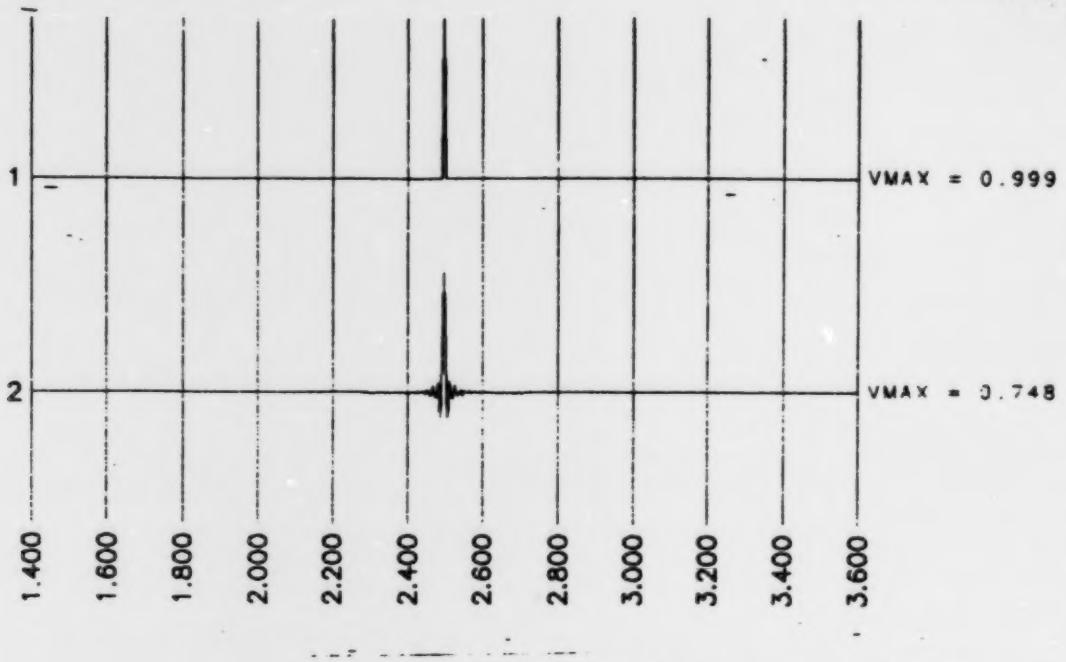

EVENT : 1988/182/12/30/59

1024 POINT FFT OF VELOCITY (μmeter/sec) DATA

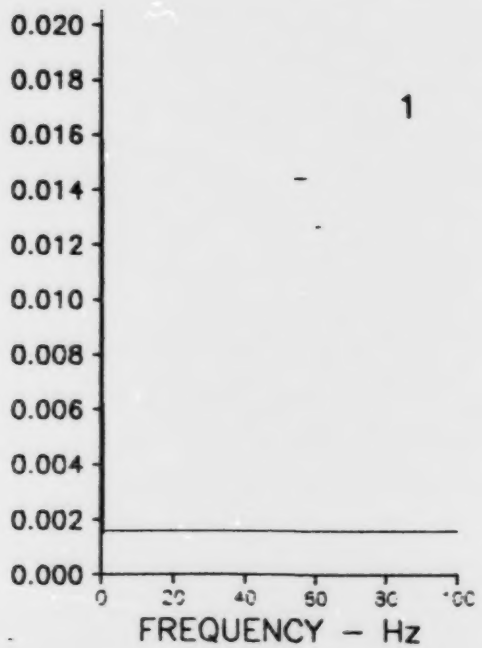

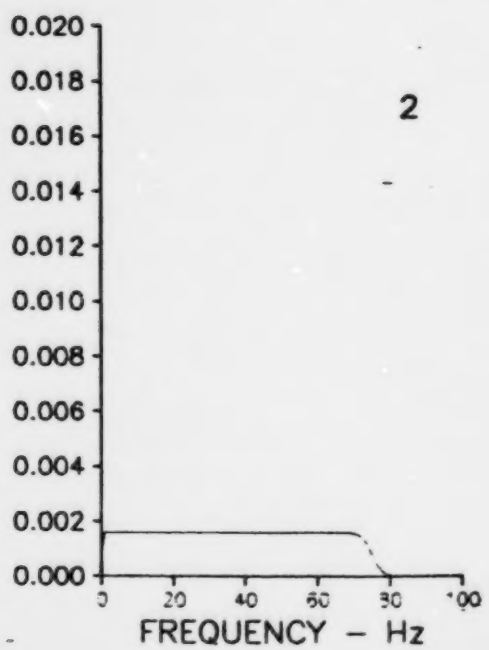

MICRO-EARTHQUAKE SEISMOGRAMS (1988/90/10/27/34)

(VELOCITY DATA IN μmeters / second)

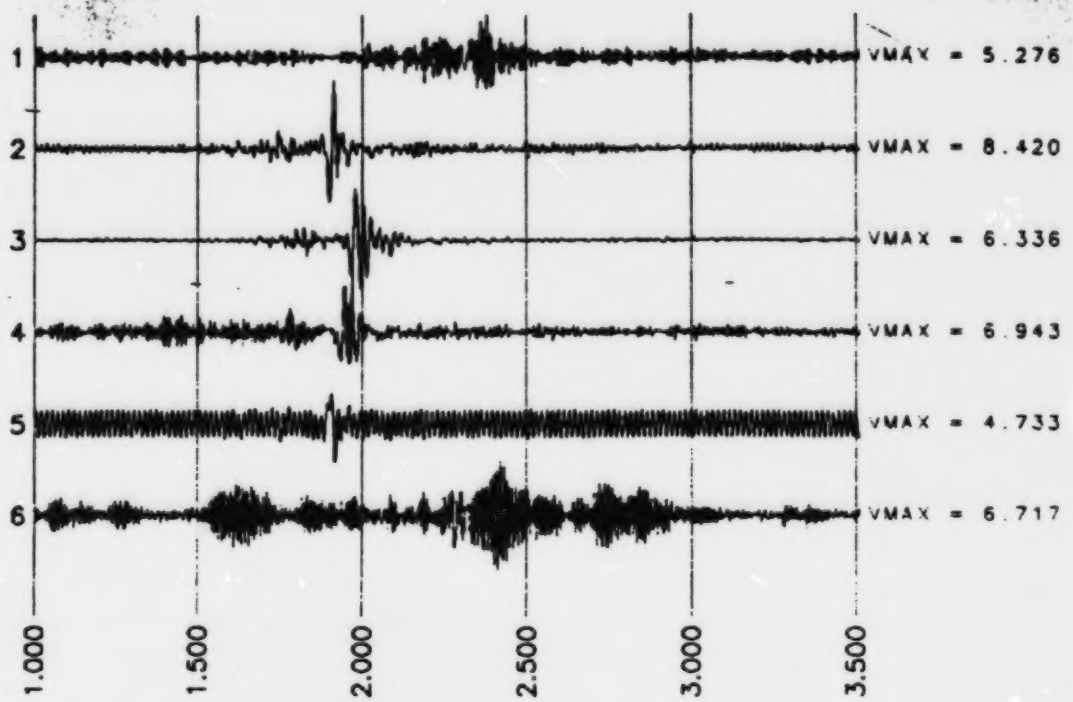

EVENT : 1988/90/10/27/34

1024 POINT FFT OF VELOCITY (μmeter/sec) DATA

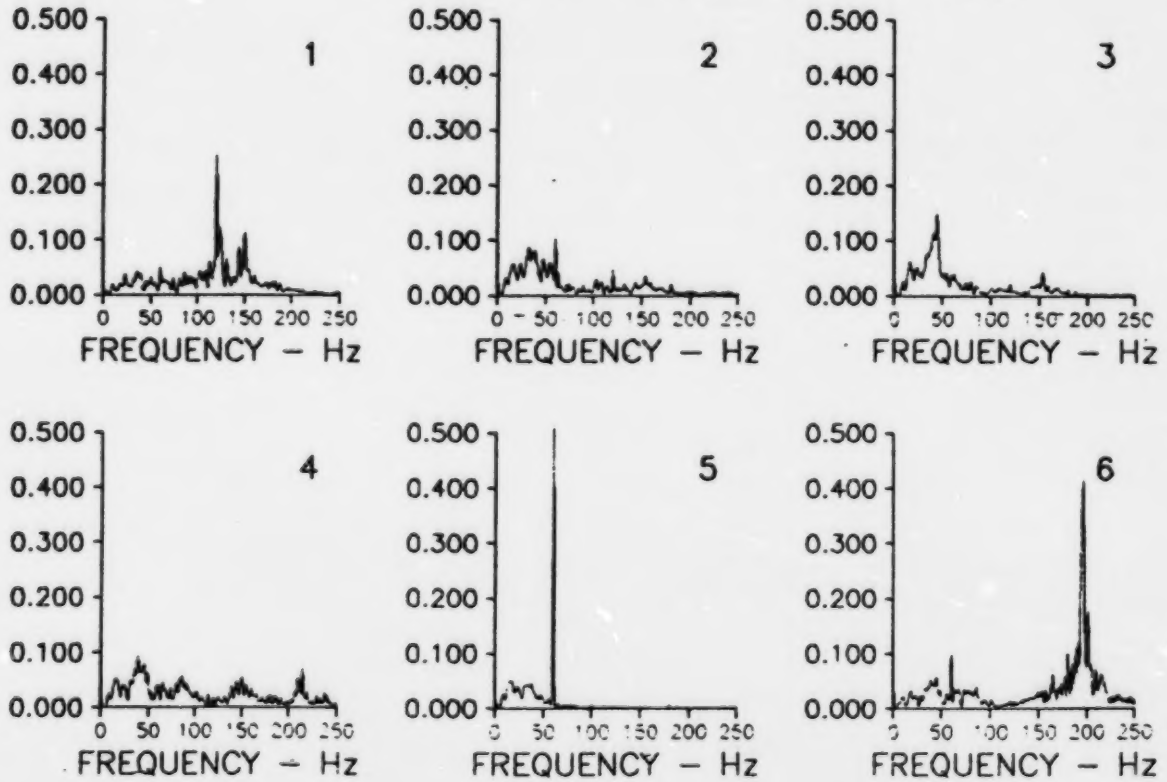

MICRO–EARTHQUAKE SEISMOGRAMS (1988/90/10/27/34)

(VELOCITY DATA IN μmeters / second)

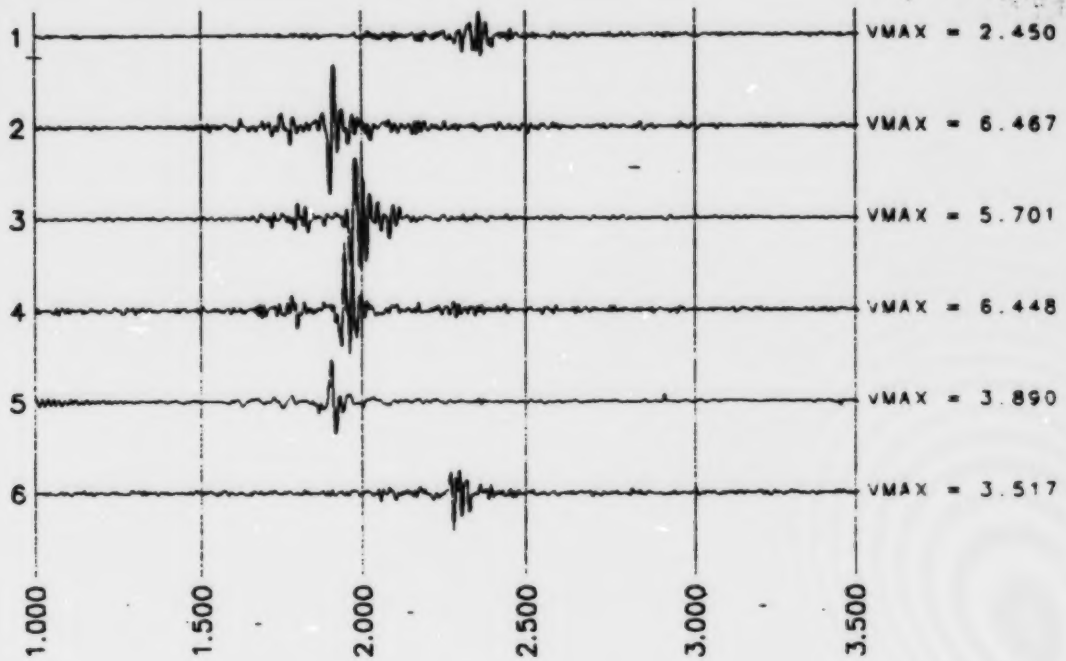

EVENT : 1988/90/10/27/34

1024 POINT FFT OF VELOCITY (μmeter/sec) DATA

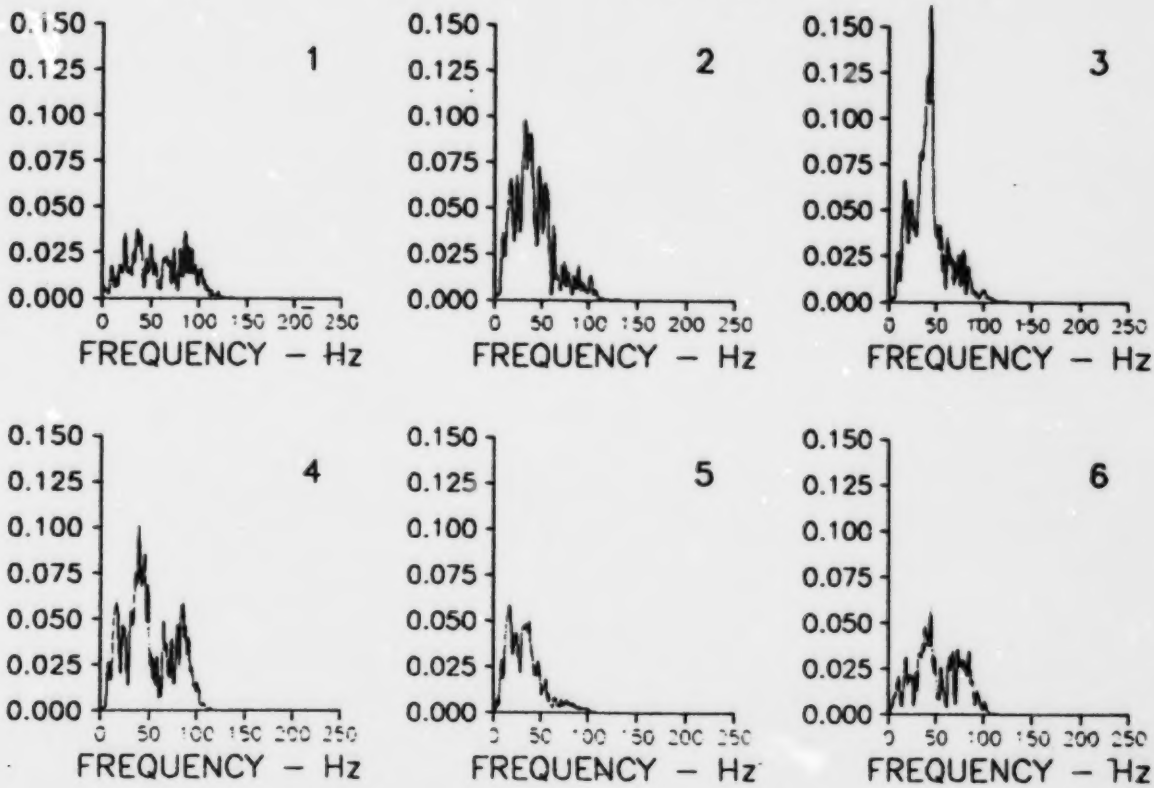

MICRO–EARTHQUAKE SEISMOGRAMS (1988/182/12/30/59)

(VELOCITY DATA IN μmeters / second)

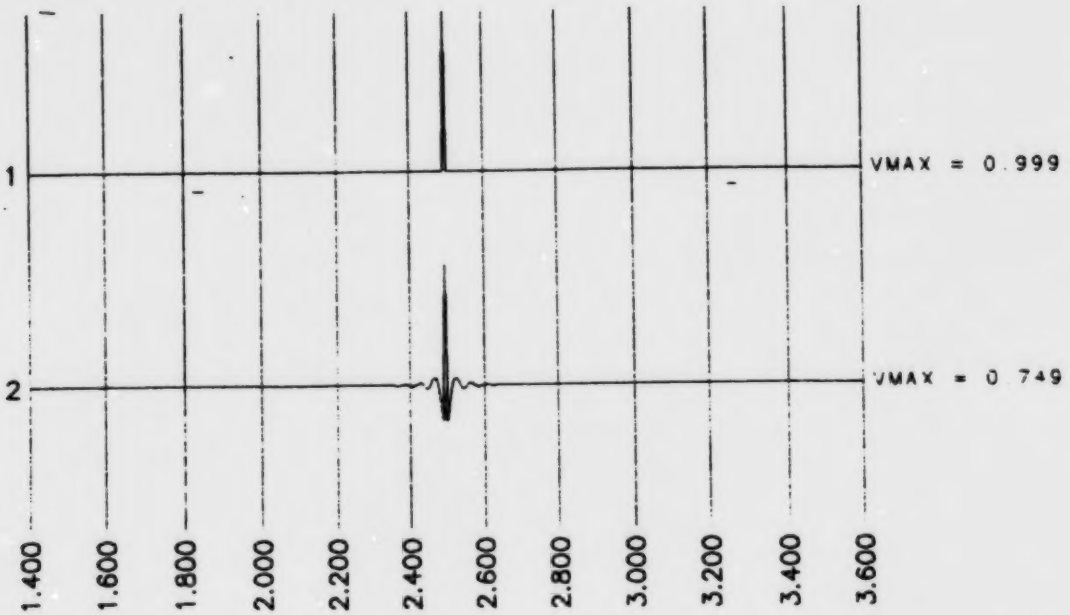

EVENT : 1988/182/12/30/59

1024 POINT FFT OF VELOCITY (μmeter/sec) DATA

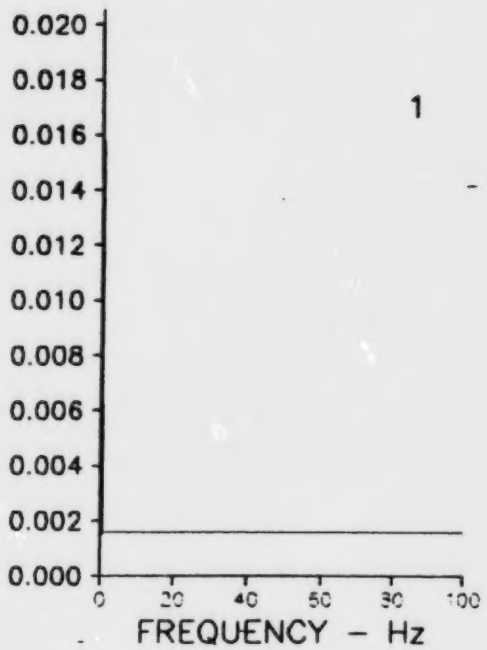

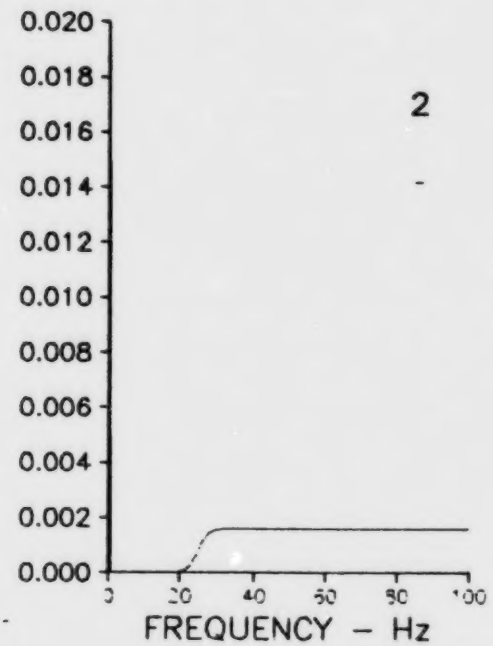

MICRO-EARTHQUAKE SEISMOGRAMS (1983/164/8/15/45)

(VELOCITY DATA IN μmeters / second)

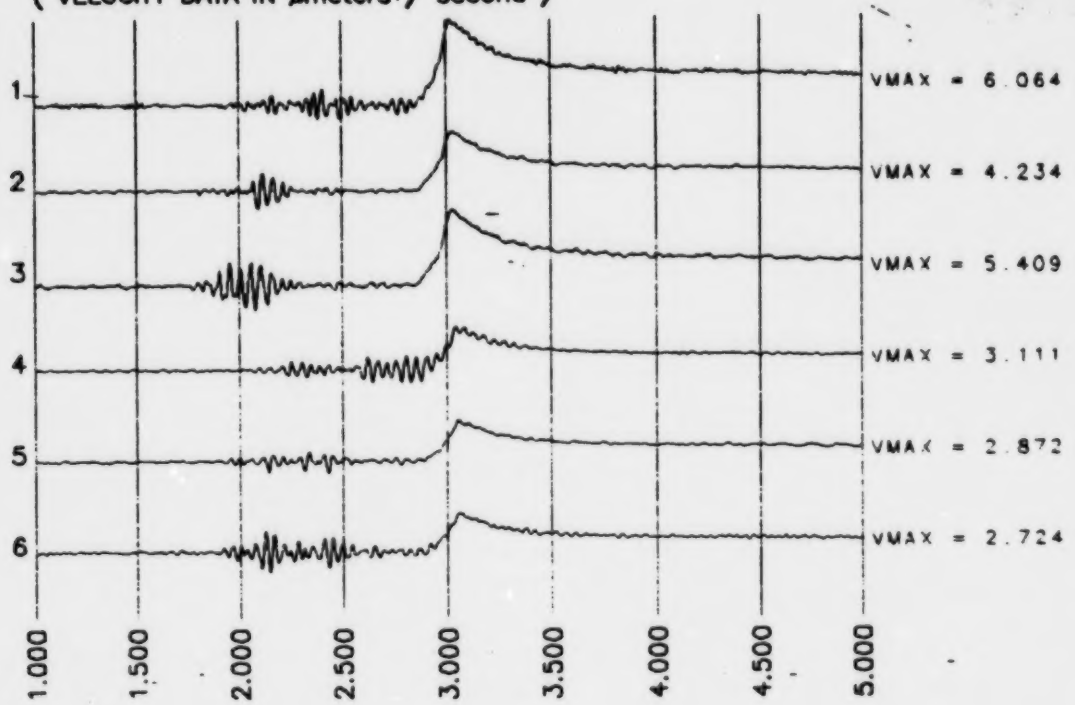

EVENT : 1983/164/8/15/45

512 POINT FFT OF VELOCITY (μmeter/sec) DATA

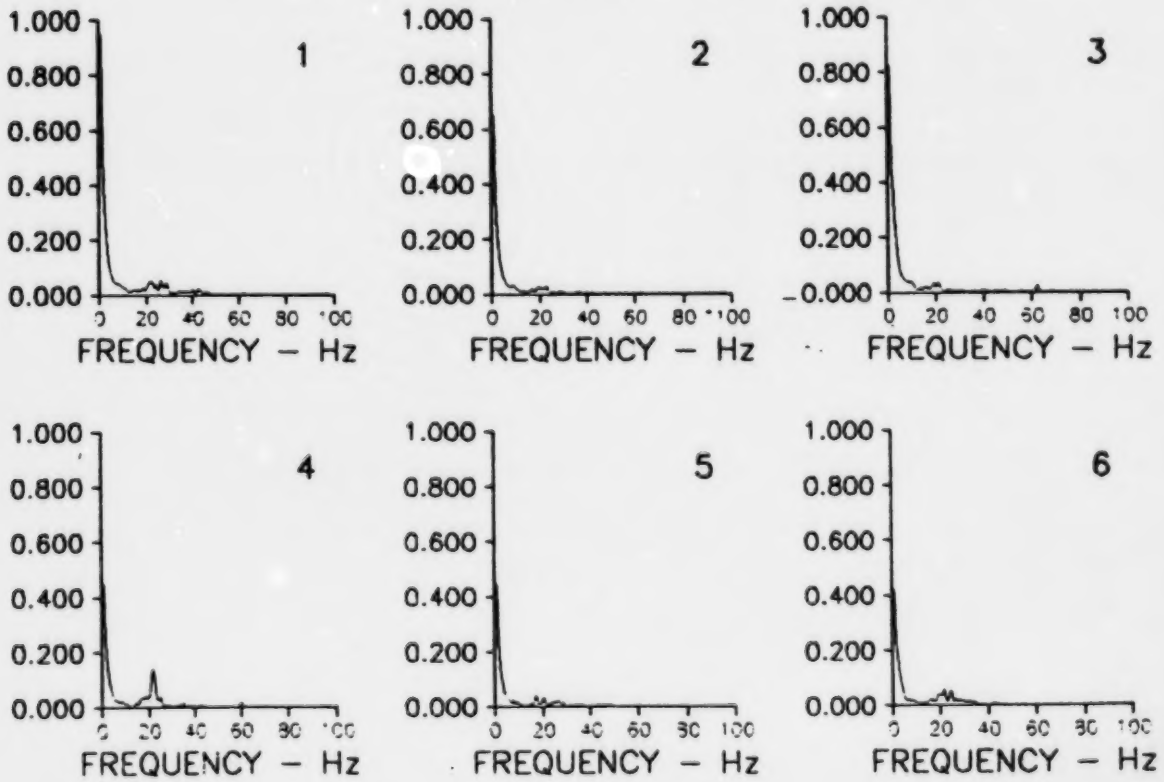

MICRO-EARTHQUAKE SEISMOGRAMS (1983/164/8/15/45)

(VELOCITY DATA IN μmeters / second)

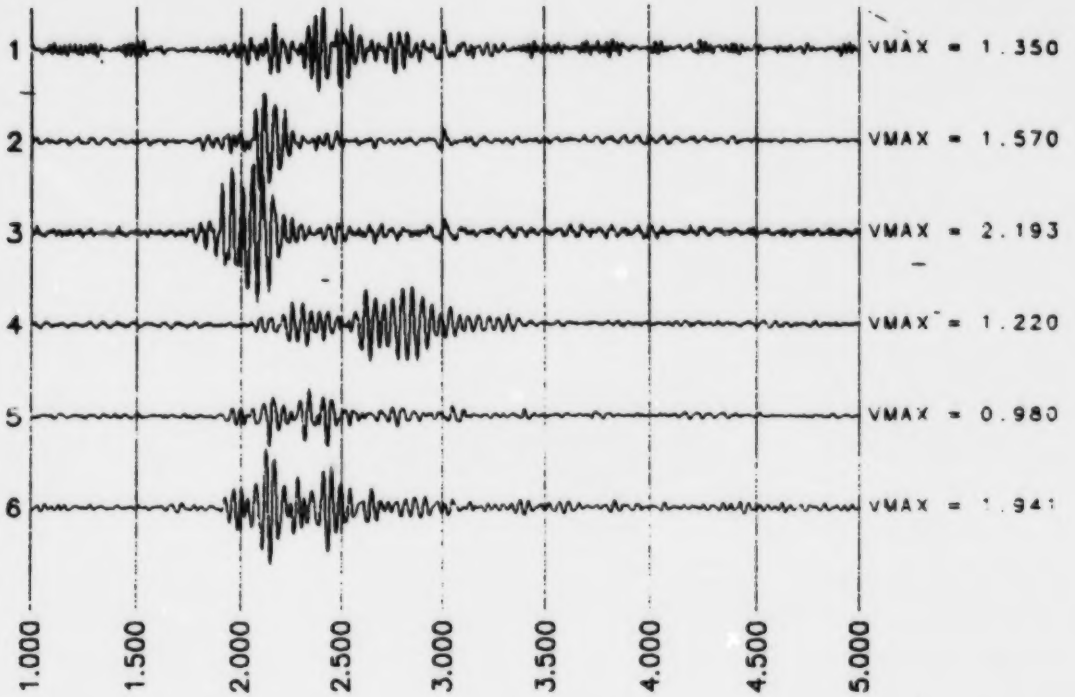

EVENT : 1983/164/8/15/45

512 POINT FFT OF VELOCITY (μmeter/sec) DATA

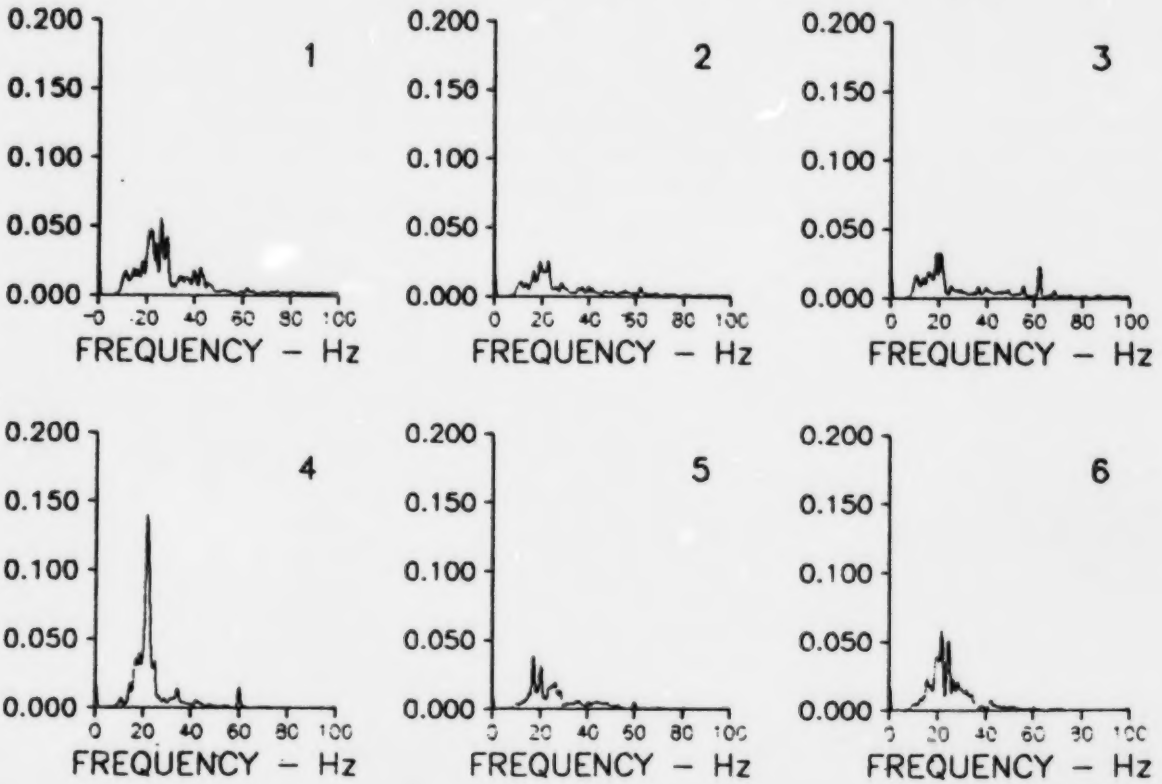

```
C*
C*
C*
C*
      SUBROUTINE FLTNCH(I,FRQ)
C*
C*
C*****************************************************************
C*
C*    NOTCH FILTER TO BE APPLIED TO SINGLE CHANNEL MICRO-
C*    EARTHQUAKE DATA.  METHODOLOGY FOLLOWED IS THAT OF
C*    SHANKS,1967, 'RECURSION FILTERS FOR DIGITAL PRO-
C*    CESSING', GEOPHYSICS, VOL.32, PP.33-51.
C*
C*    'I' is the trace to be filtered;
C*    'FRQ' is the single frequency to be removed.
C*
C*    ARNFINN PRUGGER
C*    NOVEMBER, 1986.
C*
C*****************************************************************
C*
C*
      DIMENSION VTMP(3500),VFLT(3500)
      COMMON NDP,NGF,TSTP,VDAT(16,6050)
      NCNT = 0
      PI = 4.0 * ATAN(1.0)
C*
C*
C*****************************************************************
C*
C*    DEFINITION OF VARIABLES :
C*
C*    1. VTMP(3500), VFLT(3500) are temporary work vectors;
C*    2. NDP is the Number of Data Points;
C*    3. NGF is the Number of Geophones;
C*    4. TSTP is the Time-STeP, or digital sampling interval;
C*    5. VDAT(NGF,NDP) is the vector containing the seismogram
C*       data and VDAT(I,NDP) the trace to be filtered ;  note
C*       that on output VDAT(I,NDP) contains the filtered data.
C*
C*    NOW SET FILTER COEFFICIENTS ("NUMETRATOR"/"DENOMINATOR"),
C*    AS DEFINED IN THE ACCOMPANYING PAPER.
C*
C*****************************************************************
C*
C*
      FNQ = 1.0 / ( 2.0 * TSTP )
      OMEGA = FRQ * PI / FNQ
      GMLT = 1.0 / 1.01
      RNUM1 =  1.0000
      RNUM2 =  -2.0 * COS(OMEGA)
      RNUM3 =  1.0000
      DNOM1 =  1.0000
      DNOM2 =  GMLT * -2.0 * COS(OMEGA)
      DNOM3 =  GMLT**2
```

```
C*
C*
C*************************************************************
C*
C*    "FOLD OVER" THE FIRST AND LAST 200 DATA POINTS
C*    AND APPLY A SINE TAPER TO AVOID END EFFECTS
C*    WHEN APPLYING THE FILTER.
C*
C*************************************************************
C*
C*
      DO 10 J=1,200
        VTMP(J) = SIN((J-1)*PI/400) * VDAT(I,201-J)
        VTMP(200+NDP+J) = SIN((200-J)*PI/400) * VDAT(I,1+NDP-J)
   10 CONTINUE
      DO 15 J=1,NDP
        VTMP(J+200) = VDAT(I,J)
   15 CONTINUE
      NNET = 400 + NDP
C*
C*
C*************************************************************
C*
C*    APPLY THE 60 HZ RECURSIVE FILTER.  NOTE THAT THE
C*    FILTER IS APPLIED IN BOTH DIRECTIONS, FIRST FROM LEFT
C*    TO RIGHT, THEN FROM RIGHT TO LEFT IN ORDER TO KEEP THE
C*    FILTER ZERO-PHASE.
C*
C*************************************************************
C*
C*
   19 VFLT(1) = GMLT * VTMP(1)
      VFLT(2) = GMLT * ( VTMP(2) + RNUM2 * VTMP(1) ) -
     *                      DNOM2 * VFLT(1)
      DO 20 J=3,NNET
        VFLT(J) = GMLT * ( VTMP(J) + RNUM2 * VTMP(J-1) + VTMP(J-2) ) -
     *                 ( DNOM2 * VFLT(J-1) + DNOM3 * VFLT(J-2) )
   20   CONTINUE
C*
C*
      DO 30 J=1,NNET
        VTMP(J) = VFLT(NNET+1-J)
   30 CONTINUE
      NCNT = NCNT + 1
      IF(NCNT.LE.1)GO TO 19
C*
C*
      DO 40 J=1,NDP
        VDAT(I,J) = VTMP(J+200)
   40 CONTINUE
C*
C*
      RETURN
      END
```

```
C*
C*
C*
C*
      SUBROUTINE FLTLOW(ITRC,NORD,FC)
C*
C*
C*********************************************************************
C*
C*    RECURSIVE 'Nth' ORDER BUTTERWORTH HIGH-PASS, OR LOW-CUT
C*    FILTER, TO BE APPLIED TO SINGLE CHANNEL MICRO-EARTHQUAKE
C*    DATA.  HIGH ORDER FILTERS ARE CREATED BY CASCADING ENOUGH
C*    2nd ORDER FILTERS TOGETHER.  N MUST BE AN EVEN NUMBER !
C*
C*    'ITRC' is the trace to be filtered;
C*    'NORD' is the order of the filter; AN EVEN NUMBER !
C*    'FC' is the corner frequency.
C*
C*    ARNFINN PRUGGER
C*    JUNE, 1987.
C*
C*********************************************************************
C*
C*
      DIMENSION X(6050),Y(6050),YREV(6050)
      COMMON NDP,NGF,TSTP,VDAT(16,6050)
      PI = 4.0 * ATAN(1.0)
C*
C*
C*********************************************************************
C*
C*    DEFINITION OF VARIABLES :
C*
C*    1. X(6050), Y(6050) & YREV(6050) are temporary work vectors;
C*    2. NDP is the Number of Data Points;
C*    3. NGF is the Number of Geophones;
C*    4. TSTP is the Time-STeP, or digital sampling interval;
C*    5. VDAT(NGF,NDP) is the vector containing the seismogram
C*       data and VDAT(ITRC,NDP) is the trace to be filtered ;
C*       on output VDAT(ITRC,NDP) contains the filtered data.
C*
C*********************************************************************
C*
C*
      DO 10 J=1,NDP
        X(J) = VDAT(ITRC,J)
   10 CONTINUE
      PI = 4.0 * ATAN(1.0)
      FNQ = 1.0 / ( 2.0 * TSTP )
      NPAS = IFIX(FLOAT(NORD) / 2.0)
```

```
C*
C*
C*************************************************************************
C*
C*    IN THIS SECTION FIRST THE FILTER COEFFICIENTS ARE
C*    CALCULATED FOR EACH PASS OF THE FILTER (LOOP 20), THEN
C*    THE FILTER IS APPLIED TO THE DATA TRACE "X" (LOOP 30),
C*    THEN THE FILTERED TRACE IS REVERSED (LOOP 40) AND THE
C*    FILTER IS APPLIED AGAIN TO GIVE A ZERO PHASE OUTPUT.
C*    THIS IS REPEATED UNTIL THE DESIRED FILTER ORDER IS
C*    ACHIEVED.
C*
C*    FILTER COEFFICIENTS ("NUMETRATOR"/"DENOMINATOR"), ARE
C*    DEFINED IN THE ACCOMPANYING PAPER.
C*
C*************************************************************************
C*
C*
      WA = TAN( PI * FC * TSTP )
      R1 =  1.000000
      R2 = -2.000000
      R3 =  1.000000
      D1 =  1.000000
      DO 20 I=1,NPAS
        IFLG = 0
        PHI = PI * FLOAT(I+I+NORD-1) / (2.0*FLOAT(NORD))
        GMLT = 1.0 / (WA**2 - 2.0*WA*COS(PHI) + 1.0)
        D2 = GMLT * 2.0 * (WA**2 - 1.0)
        D3 = GMLT * (WA**2 + 2.0*WA*COS(PHI) + 1.0)
   88   Y(1) = GMLT * X(1)
        Y(2) = GMLT * (X(2) + R2*X(1)) - D2*Y(1)
        DO 30 J=3,NDP
          Y(J) = GMLT * ( X(J) + R2*X(J-1) + X(J-2) ) -
     *           ( D2*Y(J-1) + D3*Y(J-2) )
   30   CONTINUE
        DO 40 J=1,NDP
          YREV(J) = Y(NDP-J+1)
   40   CONTINUE
        DO 50 J=1,NDP
          X(J) = YREV(J)
   50   CONTINUE
C*
C*
        IF(IFLG.LT.1)THEN
          IFLG = 2
          GO TO 88
        END IF
C*
C*
   20 CONTINUE
C*
C*
      DO 60 J=1,NDP
        VDAT(ITRC,J) = X(J)
   60 CONTINUE
C*
C*
      RETURN
      END
```

```
C*
C*
C*
C*
      SUBROUTINE FLTHIH(ITRC,NORD,FC)
C*
C*
C*************************************************************************
C*
C*    RECURSIVE 'Nth' ORDER BUTTERWORTH LOW-PASS OR HIGH-CUT
C*    FILTER, TO BE APPLIED TO SINGLE CHANNEL MICRO-EARTHQUAKE
C*    DATA.  HIGH ORDER FILTERS ARE CREATED BY CASCADING ENOUGH
C*    2nd ORDER FILTERS TOGETHER.  N MUST BE AN EVEN NUMBER !
C*
C*    'ITRC' is the trace to be filtered;
C*    'NORD' is the order of the filter; AN EVEN NUMBER !
C*    'FC' is the corner frequency.
C*
C*    ARNFINN PRUGGER
C*    JUNE, 1988.
C*
C*************************************************************************
C*
C*
      DIMENSION X(6050),Y(6050),YREV(6050)
      COMMON NDP,NGF,TSTP,VDAT(16,6050)
      PI = 4.0 * ATAN(1.0)
C*
C*
C*************************************************************************
C*
C*    DEFINITION OF VARIABLES :
C*
C*    1. X(6050), Y(6050) & YREV(6050) are temporary work vectors;
C*    2. NDP is the Number of Data Points;
C*    3. NGF is the Number of Geophones;
C*    4. TSTP is the Time-STeP, or digital sampling interval;
C*    5. VDAT(NGF,NDP) is the vector containing the seismogram
C*       data and VDAT(ITRC,NDP) is the trace to be filtered ;
C*       on output VDAT(ITRC,NDP) contains the filtered data.
C*
C*************************************************************************
C*
C*
      DO 10 J=1,NDP
        X(J) = VDAT(ITRC,J)
   10 CONTINUE
      PI = 4.0 * ATAN(1.0)
      FNQ = 1.0 / ( 2.0 * TSTP )
      NPAS = IFIX(FLOAT(NORD) / 2.0)
```

```
C*
C*
C*****************************************************************
C*
C*     IN THIS SECTION FIRST THE FILTER COEFFICIENTS ARE
C*     CALCULATED FOR EACH PASS OF THE FILTER (LOOP 20), THEN
C*     THE FILTER IS APPLIED TO THE DATA TRACE "X" (LOOP 30),
C*     THEN THE FILTERED TRACE IS REVERSED (LOOP 40) AND THE
C*     FILTER IS APPLIED AGAIN TO GIVE A ZERO PHASE OUTPUT.
C*     THIS IS REPEATED UNTIL THE DESIRED FILTER ORDER IS
C*     ACHIEVED.
C*
C*     FILTER COEFFICIENTS ("NUMETRATOR"/"DENOMINATOR"), ARE
C*     DEFINED IN THE ACCOMPANYING PAPER.
C*
C*****************************************************************
C*
C*
      WA = TAN( PI * FC * TSTP )
      R1 =  WA**2
      R2 =  2.0 * WA**2
      R3 =  WA**2
      D1 =  1.000000
      DO 20 I=1,NPAS
        IFLG = 0
        PHI = PI * FLOAT(I+I+NORD-1) / (2.0*FLOAT(NORD))
        GMLT = 1.0 / (WA**2 - 2.0*WA*COS(PHI) + 1.0)
        D2 = GMLT * 2.0 * (WA**2 - 1.0)
        D3 = GMLT * (WA**2 + 2.0*WA*COS(PHI) + 1.0)
   88   Y(1) = GMLT * X(1)
        Y(2) = GMLT * (X(2) + R2*X(1)) - D2*Y(1)
        DO 30 J=3,NDP
          Y(J) = GMLT * ( R1*X(J) + R2*X(J-1) + R3*X(J-2) ) -
     *           ( D2*Y(J-1) + D3*Y(J-2) )
   30   CONTINUE
        DO 40 J=1,NDP
          YREV(J) = Y(NDP-J+1)
   40   CONTINUE
        DO 50 J=1,NDP
          X(J) = YREV(J)
   50   CONTINUE
C*
C*
        IF(IFLG.LT.1)THEN
          IFLG = 2
          GO TO 88
        END IF
C*
C*
   20 CONTINUE
C*
C*
      DO 60 J=1,NDP
        VDAT(ITRC,J) = X(J)
   60 CONTINUE
C*
C*
      RETURN
      END
```

DISCUSSION OF ELECTRICAL INTERFERENCE PROBLEMS ENCOUNTERED DURING SEISMIC MONITORING, JANUARY - APRIL 1989, AT THE CLOVER HILL MINE, NEW BRUNSWICK.

Arnfinn Prugger

June, 1990.

Ambient electrical "noise" in the mine interfered with the seismic recording system throughout the monitoring period. The recording efficiency was therefore generally quite poor, and many rock-failure events were no-doubt missed because they happened to occur during times of increased electrical interference. This interference was due to a combination of :

i. induction of spike-transients from motors and switches into the long geophone cables - (this is apparently a common problem in mines where motors are thyrister controlled);

ii. an unstable power supply at the instrument site - (this problem was alleviated to some extent by the acquisition of a constant-voltage transformer);

iii. problems with some of the recording instruments, (ie.- some of the amplifiers failed during the course of the monitoring project).

Amplifier problems (iii.) can be avoided by installing new instruments rather than used gear (that has been running off and on in numerous experiments over many years). Properly installed hardware has been running continuously for three years at the IMC-K2 potash mine in Gerald, Saskatchewan.

Problems with an unstable power supply (ii.) and cable-induction (i.) will be more difficult to rectify. An isolated, grounded receptacle

(along with the constant-voltage transformer) would help stabilize the input line voltage, and using properly shielded, grounded geophone cable should decrease induction pickup. But these measures can sometimes be difficult to implement properly in the underground environment. A common solution to both of these electrical interference problems is to increase the amplitude of the seismic signals coming from the geophone ; seismic signals are thus boosted relative to the noise interference, which stays constant. There are many ways to achieve this increase in the signal-to-noise ratio ; here is a list of the techniques with which I have had some experience :

1. Increase the number of geophones at each station. By connecting successive sensors in SERIES a vibration signal which is the SUM of the signals from all geophones is sent down the wire. This is easy to implement, but signal levels can only be increased by a factor of two to four - it becomes impractical and expensive to install too many sensors. In most of seismic monitoring experiments that have been run in Saskatchewan two sensors were connected in series at each station.
2. Install an amplifier at each geophone station. This allows signal levels to be boosted by factors of 1000 (60 dB) or more right at the sensor. The amplified vibration signal is then commonly modulated on to an FM carrier frequency using a voltage controlled oscillator. This gives an FM signal that can be sent down very long cables with no induction pickup. As well, if a different FM carrier-frequency is chosen for each channel, modulated signals from many channels can be "multiplexed", or summed together, at a central location, then sent as one multiplexed signal along a single pair of wires

from underground, up the shaft, to the engineering office (for example). Before being digitized in the seismic recording computer the multiplexed signal is passed through a set of FM-frequency discriminators (one for each channel) which pick out the appropriate FM signal, then restore the amplified geophone signal from the carrier frequency. This procedure has been routinely used at earthquake monitoring stations for many years to get geophone signals from field stations to a central laboratory recorder ; FM modulated signals are sent via radio-telemetry from stations 30 and 60 km outside Saskatoon to the Geology building at the University of Saskatchewan. This is the method by which underground seismic signals are sent to offices on surface at the IMC-K2 mine near Gerald, Saskatchewan.

All electronic components discussed in this section can be purchased "off-the-shelf" from a number of supply companies (for example Teledyne, or Dyneer), and if treated sensibly this hardware will run continuously for years with virtually no maintenance. One difficulty with this setup is that power is required to drive the amplifier at each sensor. So except in the cases where sensors can be installed near a pre-existing power supply, cabling costs will increase substantially. As well, there might be some difficulty in ensuring a stable powerline voltage at each geophone site. A scientific limitation of this technique is that the FM frequencies that are used don't allow vibration signals with a frequency content greater than 50 Hz to be transmitted. This doesn't affect source location calculations, but failure mechanism analysis might not be possible on the band-limited signals.

3. Amplify and digitize the seismic signal at each geophone station. Sending an amplified digital signal via modem to the recording computer (set up in the engineering office on surface) is without a doubt the way seismic signals will be handled in the future. Modern seismic monitoring networks using field digitization have been set up at gold mines in South Africa and at some university earthquake recording stations in North America. The technique is so far unproven in a mine situation in North America. Hardware for carrying out field amplification / digitization is commercially available - one of the better manufacturers is based in Ottawa - but since these systems are still being developed, they require a fair amount of computer "tinkering" by the user. Again, power is required at each sensor, so the problem of ensuring a stable powerline voltage at each geophone site must be addressed. In addition to providing excellent noise suppression, a major advantage of field digitization is that seismic signals are not limited to less than 50 Hz, as with the FM-modulation systems. Apart from the potential difficulties of using new and unproven technologies, field digitization hardware tends to be more expensive than FM-modulation equipment.

The strong electrical interference so pervasive at the Clover Hill mine will have to be addressed when a permanent seismic monitoring array is placed in the mine. Hardware and cables will have to be installed with care to ensure that connections and are made properly. In addition, some thought have to be given to how to get a stable power-supply to the various instrument sites underground.

Unless a permanent, air-conditioned, dust-free office is built underground, the monitoring computer will have to be set up in the engineering office on surface ; (there are many obvious advantages to having computer on surface). This means that seismic signals will have to be amplified and either FM-modulated or digitized at each station underground (as discussed in items 2. and 3. earlier). While underground digitization has scientific advantages, it might be better for DPPC to go the FM-modulation route (2.), thus using a simpler technology that has proven itself over many years of continuous operation, the same system that is currently installed at the IMC-K2 mine in Gerald, Saskatchewan.

SUMMARY OF SEISMIC EVENT LOCATIONS, CLOVER HILL POTASH MINE, NEW BRUNSWICK

JANUARY - APRIL, 1989

Arnfinn Prugger

June, 1990

NOTE : Since geophones are all at mine level the uncertainty in calculated elevation is high. Unless events occurred near the mine level there is presently no way to tell whether they were some distance above or some distance below the mine.

1. 1989 25 16:53:20 (Jan. 25)

X (east) = 1450 +/- 50 m
Y (north) = 6750 +/- 50 m
Z (elev.) = 100 m (?)
V (speed) = 6000 m/sec
E (error) = .009 sec

2. 1989 33 15:08:37 (Feb. 02)

X (east) = 1440 +/- 40 m
Y (north) = 6520 +/- 40 m
Z (elev.) = 480 m
V (speed) = 5110 m/sec
E (error) = .007 sec

3. 1989 33 22:31:34 (Feb. 02)

X (east) = 1430 +/- 90 m
Y (north) = 6270 +/- 90 m
Z (elev.) = 230 m
V (speed) = 2440 m/sec
E (error) = .015 sec

4. 1989 34 03:23:43 (Feb. 03)

LOCATION NOT FOUND ; (small event near channel 7).

5. 1989 34 04:57:12 (Feb. 03)

LOCATION NOT FOUND ; (small event near channel 7).

6. 1989 39 11:50:07 (Feb. 08)

X (east) = 1630 +/- 30 m
Y (north) = 6600 +/- 30 m
Z (elev.) = 240 m
V (speed) = 3700 m/sec
E (error) = .004 sec

7. 1989 39 15:27:31 (Feb. 08)

X (east) = 1590 +/- 40 m
Y (north) = 6560 +/- 40 m
Z (elev.) = 100 m
V (speed) = 3170 m/sec
E (error) = .006 sec

8. 1989 40 07:04:15 (Feb. 09)

X (east) = 1490 +/- 50 m
Y (north) = 6650 +/- 50 m
Z (elev.) = 160 m
V (speed) = 3730 m/sec
E (error) = .008 sec

9. 1989 40 10:24:12 (Feb. 09)

X (east) = 2290 +/- 210 m
Y (north) = 6320 +/- 210 m
Z (elev.) = 300 m
V (speed) = 2640 m/sec
E (error) = .036 sec

10. 1989 41 11:30:20 (Feb. 10)

X (east) = 1890 +/- 50 m
Y (north) = 6320 +/- 50 m
Z (elev.) = 260 m
V (speed) = 4790 m/sec
E (error) = .006 sec

11. 1989 41 11:30:29 (Feb. 10)

X (east) = 1940 +/- 50 m
Y (north) = 6220 +/- 50 m
Z (elev.) = 240 m
V (speed) = 4960 m/sec
E (error) = .009 sec

12. 1989 41 17:50:18 (Feb. 10)

X (east) = 2110 +/- 30 m
Y (north) = 6020 +/- 30 m
Z (elev.) = 290 m
V (speed) = 2940 m/sec
E (error) = .005 sec

13. 1989 42 02:43:31 (Feb. 11)

X (east) = 1550 +/- 20 m
Y (north) = 6670 +/- 20 m
Z (elev.) = 490 m
V (speed) = 5140 m/sec
E (error) = .003 sec

14. 1989 42 03:24:34 (Feb. 11)

X (east) = 2150 +/- 50 m
Y (north) = 5990 +/- 50 m
Z (elev.) = 360 m
V (speed) = 3300 m/sec
E (error) = .008 sec

15. 1989 43 07:58:48 (Feb. 12)

X (east) = 1970 +/- 30 m
Y (north) = 6780 +/- 30 m
Z (elev.) = 270 m
V (speed) = 3670 m/sec
E (error) = .005 sec

16. 1989 45 15:07:16 (Feb. 14)

X (east) = 1200 +/- 20 m
Y (north) = 6940 +/- 20 m
Z (elev.) = -250 m (?)
V (speed) = 5260 m/sec
E (error) = .003 sec

17. 1989 47 00:14:47 (Feb. 16)

X (east) = 2520 +/- 30 m
Y (north) = 6050 +/- 30 m
Z (elev.) = 490 m
V (speed) = 3680 m/sec
E (error) = .005 sec

BB. 1989 48 04:39:57 (Feb. 17) (Rubble blast ?)

X (east) = 1880 +/- 50 m
Y (north) = 6760 +/- 50 m
Z (elev.) = 250 m
V (speed) = 4920 m/sec
E (error) = .008 sec

BB. 1989 48 04:42:33 (Feb. 17) (Rubble blast ?)

X (east) = 1710 +/- 50 m
Y (north) = 6700 +/- 50 m
Z (elev.) = 200 m
V (speed) = 3240 m/sec
E (error) = .008 sec

BB. 1989 48 04:43:19 (Feb. 17) (Rubble blast ?)

X (east) = 1950 +/- 40 m
Y (north) = 7200 +/- 40 m
Z (elev.) = 150 m
V (speed) = 4890 m/sec
E (error) = .006 sec

BB. 1989 48 04:45:52 (Feb. 17) (Rubble blast ?)

X (east) = 1710 +/- 40 m
Y (north) = 7000 +/- 40 m
Z (elev.) = 300 m
V (speed) = 4700m/sec
E (error) = .006 sec

BB. 1989 48 05:07:03 (Feb. 17) (Rubble blast ?)

X (east) = 2050 +/- 120 m
Y (north) = 6770 +/- 120 m
Z (elev.) = 270 m
V (speed) = 4960 m/sec
E (error) = .019 sec

BB. 1989 48 05:45:10 (Feb. 17) (Rubble blast ?)

X (east) = 1710 +/- 60 m
Y (north) = 6660 +/- 60 m
Z (elev.) = 220 m
V (speed) = 2990 m/sec
E (error) = .010

BB. 1989 48 05:45:54 (Feb. 17) (Rubble blast ?)

X (east) = 1790 +/- 30 m
Y (north) = 6890 +/- 30 m
Z (elev.) = 500 m
V (speed) = 6000 m/sec
E (error) = .004

BB. 1989 48 05:48:30 (Feb. 17) (Rubble blast ?)

X (east) = 1790 +/- 30 m
Y (north) = 6740 +/- 30 m
Z (elev.) = 200 m
V (speed) = 3040 m/sec
E (error) = .003

BB. 1989 48 05:49:16 (Feb. 17) (Rubble blast ?)

X (east) = 1800 +/- 30 m
Y (north) = 6710 +/- 30 m
Z (elev.) = 170 m
V (speed) = 2980 m/sec
E (error) = .004

BB. 1989 48 05:49:53 (Feb. 17) (Rubble blast ?)

X (east) = 1630 +/- 60 m
Y (north) = 7490 +/- 60 m
Z (elev.) = 300 m
V (speed) = 4320 m/sec
E (error) = .010

18. 1989 49 13:55:38 (Feb. 18)

X (east) = 1570 +/- 20 m
Y (north) = 6590 +/- 20 m
Z (elev.) = 240 m
V (speed) = 2910m/sec
E (error) = .002 sec

19. 1989 51 20:29:39 (Feb. 20)

X (east) = 1500 +/- 30 m
Y (north) = 6130 +/- 30 m
Z (elev.) = 200 m
V (speed) = 2830m/sec
E (error) = .004 sec

**. 1989 52 08:08:04 (Feb. 21) --- BLAST

X (east) = 2120 +/- 20 m
Y (north) = 6140 +/- 20 m
Z (elev.) = 320 m
V (speed) = 4540 m/sec
E (error) = .001 sec

**. 1989 52 19:59:08 (Feb. 21) --- BLAST

X (east) = 2130 +/- 20 m
Y (north) = 6110 +/- 20 m
Z (elev.) = 380 m
V (speed) = 4860 m/sec
E (error) = .002 sec

20. 1989 53 02:21:05 (Feb. 22)

X (east) = 1840 +/- 30 m
Y (north) = 6660 +/- 30 m
Z (elev.) = 260 m
V (speed) = 5240 m/sec
E (error) = .004 sec

21. 1989 53 04:37:03 (Feb. 22)

X (east) = 1660 +/- 30 m
Y (north) = 6560 +/- 30 m
Z (elev.) = 180 m
V (speed) = 3600 m/sec
E (error) = .005 sec

22. 1989 53 07:07:57 (Feb. 22)

X (east) = 1910 +/- 30 m
Y (north) = 6860 +/- 30 m
Z (elev.) = 260 m
V (speed) = 3230 m/sec
E (error) = .005 sec

**. 1989 53 08:09:18 (Feb. 22) --- BLAST

X (east) = 2120 +/- 20 m
Y (north) = 6120 +/- 20 m
Z (elev.) = 340 m
V (speed) = 4810 m/sec
E (error) = .003 sec

23. 1989 53 13:44:57 (Feb. 22)

X (east) = 1680 +/- 20 m
Y (north) = 6670 +/- 20 m
Z (elev.) = 150 m
V (speed) = 3320 m/sec
E (error) = .002 sec

**. 1989 53 17:32:55 (Feb. 22) --- BLAST

X (east) = 1750 +/- 60 m
Y (north) = 6430 +/- 60 m
Z (elev.) = 100 m
V (speed) = 2520 m/sec
E (error) = .011 sec

**. 1989 53 17:33:00 (Feb. 22) --- BLAST

X (east) = 1670 +/- 40 m
Y (north) = 6470 +/- 40 m
Z (elev.) = 240 m
V (speed) = 4420 m/sec
E (error) = .006 sec

**. 1989 53 17:33:45 (Feb. 22) --- BLAST

X (east) = 1630 +/- 20 m
Y (north) = 6470 +/- 20 m
Z (elev.) = 500 m
V (speed) = 5330 m/sec
E (error) = .004 sec

**. 1989 53 19:50:46 (Feb. 22) --- BLAST

X (east) = 2190 +/- 40 m
Y (north) = 6170 +/- 40 m
Z (elev.) = 280 m
V (speed) = 4610 m/sec
E (error) = .006 sec

**. 1989 53 19:50:54 (Feb. 22) --- BLAST

X (east) = 2130 +/- 50 m
Y (north) = 6130 +/- 50 m
Z (elev.) = 230 m
V (speed) = 2270 m/sec
E (error) = .009 sec

**. 1989 53 19:51:32 (Feb. 22) --- BLAST

X (east) =
Y (north) =
Z (elev.) =
V (speed) =
E (error) =

24. 1989 54 08:48:28 (Feb. 23)

X (east) = 1940 +/- 50 m
Y (north) = 6800 +/- 50 m
Z (elev.) = 260 m
V (speed) = 3040 m/sec
E (error) = .009 sec

25. 1989 54 19:54:17 (Feb. 23)

X (east) = 1660 +/- 20 m
Y (north) = 6620 +/- 20 m
Z (elev.) = 240 m
V (speed) = 3520 m/sec
E (error) = .002 sec

26. 1989 55 02:07:08 (Feb. 24)

X (east) = 1710 +/- 30 m
Y (north) = 6550 +/- 30 m
Z (elev.) = 70 m
V (speed) = 3500 m/sec
E (error) = .005 sec

27. 1989 55 16:29:07 (Feb. 24)

X (east) = 1700 +/- 30 m
Y (north) = 5920 +/- 30 m
Z (elev.) = 290 m
V (speed) = 4470 m/sec
E (error) = .003 sec

28. 1989 55 16:29:12 (Feb. 24)

X (east) = 1710 +/- 30 m
Y (north) = 5870 +/- 30 m
Z (elev.) = 490 m
V (speed) = 2670 m/sec
E (error) = .004 sec

**. 1989 55 19:54:48 (Feb. 24) --- BLAST

X (east) =
Y (north) =
Z (elev.) =
V (speed) =
E (error) =

**. 1989 56 12:12:32 (Feb. 25) BLAST ???

X (east) = 2090 +/- 20 m
Y (north) = 6120 +/- 20 m
Z (elev.) = 330 m
V (speed) = 4740 m/sec
E (error) = .001 sec

**. 1989 56 12:37:35 (Feb. 25) BLAST ???

X (east) = 2100 +/- 20 m
Y (north) = 6110 +/- 20 m
Z (elev.) = 260 m
V (speed) = 4590 m/sec
E (error) = .002 sec

29. 1989 56 15:13:48 (Feb. 25)

X (east) = 1260 +/- 40 m
Y (north) = 6330 +/- 40 m
Z (elev.) = 170 m
V (speed) = 4800 m/sec
E (error) = .007 sec

30. 1989 57 14:17:12 (Feb. 26)

X (east) = 1140 +/- 20 m
Y (north) = 6390 +/- 20 m
Z (elev.) = 100 m
V (speed) = 4090 m/sec
E (error) = .003 sec

31. 1989 58 17:35:23 (Feb. 27)

X (east) = 1530 +/- 40 m
Y (north) = 6510 +/- 40 m
Z (elev.) = 260 m
V (speed) = 3090 m/sec
E (error) = .002 sec

**. 1989 58 19:57:08 (Feb. 27) --- BLAST

X (east) =
Y (north) =
Z (elev.) =
V (speed) =
E (error) =

32. 1989 58 22:16:32 (Feb. 27)

X (east) = 1940 +/- 200 m
Y (north) = 6870 +/- 200 m
Z (elev.) = ??
V (speed) = 5200 m/sec (FIXED)
E (error) = 0.046 sec

33. 1989 60 04:40:06 (Mar. 01)

X (east) = 1630 +/- 20 m
Y (north) = 6550 +/- 20 m
Z (elev.) = 330 m
V (speed) = 3235 m/sec
E (error) = .003 sec

34. 1989 60 18:26:14 (Mar. 01)

X (east) = 1620 +/- 60 m
Y (north) = 6540 +/- 60 m
Z (elev.) = 230 m
V (speed) = 3130 m/sec
E (error) = .010 sec

35. 1989 61 10:23:18 (Mar. 03)

X (east) = NO SOLUTION (close to channel # 9).
Y (north) =
Z (elev.) =
V (speed) =
E (error) =

36. 1989 62 02:08:51 (Mar. 03)

X (east) = 1580 +/- 40 m
Y (north) = 6530 +/- 40 m
Z (elev.) = 200 m
V (speed) = 4050 m/sec
E (error) = .007 sec

37. 1989 62 05:20:49 (Mar. 03)

X (east) = 1880 +/- 30 m
Y (north) = 5950 +/- 30 m
Z (elev.) = 250 m
V (speed) = 2710 m/sec
E (error) = .005 sec

38. 1989 62 07:58:21 (Mar. 03)

X (east) = 1470 +/- 20 m
Y (north) = 6640 +/- 20 m
Z (elev.) = 270 m
V (speed) = 2810 m/sec
E (error) = .003 sec

39. 1989 62 09:33:52 (Mar. 03) BLAST ???

X (east) = 1890 +/- 40 m
Y (north) = 6000 +/- 40 m
Z (elev.) = 400 m
V (speed) = 3220 m/sec
E (error) = .006 sec

40. 1989 62 14:10:19 (Mar. 03) (like Jan. 25 event)

X (east) = 1350 +/- 20 m
Y (north) = 6670 +/- 20 m
Z (elev.) = 250 m
V (speed) = 4910 m/sec
E (error) = .003 sec

41. 1989 65 17:46:48 (Mar. 06)

X (east) = 1650 +/- 20 m
Y (north) = 6480 +/- 20 m
Z (elev.) = 150 m
V (speed) = 2760 m/sec
E (error) = .003 sec

42. 1989 69 07:46:58 (Mar. 10)

X (east) = 1650 +/- 20 m
Y (north) = 6150 +/- 20 m
Z (elev.) = 220 m
V (speed) = 2550 m/sec
E (error) = .003 sec

43. 1989 70 08:03:37 (Mar. 11)

X (east) = 1720 +/- 20 m
Y (north) = 6700 +/- 20 m
Z (elev.) = 160 m
V (speed) = 3160 m/sec
E (error) = .002 sec

44. 1989 70 11:00:46 (Mar. 11)

X (east) = 1830 +/- 60 m
Y (north) = 6740 +/- 60 m
Z (elev.) = 230 m
V (speed) = 3440 m/sec
E (error) = .010 sec

45. 1989 72 19:16:43 (Mar. 13)

X (east) = 1020 +/- 40 m
Y (north) = 5650 +/- 40 m
Z (elev.) = 300 m
V (speed) = 2290 m/sec
E (error) = .007 sec

**. 1989 73 20:25:00 (Mar. 14) BLAST

X (east) = 1650 +/- 20 m
Y (north) = 6560 +/- 20 m
Z (elev.) = 440 m
V (speed) = 5220 m/sec
E (error) = .002 sec

46. 1989 75 19:24:58 (Mar. 16)

X (east) = 1650 +/- 70 m
Y (north) = 6690 +/- 70 m
Z (elev.) = 140 m
V (speed) = 2500 m/sec
E (error) = .012 sec

47. 1989 87 14:40:46 (Mar. 28)

X (east) = 2070 +/- 40 m
Y (north) = 7180 +/- 40 m
Z (elev.) = 340 m
V (speed) = 2490 m/sec
E (error) = .006 sec

48. 1989 87 18:47:03 (Mar. 28)

X (east) = 2170 +/- 50 m
Y (north) = 6920 +/- 50 m
Z (elev.) = 380 m
V (speed) = 3880 m/sec
E (error) = .009 sec

49. 1989 89 01:32:31 (Mar. 30)

X (east) = 1360 +/- 20 m
Y (north) = 6430 +/- 20 m
Z (elev.) = 220 m
V (speed) = 3290 m/sec
E (error) = .001 sec

50. 1989 89 11:04:08 (Mar. 30)

X (east) = 2430 +/- 50 m
Y (north) = 6400 +/- 50 m
Z (elev.) = 340 m
V (speed) = 5360 m/sec
E (error) = .009 sec

51. 1989 91 09:43:45 (Apr. 01)

X (east) = 1550 +/- 20 m
Y (north) = 6610 +/- 20 m
Z (elev.) = 130 m
V (speed) = 3600 m/sec
E (error) = .003 sec

52. 1989 93 05:00:26 (Apr. 03)

X (east) = 2250 +/- 60 m
Y (north) = 6340 +/- 60 m
Z (elev.) = 310 m
V (speed) = 2670 m/sec
E (error) = .010 sec

53. 1989 95 13:43:17 (Apr. 05)

X (east) = 1930 +/- 40 m
Y (north) = 6030 +/- 40 m
Z (elev.) = 260 m
V (speed) = 5260 m/sec
E (error) = .007 sec

54. 1989 95 15:28:47 (Apr. 05)

X (east) = 2010 +/- 50 m
Y (north) = 6060 +/- 50 m
Z (elev.) = 290 m
V (speed) = 2550 m/sec
E (error) = .008 sec

55. 1989 96 08:10:15 (Apr. 06)

X (east) = 1890 +/- 30 m
Y (north) = 6870 +/- 30 m
Z (elev.) = 260 m
V (speed) = 3940 m/sec
E (error) = .005 sec

56. 1989 96 12:02:11 (Apr. 06)

X (east) = 2170 +/- 30 m
Y (north) = 7030 +/- 30 m
Z (elev.) = 330 m
V (speed) = 5970 m/sec
E (error) = .005 sec

57. 1989 97 05:39:36 (Apr. 07)

X (east) = 1620 +/- 20 m
Y (north) = 6490 +/- 20 m
Z (elev.) = 350 m
V (speed) = 2650 m/sec
E (error) = .002 sec

Microseis Systems Inc.
105 - 902 Spadina Crescent East, Saskatoon, Sask. S7K 3H5
(306) 244-3878

System Overview

microseis
systems inc.

System Hardware

Main Unit

The main unit is an Intel System 286/310 AP, based on the Multibus (IEEE 796 System Backplane Bus). It has two 16 bit processors, one megabyte of RAM, two RS232C serial ports and one Centronics compatible parallel port.

Main Processor

The main processor is an Intel iSBC 286/12, which uses an 80286 CPU with 80287 math co-processor. The clock speed is 8 MHz. The board has one megabyte of 0 wait state RAM.

Slave Processor

The second, or slave, processor board is an Intel iSBC 86/30, which uses an 8086 CPU with a clock speed of 8 MHz. The board has 128 KB of RAM dual-ported into the main board's address space.

Analog Input Board

The analog input is handled by one or two Intel iSBX 311 boards, controlled by the slave processor. Each board can handle 8 double ended or 16 single ended channels. Conversion speed is 50 microseconds per channel. Conversion accuracy is 12 bits, therefore the dynamic range is 72 dB. The common mode rejection ratio is 60 dB minimum. Input impedance is 20 megohms minimum. The input may range from - 5 to + 5 Volts with overload protection of +/- 30 Volts.

Input Amplification, Filtering and Protection

Surge protection and filtering are best provided via the external geophone amplification. There are a variety of makes of field amplification systems. We have worked with Teledyne Geotech 42.50 amplifiers, which are modified at the factory for our use. They have a low pass filter which is switch selectable at .4, 10 or 20 Hz and a high pass filter which is switch selectable at 10, 25, 50, 100 or 200 Hz. Gain is selectable in 6 dB steps from 0 to 120 dB. Lightning surge protectors are available from Teledyne which provide good high voltage transient protection.

If desired, telemetry may be used, either over wire for underground arrays or over radio for surface arrays. This allows remote monitoring of the geophone array, allowing the operator to maintain the system and interpret the data in the mine office, as opposed to an underground office or field office.

However, the array electronics do not necessarily have to be Teledyne. As long as the output of the array is compatible with the iSBX 311 A/D inputs, any system may be used.

Graphics Terminal

User input to the system is provided through a Qume QVT211GX graphics terminal. This terminal communicates over one of the RS232C ports at 9600 baud. The keyboard is a QWERTY type which includes the full ASCII character set. The terminal provides monochrome graphics with a resolution of 644 by 288 pixels. It can operate in terminal, native graphics or Tektronix 4010/4014 emulation modes.

Colour Plotter

Hard copy graphics are provided by a Hewlett-Packard 7475A colour plotter. This plotter communicates over the second RS232C port at 9600 baud. It plots in six colours on either A or B-sized paper with a resolution of 0.025 mm. For heavier duty use, the 8-pen 7550A may also be used.

Parallel Printer

An ASCII printer with a Centronics compatible parallel interface is used to produce non-graphical hard copy. Any popular make of printer will work with the system. Recommended here is the Panasonic KX-P1092 printer. It is a narrow carriage dot matrix printer which can print at 180 cps in draft mode and also produce very nice near letter quality text at about 30 cps.

Mass Storage

Mass storage is provided through a choice of 40, 80 or 140 MB Winchester disk drives. A 320 KB floppy disk drive is also provided. These devices are controlled by an Intel iSBC 214, which is an 80186 based intelligent peripheral controller with 32 KB of cache memory and DMA access.

Mass Storage Expansion

The peripheral controller provided with the system can control a second Winchester disk drive with ST506/412 interface, up to three additional floppy disk drives with SA 450/460 interface and up to four 1/4" streaming tape drives with QIC-02 interface. An optional half-height 60 MB streaming tape drive utilizing QIC-04 format may be incorporated into the system chassis. Any further expansion of mass storage devices would require an Intel System 311 expansion chassis, but is easily done.

Communications Expansion

Intelligent communications boards and software may be added to provide further communications capabilities. An Intel iSXM 544A may be used to add up to 4 additional RS232C channels. An Intel iSXM 188/48 may be used to add up to 8 additional RS232C channels. An Intel iSXM552A and additional software may

be used to provide LAN communications through Intel's OpenNET system, which is an implementation of the EtherNET standard. This system allows communications and file access between the Microseis and systems running the iRMX86, XENIX, iNDX, MS-DOS 3.1 or PC-DOS 3.1 operating systems. An Intel iSBX 488 may be used to add IEEE 488-1978 (GPIB) capabilities.

Memory Expansion

The current version of the Microseis System runs under iRMX86, which allows only 1 megabyte of RAM. However, future versions will run under iRMX286, which allows up to 16 megabytes of RAM. RAM expansion is accomplished by inserting additional RAM boards and then configuring the operating system to recognize the additional memory.

Packaging

Processors, analog input boards, communications, peripheral control and mass storage devices are all contained within the System 310AP chassis, which has dimensions of 6.5" high, 17" wide and 22" deep, and weighs less than 55 pounds. Access to the parallel port is provided through a 36 pin delta connector on the backplane. Access to the serial ports is provided through two 25 pin D subminiature connectors (female) on the backplane.

Access to the analog inputs is provided through one or two 25 pin D subminiature connectors (male) on the backplane. Unless contracted to provide a geophone array system or to provide a specific interface, Microseis Systems will provide a connector panel which plugs into the analog input D-type connector(s) and provides a series of BNC connectors for the geophone inputs.

Environment and Space Requirements

A dry, temperature controlled building should be provided for the equipment. The temperature may range from 50 to 95 degrees F. Humidity may range from 20% to 80% non-condensing, 79 degrees F wet bulb maximum. An effort must be made to keep the environment fairly dust-free. If excessive dust exists, the machine should be cleaned periodically to prevent overheating due to clogged ventilation fans or dust-covered electronics. Excessive dust may eventually cause problems with the floppy disk drive, but should not present a problem to the hermetically sealed Winchester drive.

Ideally, the equipment should be located in the office where the information is compiled and used. Space requirements are minimal: a large desk or table is sufficient space for the main unit, terminal, plotter and printer, as A/D conversion, event storage, analysis and display are all performed with just these components. Extra space and arrangements will be necessary for the geophone array and accompanying electronics.

System Software

Operating System

The Microseis software runs under iRMX86, an operating system designed by Intel for real-time, multi-tasking applications. The operating system is a prioritized, event-driven system which uses such features as mailboxes, semaphores, regions and dynamically allocated memory to enable the systems programmer to easily implement real-time operations.

The Microseis software was written in 8086 assembler and PL/M 86. Compilers are available for these two languages, as well as C, FORTRAN and PASCAL. The the formats of the event storage files are known to the user. This enables him to write his own applications in a language he feels comfortable with.

General Organization

There are two processors on board the Microseis. The secondary, or slave processor spends all of it's time examining the incoming data for events. When it recognizes an event (see "Event Capture" below), it alerts the main processor, which interrupts whatever it is doing and records the event to hard disk immediately. Because the whole process utilizes buffers and is managed by a real time operating system, no events are missed. An event that arrives immediately after a recorded event is also recorded. The analysis of the events is performed in-between the actual recording of the raw data. Thus, the Microseis is able to perform some fairly sophisticated analysis without ever missing incoming events. The whole procedure is prioritized. Event recording gets highest priority, automatic analysis the next highest and the user the lowest. Example: the user is plotting a seismogram when event A triggers the system. The plotter slows down and occasionally stops while the event is recorded. Analysis begins on event A when event B triggers the system. Analysis is slowed down or halted while event B is recorded. When B is recorded, analysis is completed on A. Analysis is then performed on event B. When both events have been recorded and analyzed, the plotter continues where it left off. No data is lost, programs in progress are just temporarily halted while more important things happen.

Event Recognition

The system recognises a "trigger" or "hit" using the STA/LTA algorithm. It keeps track of three averages: a signed average, a short term average (STA) and a long term average (LTA). The signed average is used to correct for DC amplifier drift, in order that zero-mean data is produced. The STA and LTA averages are used to provide a hit recognition algorithm which adapts itself to background noise.

If a seismic event occurs, then the STA will rise more quickly than the LTA; the ratio of the two increases. A threshold is chosen to compare with this ratio. If a constant noise source

is nearby, then the LTA will rise until it equals the STA; spurious triggers are then eliminated. If a moving noise source approaches such as a truck or train, then the LTA will rise roughly with the STA. Because the increase in signal level is gradual, the threshold ratio is never crossed.

If, however, there is a quick increase in signal level, such as is caused by a microseism, then the STA will rise relatively quickly compared to the LTA, the threshold will be crossed and the channel will be declared as hit.

Therefore, the signal level must always rise quickly above the background level for a trigger to be declared. This is a vast improvement over a simple voltage threshold check. The length of both averages and the threshold ratio may be set by the user. This allows "tuning" of the recognition algorithm to the magnitude and frequency content expected.

Additionally, channels may be declared as valid or invalid trigger channels, and a certain number of them required to trigger before an event is declared. Example: In an eight channel system, channels 3 and 7 are known to be noisy. Experience has shown that a real microseism will trigger at least four channels. The user would disable channels 3 and 7 and require that four channels trigger in order that an event be declared. Therefore, if any four of channels 1, 2, 4, 5, 6, or 8 trigger within a certain time period, an event is declared. All eight channels are then recorded for the specified pre-hit and post-hit times. Once an event is captured, then it may be automatically filtered, picked for first breaks and located.

This sophisticated recognition algorithm may be disabled to allow for full data throughput, in which case a simpler trigger detection algorithm is enabled. With STA/LTA event recognition, rates of 500 samples per second per channel on a 16 channel system are typical, trading sampling rate for channels as the number of channels is increased or decreased. The simpler algorithm is currently under development. When finished, the A/D boards will be allowed to run closer to the maximum rate, for a total throughput of 15 kHz per iSBX 311 board.

First Break Picker

First breaks are picked using a more sophisticated form of the STA/LTA algorithm discussed previously. Because the picker is not under severe time constraints as is the event detection routine, it may look for a more precise spot on the wave - the initial up or down sweep of the first break. In addition, the picker may be set to calculate it's averages on the difference function of the wave, thus making it sensitive to frequency changes as well as amplitude changes. In addition to picking the first breaks, the picker records the maximum amplitude, used in the magnitude determination.

Seismogram Display and Manual Picking

Optionally, manual picking may be applied after the automatic interpretation has been completed. This is done with a very nice multi-channel screen seismogram display. A vertical line cursor is moved over the data, showing time and amplitude of it's location in a continuous display. The pick is performed by pressing one key, which records the selection in the event's short file. Picks may be changed or old picks restored.

Any combination of channels may be displayed, up to a maximum of sixteen displayed simultaneously. Both the time and amplitude scales of the display may be varied, to allow for a flexible display. A clipping feature may be enabled, to prevent large peaks from obscuring other channel signals. Time lines may be added; the time between these lines is variable. A zero line may be added to each channel.

Source Location

The source location program is an iterative procedure which utilizes all available hit times. The program uses the Simplex method of curve fitting to search for a location where the error between the actual and the theoretical travel times is at a minimum.

The program uses a layered model of the earth. The user specifies, through menu control, a number of strata of varying thicknesses and velocities. The layers may dip at any angle and strike in any direction, although all the layer boundaries are parallel. The program utilizes ray-tracing techniques to account for both critically and non-critically refracted waves. There are no restrictions placed on the ordering of velocities; reversals are allowed. Both compressive (P) and shear (S) wave velocities are entered; the operator may choose to run the location utilizing either model depending on what wave type is being picked as the first break. Geophones may be placed anywhere in any of the layers.

Optionally, the user may specify a uniform velocity earth. In this case, the program also searches for the best average velocity. If desired, the search may be limited to a planar solution. These two options are useful where the earth is too complicated to be represented by a layer structure; a planar solution is useful in this case when the geophone array is two-dimensional and events are known to occur in the same plane.

One of the big advantages of the Simplex technique is that it allows a system to be less channel-intensive. A three-dimensional solution may be found with only four channels. Because the Simplex location utilizes all available picks and searches for the location based on best average error, the effect of a bad pick tends to be minimized. The combination of a sophisticated automatic picker and a screen graphics manual picker produces a further reduction in location error. The result of

this is that a large area can typically be monitored with only six or eight channels.

The magnitude of the event is calculated based on a statistical fit of the logarithmic amplitude-distance function to the amplitudes at all recorded channels. The coefficients used in this calculation may be adjusted so that the magnitude ratings may be calibrated.

Notch Filter

The Microseis system employs an optional 60 Hz notch filter. This recursive software filter is run over the data once it has been recorded to hard disk. It has proven very effective in removing power-line induced 60 Hz noise from the seismic signal. This may be run automatically on any, all or none of the channels.

File Management

A short and long file are kept for every event. The short file contains all the pertinent facts: time, date, location, magnitude, geophone parameters, first break picks and amplitudes and other factors are all stored as part of the short file. The long file contains the multiplexed raw data.

The events are kept in order of date, time and daily event number. When the hard disk becomes full, the system starts automatically deleting the oldest files, long records first. The user is given a warning when available disk space is low.

Events may be called up for plotting, printing, display or reinterpretation. In addition, they may be copied from hard disk to floppy, floppy to hard disk or floppy to floppy. They may be backed up to an optional streaming tape drive. They may be deleted, either partially (just the long file) or completely. Any of these functions may be performed on a group of files selected for any combination of criteria. For example, the user may wish to plot the locations of all events for the second week of February that had a magnitude greater than 1.0 and were located below mine level. This can easily be done, using menu control.

Manual Analysis

The automatic picking, notch filter and source location programs may be re-run on events by the user under menu control. As well, the event may be manually picked, then located using the manual picks. The automatic analysis functions may be disabled by the user.

Location Plotting

Plotting of seismic hypocentres is done using the Hewlett-Packard plotter. Rather than store the details of the site map and plot them every time, the Microseis uses the paper maps

produced by the user. The user obtains the latest version of the site map, inputs two coordinates using the interactive plotter, and then the locations are plotted directly onto the map. Once a particular map has been used once, the user no longer has to enter the two coordinates. He merely calls the map up by name. This is a simple solution which eliminates the time consuming process of having to update a site map stored in the computer.

Seismogram Plotting

The full wave seismograms may be plotted on paper, in colour. The same options available for screen display are also available for the hard copy output: variable scaling, multiple channel plotting, variable-width time lines, optional zero lines and optional clipping. In addition, the user can elect not to plot the first break information. Basic information such as time, event number, location and magnitude is printed along with the seismogram.

Event Lists

The principle facts of events may be listed on paper using the printer. The user may opt to print only the basic facts, such as event time, location, magnitude, number of channels, and number of triggered channels. An extended list may be printed in which the individual channel parameters are listed such as geophone location, first break time, maximum amplitude and trigger flag.

First Motion Plotting

The Microseis incorporates a first motion analysis routine. This routine uses the initial direction of the first break wave, calculated by the source location program, to plot a set of first motion vectors for use with a stereo net overlay. This information is used to determine the orientation and direction of motion of the fault plane.

System Parameters

All system parameters are specified through a set of user-friendly menus. Geophone coordinates, amplification and sensitivity are input through a menu. The analog input parameters, such as number of channels, sampling rate, storage lengths, STA/LTA lengths and threshold level, are specified through another menu. The system may be easily adapted to suit the users requirements through this software control.

Under Development

Spectral analysis will be incorporated into the menu structure, including graphical display of Fourier transforms and calculation of the Brune parameters. These parameters determine seismic moment, fault area and stress drop, giving a more accurate picture of the size of an event than a simple magnitude calculation.

APPENDIX B

NUMERICAL MODELLING USING GEOROC

1.0 Introduction

The purpose of the GEOROC run was to evaluate the performance of the code in comparison with other programs of similar capabilities, notably VISCOT and FLAC.

GEOROC and VISCOT are very similar finite element codes, both based on a set of subroutines originating from a well-known text of Owen and Hinton "Finite Element Analysis in Plasticity and Viscoelasticity". FLAC produces solutions very similar to finite element codes, but uses an explicit finite difference method to model a variety of geotechnical problems.

2.0 Technical Aspects

The difference between the GEOROC and VISCOT codes are their input/output structure and time step control. Both codes utilize isoparametric elements, with four and eight node quadrilaterals being the most commonly used elements. In the course of this project, VISCOT used four-node elements, while the GEOROC manual recommended eight-node quadrilaterals. Experience indicates that four-node elements are more efficient, provided mesh lock-up is prevented.

Mesh lock-up is a subtle phenomenon manifesting itself in transition to steady state with respect to shear stress while hydrostatic pressure in elements is usually growing. This type of performance occurs due to incompressibility of viscous flow demanded by constitutive relationships. The incompressibility of flow becomes a strong constraint on mesh deformations if an attempt is made to satisfy incompressibility at Gaussian points within the element.

Four-node elements are most prone to mesh lock-up unless special care is taken to eliminate this phenomenon. This is usually achieved by utilizing the Nategaal-Parks-Rice variational principle in FEM formulation. This feature is implemented in VISCOT. In simple terms, the procedure leads to preservation of volume for the entire element but incompressibility is not demanded at each Gaussian point. The accuracy of the solution is not affected by this formulation. Eight-node quadrilaterals are less prone to mesh lock-up since this type of element has more kinematic freedom. Nevertheless, numerical experiments with eight-node elements within VISCOT indicated mesh lock-up could occur for some geometries. For this reason VISCOT is used with four-node quadrilaterals in conjunction with the Nategaal-Parks-Rice formulation. It is not clear if GEOROC has similar provisions to avoid mesh lock-up. Mesh lock-up does not occur in the finite difference code FLAC.

3.0 Verification of GEOROC Against VISCOT and FLAC

3.1 Input

To assure identical conditions for comparison of the three codes under investigation, calculations were carried out on an identical mesh consisting of 1784 elements (Figures 1 & 2). VISCOT and FLAC consisted of 1880 nodes and GEOROC contained 5543 nodes, since GEOROC elements are eight-node quadrilaterals.

The amount of memory required to run the GEOROC mesh would not allow processing on a personal computer, therefore the version of GEOROC received was installed on a SUN IV workstation. Installation on the SUN IV did not require any modification of the code. Some difficulties were encountered in running GEOROC, but these were partially related to discrepancies between the input file structure in the supplied version of GEOROC and the manual. Results of a test run matched numerical data presented

FIGURE 1

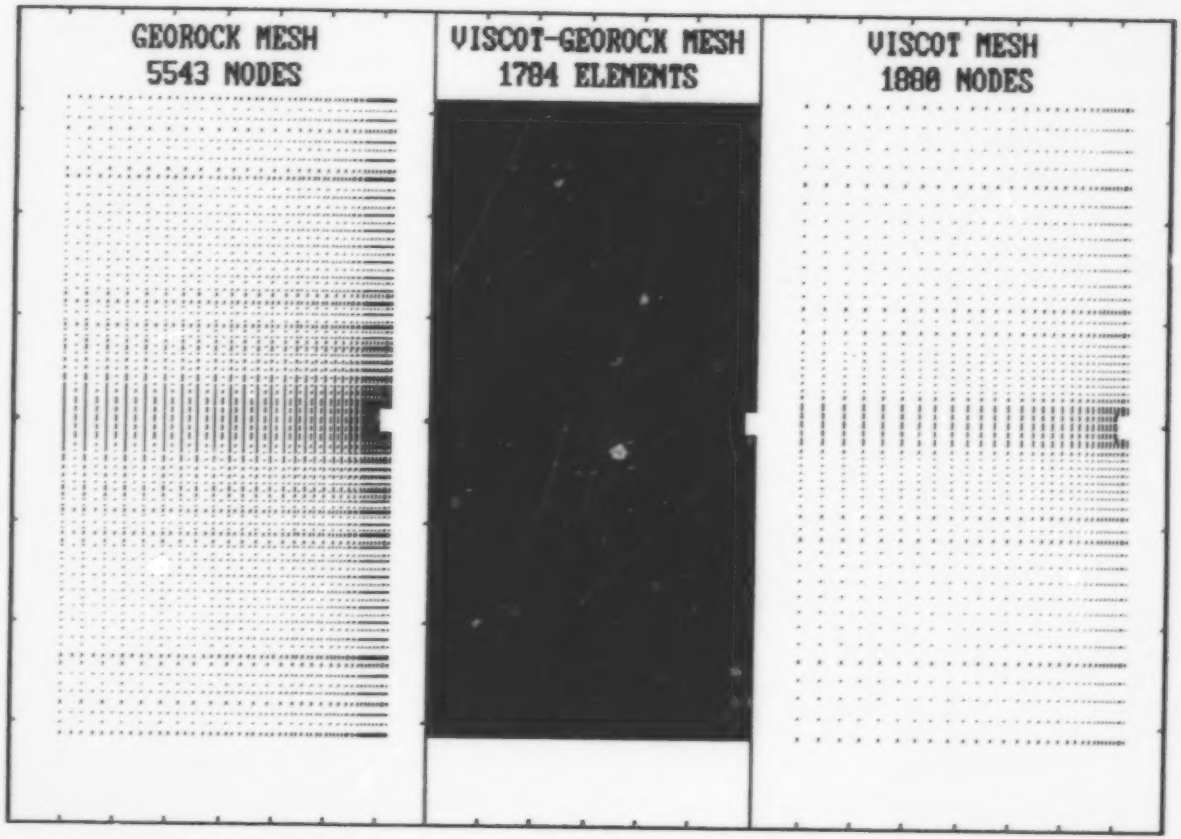
GEOROCK MESH
5543 NODES
VISCOT-GEOROCK MESH
1784 ELEMENTS
VISCOT MESH
1880 NODES

FIGURE 2

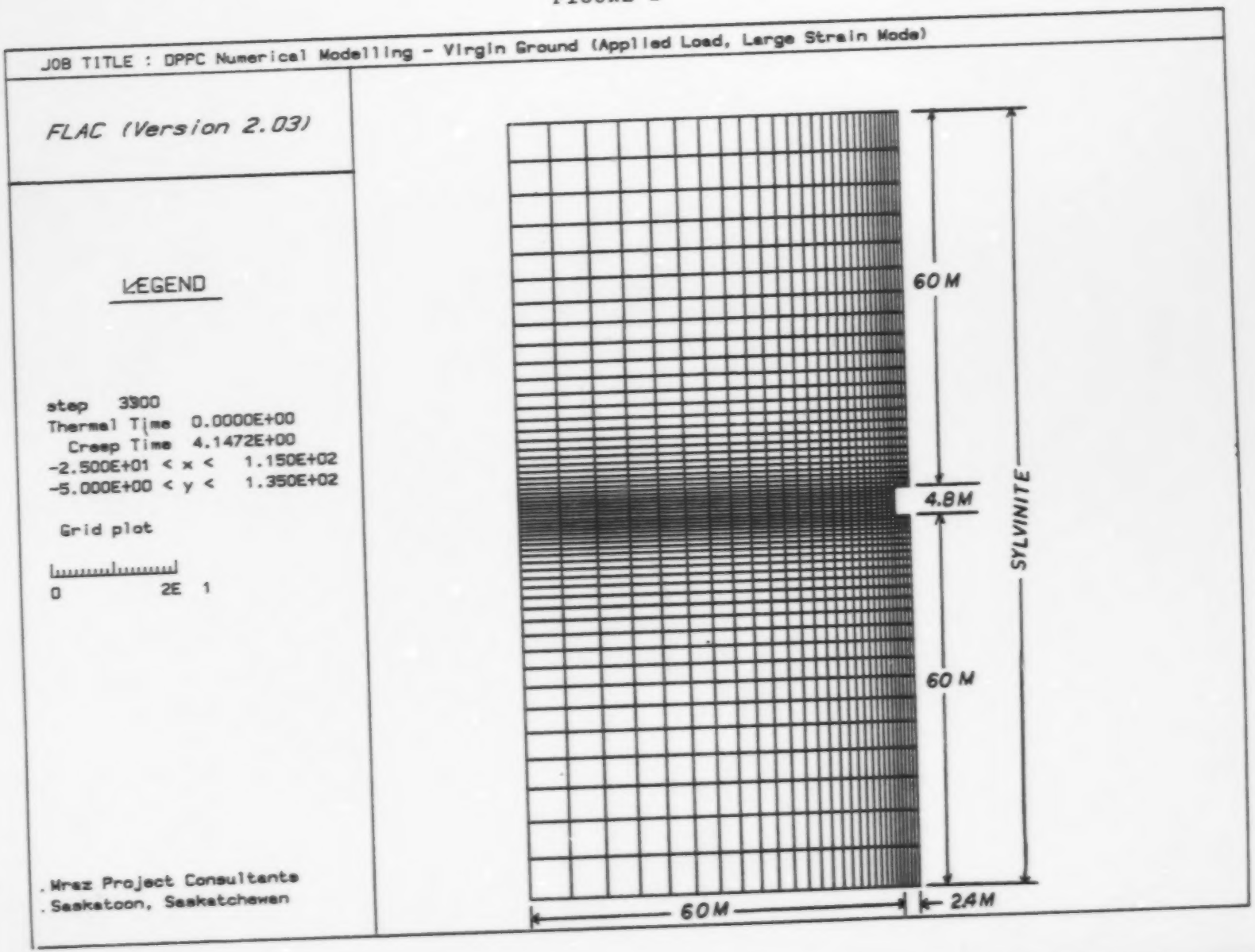
JOB TITLE : DPPC Numerical Modelling - Virgin Ground (Applied Load, Large Strain Mode)
FLAC (Version 2.03)
LEGEND
step 3900
Thermal Time 0.0000E+00
Creep Time 4.1472E+00
-2.500E+01 < x < 1.150E+02
-5.000E+00 < y < 1.350E+02
Grid plot
0 2E 1
. Mraz Project Consultants
. Saskatoon, Saskatchewan
60 M
4.8M
60 M
SYLVINITE
60 M
2.4M

in the manual (ie. thick cylinder problem) precisely.

The current version of GEOROC utilizes a single mechanism power creep law that grossly oversimplifies salt rock creep behaviour. In the course of the project a more realistic two-mechanism creep law was adopted using closure data from the DPPC Virgin Ground Opening (ie. Test Room) to determine material parameters for potash. In order to provide a valid comparison of the codes involved, the portion of the code in GEOROC implementing material behaviour was modified to account for the material behaviour adopted in this study.

All three codes, VISCOT, FLAC, and GEOROC, utilized the following steady-state creep law:

$$\dot{\epsilon}_{ss} = \begin{cases} \dot{\epsilon}_o \left(\frac{\sigma_{eff}}{\sigma_o}\right)^m & \sigma_{eff} \leq \sigma_o \\ \dot{\epsilon}_o \left(\frac{\sigma_{eff}}{\sigma_o}\right)^n & \sigma_{eff} > \sigma_o \end{cases}$$

σ_{eff} = effective stress
$\dot{\epsilon}_{ss}$ = steady state strain rate
m,n = exponents
$\dot{\epsilon}_o$ = reference strain rate
σ_o = critical effective stress

Specific values of creep parameters are as follows:

m = 3.0
n = 6.9
σ_o = 10.2 MPa
$\dot{\epsilon}_o$ = 3.24 x 10^{-11} sec^{-1}

3.2 Output

Comparison of the results of the computations are listed in Table 1.0. In all cases instantaneous excavation was assumed. Mesh size and time steps involved were identical for the finite element codes, VISCOT and GEOROC. The time steps for the finite difference solution (ie. FLAC) were different, but the mesh size was identical. Horizontal and vertical closure amounts 4 years after excavation were determined by extrapolation for the GEOROC and VISCOT solutions. Horizontal and vertical closure and accompanying closure rates, for each numerical model and in situ, are illustrated in Figures 3 to 9.

The comparison (Table 1.0) shows that the steady state closure rates predicted VISCOT solution are in close agreement with in situ data. This is expected because VISCOT was used to determine the creep parameters that govern the rock mass behaviour. The difference in computed closure and rates between VISCOT and GEOROC is approximately 16 percent. The steady state closure rates produced by FLAC were in-between those predicted by GEOROC and VISCOT, and approximately 10 percent greater than in situ rates. The closures predicted by FLAC were almost twice that of closures predicted by the other codes, and measured in situ. However, the in situ measurements do not account for transient closure that occur between the time of excavation and instrumentation installation. If transient closure was included in situ closures would be similar to the closures predicted by FLAC.

The only immediately identifiable difference in computational conditions between VISCOT and GEOROC is the fact that VISCOT was operating in double precision (ie. 15 significant figure accuracy in floating point arithmetic), and GEOROC operated in single precision (ie. 7 significant figures). It is conceivable that over 11,000 degrees of freedom involved in the GEOROC mesh may require double precision for matrix inversion. A slight

Table 1.0

Comparison of Computational Results After 4.0 Years

Numerical Model	Vertical Closure (cm)	Horizontal Closure (cm)	Vertical Steady-State Closure Rate (cm/yr)	Horizontal Steady-State Closure Rate (cm/yr)
* In Situ	7.0	7.0	1.13	1.13
VISCOT	4.79	4.75	1.136	1.138
FLAC	13.21	13.20	1.264	1.276
GEOROC	5.69	5.66	1.352	1.361

* NOTE : In situ closure measurements do not include transient creep closure. The amount of in situ closure would be approximately the same as predicted by FLAC, if transient closure was measured.

FIGURE 3

DPPC VIRGIN GROUND OPENING

HORIZONTAL DISPLACEMENT

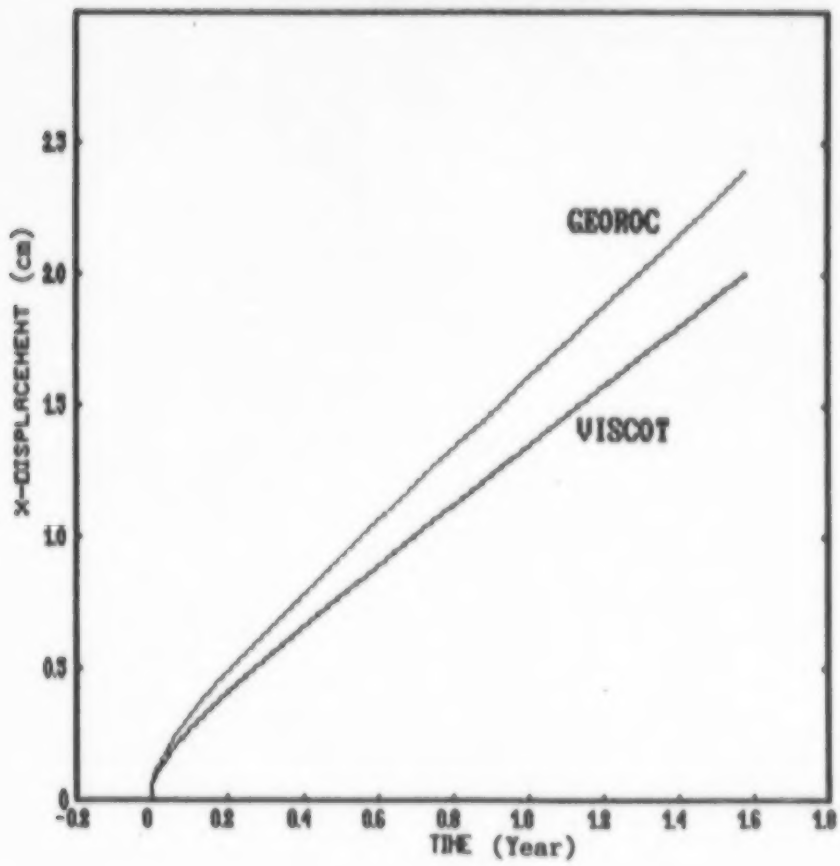

FIGURE 4

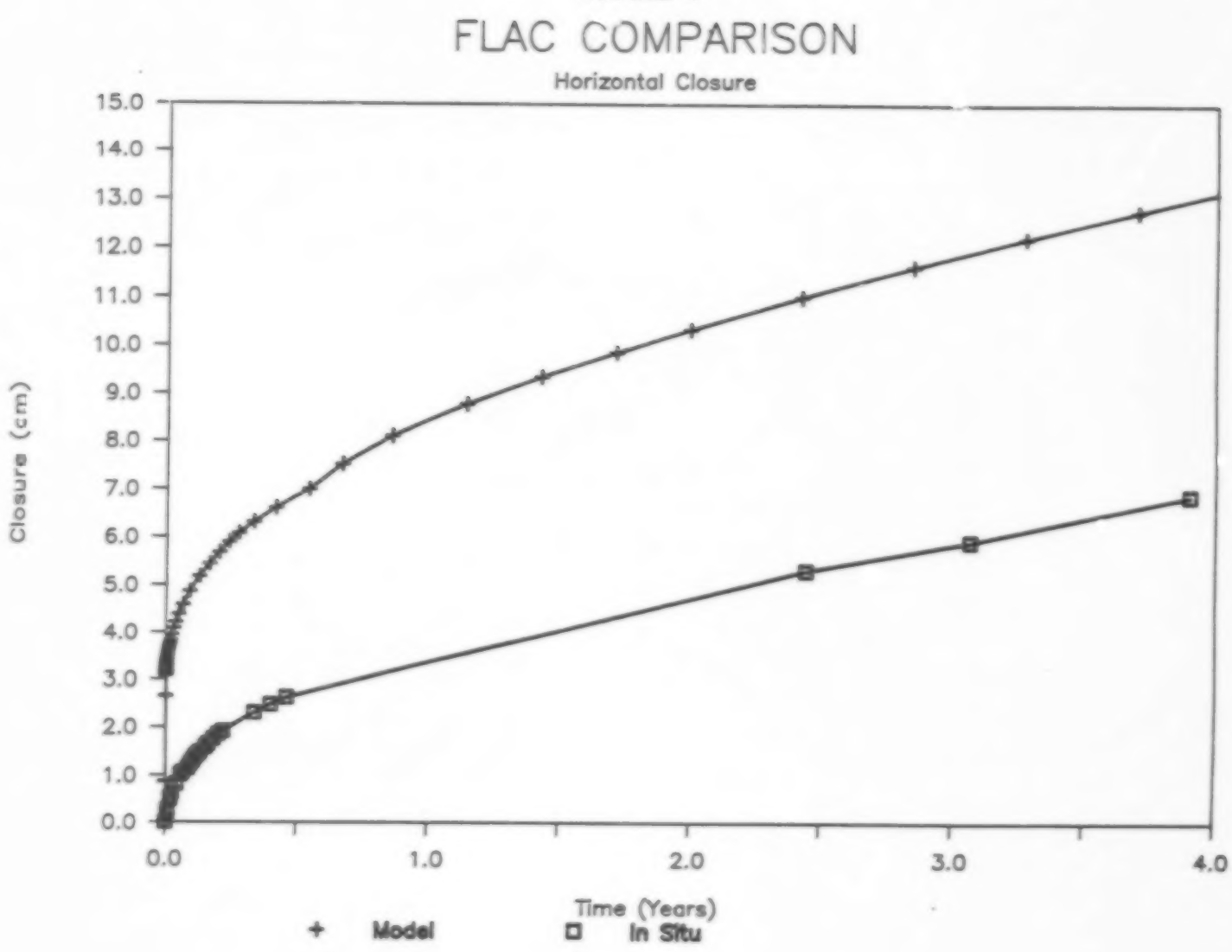
FLAC COMPARISON
Horizontal Closure
Closure (cm)
15.0
14.0
13.0
12.0
11.0
10.0
9.0
8.0
7.0
6.0
5.0
4.0
3.0
2.0
1.0
0.0
0.0
1.0
2.0
3.0
4.0
Time (Years)
+ Model
□ In Situ

FIGURE 5

DPPC VIRGIN GROUND OPENING

VERTICAL DISPLACEMENT

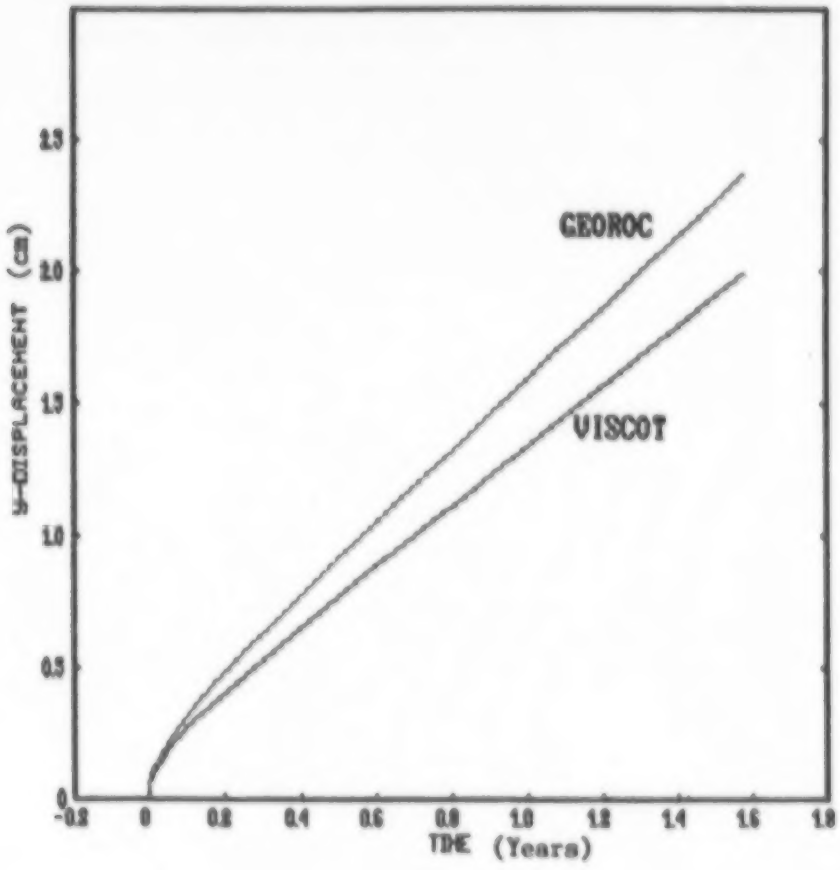

FIGURE 6

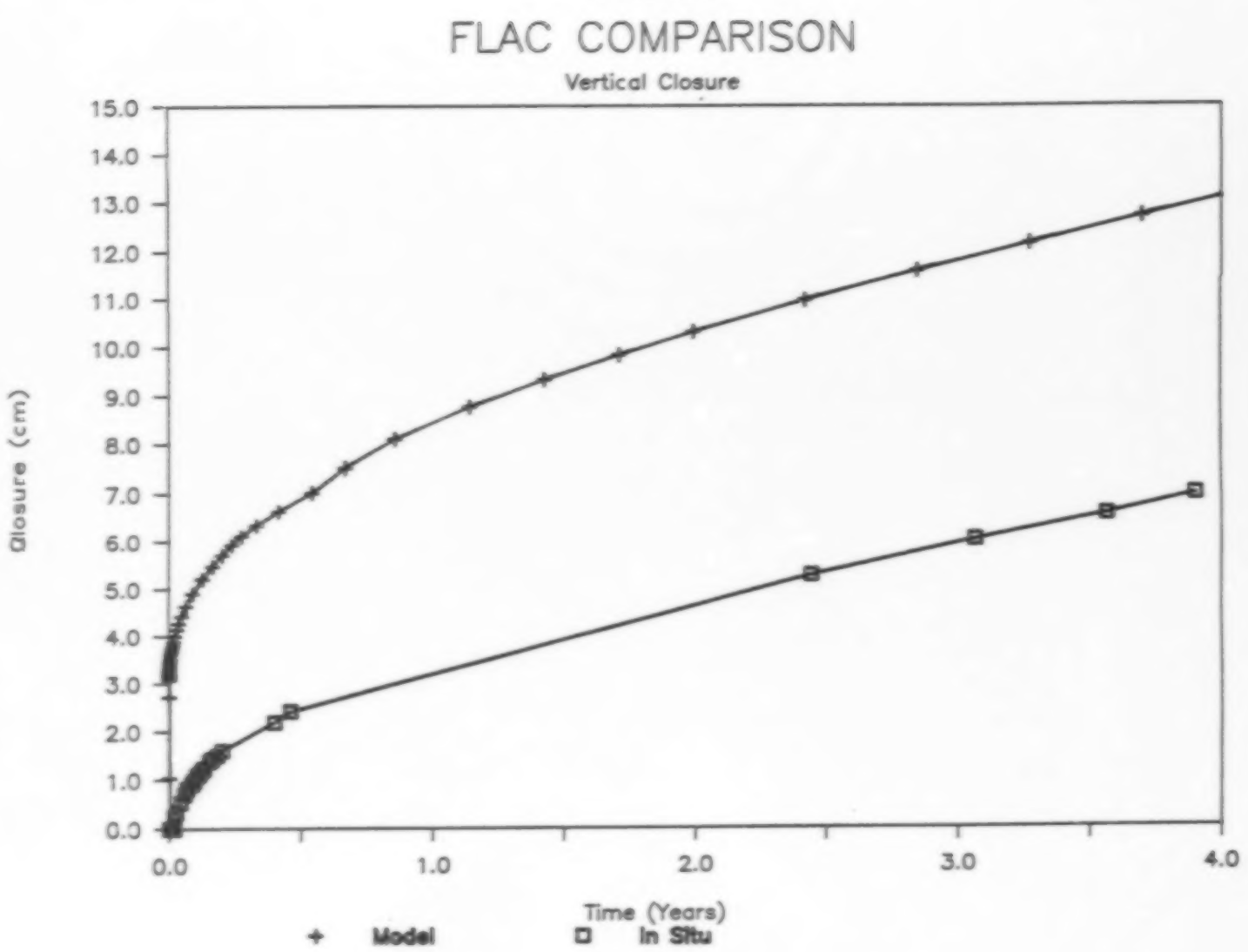
FLAC COMPARISON
Vertical Closure
Closure (cm)
15.0
14.0
13.0
12.0
11.0
10.0
9.0
8.0
7.0
6.0
5.0
4.0
3.0
2.0
1.0
0.0
0.0
1.0
2.0
3.0
4.0
Time (Years)
Model
In Situ

FIGURE 7

DPPC VIRGIN GROUND OPENING

HORIZONTAL CLOSURE RATE

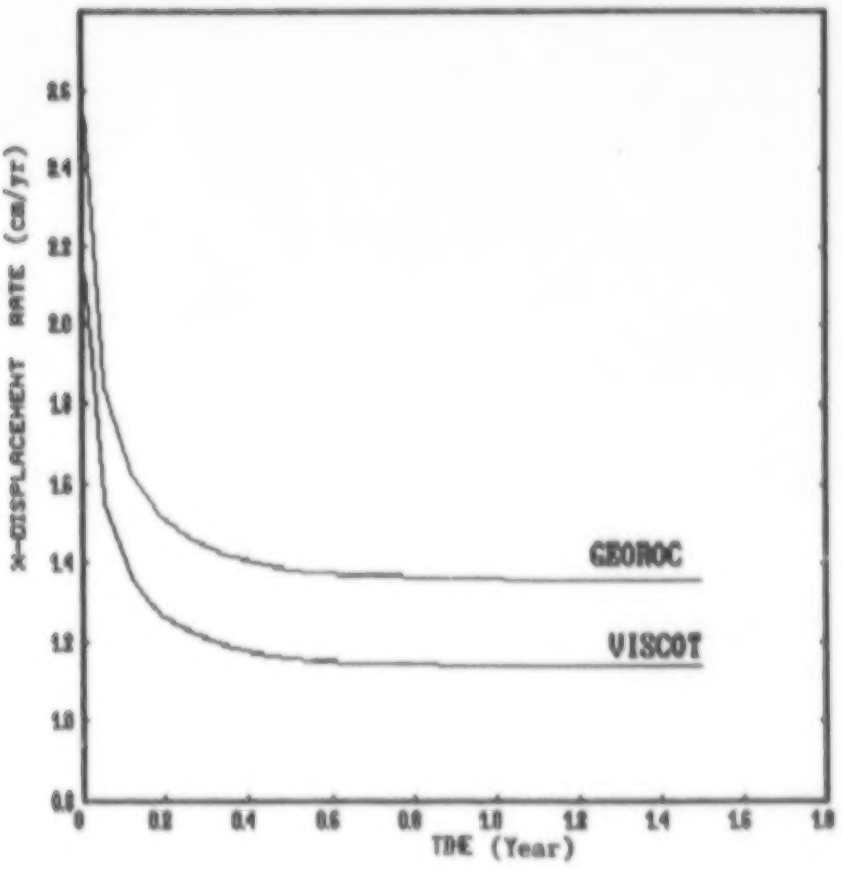

FIGURE 8

DPPC VIRGIN GROUND OPENING

VERTICAL CLOSURE RATE

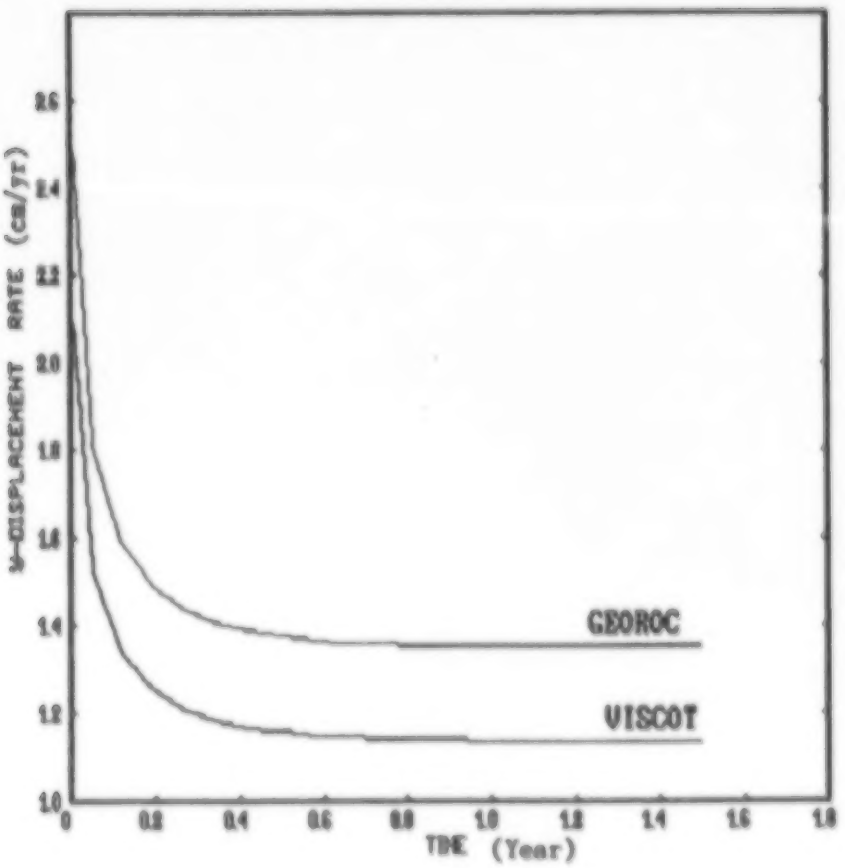

FIGURE 9

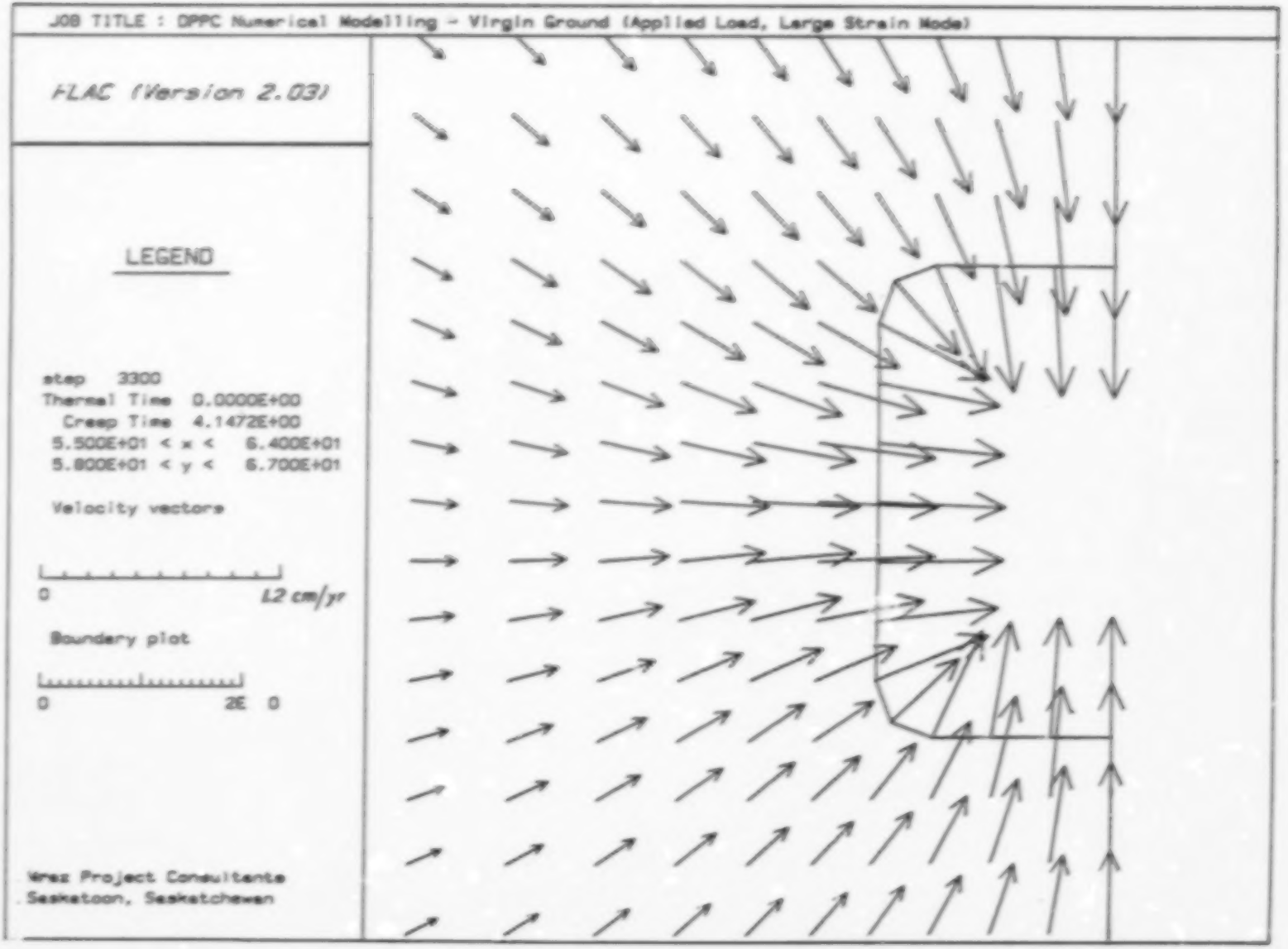
JOB TITLE : DPPC Numerical Modelling - Virgin Ground (Applied Load, Large Strain Mode)
FLAC (Version 2.03)
LEGEND
step 3300
Thermal Time 0.0000E+00
Creep Time 4.1472E+00
5.500E+01 < x < 6.400E+01
5.800E+01 < y < 6.700E+01
Velocity vectors
0
L2 cm/yr
Boundary plot
0
2E 0
Vrez Project Consultants
Saskatoon, Saskatchewan

numerical "drift" over 2000 time steps may have resulted in an accumulated discrepancy of 16 percent.

The difference in computational conditions between the FEM codes and FLAC is the fact that the FEM codes are operated under small strain mode, and FLAC is run using large strain mode. Large strain mode is a function which updates the coordinate system of a mesh for each time step, reflecting the distortion that is occurring within the mesh. Finite element codes used do not contain a coordinate updating system. The large strain mode in FLAC produced slightly higher closure rates and significantly higher room closure than the finite element codes. In actuality, the amount of in situ closure situ would probably be similar to the amount of closure predicted by the finite difference difference code, if transient closure is included.

4.0 DISCUSSION ON GEOROC

Generally, GEOROC is an excellent code with many advanced features. Nevertheless, it is not immediately clear if the mathematical formulation of the code eliminates the possibility of mesh lock-up.

The material law implemented in GEOROC is simplistic and it would likely be worthwhile incorporating more advanced models, such as Munson-Dawson, and the two exponent power law used in this study.

Pre- and post-processing programs supplied with the code are antiquated by today's standards. Moreover, in order to graphically display results, the user must purchase a proprietary program. More advanced pre- and post-processing capabilities would reduce the time spent on analysis considerably by a factor of five or more.

The current PC version of the GEOROC code has limited capabilities in terms of mesh sizes that can be processed. With the current availability of personal computers based on a 80386 processor, this limitations can be removed with minimal effort.

Generally, all three codes produce exceptable solutions in terms of closure rates, but FLAC appears to be the superior code because of its ability to predicted more realistic closures.

MAPS
NOT
FILMED

CARTES
OMISES